SARS-CoV-2 variants of concern: study of Spike antigenicity and interaction with hACE2

Shang Yu Gong

Department of Microbiology and Immunology

Faculty of Medicine and Health Sciences

McGill University, Montréal, Québec, Canada

December 2022

A thesis submitted to McGill University in partial fulfillment

of the requirements of the degree of

Master of Science

TABLE OF CONTENTS

TABLE OF CONTENTS ..... **II**

PREFACE ..... **IV**

CONTRIBUTION OF AUTHORS ..... **VIII**

ABSTRACT ..... **IX**

RÉSUMÉ ..... **X**

ACKNOWLEDGEMENTS ..... **XII**

LIST OF ABBREVIATIONS ..... **XIV**

LIST OF FIGURES ..... **XVII**

CHAPTER 1 XVII
CHAPTER 2 XVII
CHAPTER 3 XVII

LIST OF TABLES ..... **XVIII**

CHAPTER 1 XVIII

CHAPTER 1. INTRODUCTION **19**

1.1 SARS-CoV-2 AND COVID-19 19
1.2 VIRAL ORIGIN AND RESERVOIR 19
1.3 VIRAL STRUCTURE AND GENOME ORGANIZATION 20
1.4 REPLICATION CYCLE 23
1.4.1 Entry *23*
1.4.2 Translation of viral non-structural proteins *24*
1.4.3 Genome Replication and Transcription *25*
1.4.4 Viral Assembly and Budding *26*
1.5 STRUCTURAL PROTEINS 27
1.5.1 Spike Glycoproteins *27*
1.5.2 S1 subunit *29*
1.5.3 S2 subunit *29*
1.5.4 Membrane Protein *30*
1.5.5 Envelope Protein *30*
1.5.6 Nucleocapsid *30*
1.6 ACCESSORY PROTEINS 31
1.6.1 ORF3a *31*
1.6.2 ORF6 ..... *31*
1.6.3 ORF7a *31*
1.6.4 ORF8 ..... *31*
1.6.5 ORF10 ..... *32*
1.7 VARIANTS 32
1.7.1 B.1.1.7 (ALPHA) 35
1.7.2 B.1.351 (BETA) AND P.1 (GAMMA) 35
1.7.3 B.1.617.2 (DELTA) 35
1.7.4 B.1.1.529 (OMICRON) 35

1.8 PATHOLOGY....38
1.9 VACCINE STRATEGIES....38
1.10 HUMORAL IMMUNE RESPONSES TO SARS-COV-2 INFECTION....40
1.10.1. Neutralization....41
1.10.2 ADCC....41
1.10.3 Spike is the main target of Abs with neutralizing and Fc-effector functions....42
1.11 TREATMENT OPTIONS....42
1.11.1 Monoclonal Abs Therapy....42
1.11.2 Small Molecule inhibitors....43
1.12 EXPERIMENTAL METHODS....43
1.12.1 Flow Cytometry....43
1.12.2 Virus Capture Assay....44
1.12.3 Biolayer Interferometry (BLI)....44
1.13 THESIS RATIONALE AND OBJECTIVES....45

CHAPTER 2. CONTRIBUTION OF SINGLE MUTATIONS TO SELECTED SARS-COV-2 EMERGING VARIANTS SPIKE ANTIGENICITY....46

2.1 PREFACE TO CHAPTER 2....46
2.2. ABSTRACT....46
2.3 INTRODUCTION....47
2.4 MATERIALS AND METHODS....48
2.5 RESULTS....51
2.6 DISCUSSION....62
2.7 CONCLUSIONS....63
2.8 REFERENCES....65

CHAPTER 3. TEMPERATURE INFLUENCES THE INTERACTION BETWEEN SARS-COV-2 SPIKE FROM OMICRON SUBVARIANTS AND HUMAN ACE2....69

3.1 PREFACE....69
3.2 ABSTRACT....69
3.3 INTRODUCTION....70
3.4 MATERIALS AND METHODS....71
3.5 RESULTS....74
3.6 DISCUSSION....78
3.7 REFERENCES....81

CHAPTER 4. DISCUSSION....86

4.1 SUMMARY OF FINDINGS....86
4.2 CONTRIBUTION TO KNOWLEDGE....87
4.3 SIGNIFICANCE....90
4.3.1 The importance of single mutations....90
4.3.2 Implications for increased Spike—ACE2 cooperativity in the cold....92
4.4 EXPERIMENTAL LIMITATIONS....92
4.5 NEXT STEPS....92
4.6 OUTSTANDING QUESTIONS....93

CONCLUSION....95

REFERENCES....96

APPENDIX....117

PREFACE

This thesis was written in accordance with the guidelines provided for a "Manuscript-based (Article-based) thesis" format from McGill University's Graduate and Postdoctoral Studies "Guidelines for Preparation of a Thesis":

"As an alternative to the traditional format, a thesis may be presented as a collection of scholarly papers of which the student is the first author or co-first author. A manuscript-based Master's thesis must include the text of one or more manuscripts. Manuscripts for publication in journals are frequently very concise documents. A thesis, however, is expected to consist of more detailed, scholarly work. A manuscript-based thesis will be evaluated by the examiners as a unified, logically coherent document in the same way a traditional thesis is evaluated."

This thesis consists of 4 chapters. Chapter 1 presents a literature review of the newly-emerged SARS-CoV-2 virus and topics relevant to this thesis, and introduces the research aims of this thesis. Chapter 2 and 3 are two peer-reviewed and published manuscripts for which the candidate is the first or co-first author. Chapter 4 is the general discussion of the work presented in this thesis The contribution of all authors can be found in the following "Contribution of Authors" Section.

Manuscript which the candidate has included in this thesis are the following publications:

1. **Gong, S. Y**.; Chatterjee, D.; Richard, J.; Prévost, J.; Tauzin, A.; Gasser, R.; Bo, Y.; Vézina, D.; Goyette, G.; Gendron-Lepage, G.; Medjahed, H.; Roger, M.; Côté, M.; Finzi, A., **Contribution of single mutations to selected SARS-CoV-2 emerging variants spike antigenicity**. *Virology.* (Nov 2021)
2. **Gong, S. Y.**; Ding, S.; Benlarbi, M.; Chen, Y.; Vezina, D.; Marchitto, L.; Beaudoin-Bussieres, G.; Goyette, G.; Bourassa, C.; Bo, Y.; Medjahed, H.; Levade, I.; Pazgier, M.; Cote, M.; Richard, J.; Prevost, J.; Finzi, A., **Temperature Influences the Interaction between SARS-CoV-2 Spike from Omicron Subvariants and Human ACE2**. *Viruses.* (Sept 2022)

Manuscripts not included in this thesis, for which the candidate has made significant contributions during the course of her M.Sc. training include the following publications:

3. Tauzin, A.; **Gong, S. Y**.; Chatterjee, D.; Ding, S.; Painter, M. M.; Goel, R. R.; Beaudoin-Bussieres, G.; Marchitto, L.; Boutin, M.; Laumaea, A.; Okeny, J.; Gendron-Lepage, G.; Bourassa, C.; Medjahed, H.; Goyette, G.; Williams, J. C.; Bo, Y.; Gokool, L.; Morrisseau, C.; Arlotto, P.; Bazin, R.; Fafard, J.; Tremblay, C.; Kaufmann, D. E.; De Serres, G.; Richard, J.; Cote, M.; Duerr, R.; Martel-Laferriere, V.; Greenplate, A. R.; Wherry, E. J.; Finzi, A., **A boost with SARS-CoV-2 BNT162b2 mRNA vaccine elicits strong humoral responses independently of the interval between the first two doses.** *Cell Rep.* (Oct 2022)

4. Sannier, G.; Nicolas, A.; Dubé, M.; Marchitto, L.; Nayrac, M.; Tastet, O.; Tauzin, A.; Lima-Barbosa, R.; Laporte, M.; Cloutier, R.; Flores, A. S.; Boutin, M.; **Gong, S. Y.**; Benlarbi, M.; Ding, S.; Bourassa, C.; Gendron-Lepage, G.; Medjahed, H.; Goyette, G.; Brassard, N.; Ortega-Delgado, G.-G.; Niessl, J.; Gokool, L.; Morrisseau, C.; Arlotto, P.; Rios, N.; Tremblay, C.; Martel-Laferrière, V.; Prat, A.; Bélair, J.; Beaubien-Souligny, W.; Goupil, R.; Nadeau-Fredette, A.-C.; Lamarche, C.; Finzi, A.; Suri, R. S.; Kaufmann, D. E., A third SARS-CoV-2 mRNA vaccine dose in people receiving hemodialysis overcomes B cell defects but elicits a skewed CD4+ T cell profile. bioRxiv (Sept 2022)

5. Tauzin, A.; Beaudoin-Bussieres, G.; **Gong, S. Y.;** Chatterjee, D.; Gendron-Lepage, G.; Bourassa, C.; Goyette, G.; Racine, N.; Khrifi, Z.; Turgeon, J.; Tremblay, C.; Martel-Laferriere, V.; Kaufmann, D. E.; Cardinal, H.; Cloutier, M.; Bazin, R.; Duerr, R.; Dieude, M.; Hebert, M. J.; Finzi, A., **Humoral immune responses against SARS-CoV-2 Spike variants after mRNA vaccination in solid organ transplant recipients**. *iScience.* (Sept 2022)

6. Ding, S.; Ullah, I.; **Gong, S. Y.**; Grover, J. R.; Mohammadi, M.; Chen, Y.; Vézina, D.; Beaudoin-Bussières, G.; Verma, V. T.; Goyette, G.; Gaudette, F.; Richard, J.; Yang, D.; Smith, A. B., 3rd; Pazgier, M.; Côté, M.; Abrams, C.; Kumar, P.; Mothes, W.; Uchil, P. D.; Finzi, A.; Baron, C., **VE607 stabilizes SARS-CoV-2 Spike in the "RBD-up" conformation and inhibits viral entry.** *iScience*. (Jul 2022)

7. Nayrac, M.; Dube, M.; Sannier, G.; Nicolas, A.; Marchitto, L.; Tastet, O.; Tauzin, A.; Brassard, N.; Lima-Barbosa, R.; Beaudoin-Bussieres, G.; Vezina, D.; **Gong, S. Y**.; Benlarbi, M.; Gasser, R.; Laumaea, A.; Prevost, J.; Bourassa, C.; Gendron-Lepage, G.; Medjahed, H.; Goyette, G.; Ortega-Delgado, G. G.; Laporte, M.; Niessl, J.; Gokool, L.; Morrisseau, C.; Arlotto, P.; Richard, J.; Belair, J.; Prat, A.; Tremblay, C.; Martel-Laferriere, V.; Finzi, A.; Kaufmann, D. E**., Temporal associations of B and T cell immunity with robust vaccine responsiveness in a 16-week interval BNT162b2 regimen.** *Cell Rep.* (Jun 2022)

8. Chatterjee, D.; Tauzin, A.; Marchitto, L.; **Gong, S. Y.**; Boutin, M.; Bourassa, C.; Beaudoin-Bussières, G.; Bo, Y.; Ding, S.; Laumaea, A.; Vézina, D.; Perreault, J.; Gokool, L.; Morrisseau, C.; Arlotto, P.; Fournier, É.; Guilbault, A.; Delisle, B.; Levade, I.; Goyette, G.; Gendron-Lepage, G.; Medjahed, H.; De Serres, G.; Tremblay, C.; Martel-Laferrière, V.; Kaufmann, D. E.; Bazin, R.; Prévost, J.; Moreira, S.; Richard, J.; Côté, M.; Finzi, A., **SARS-CoV-2 Omicron Spike recognition by plasma from individuals receiving BNT162b2 mRNA vaccination with a 16-week interval between doses.** *Cell Rep*. (Mar 2022)

9. Beaudoin-Bussieres, G.; Chen, Y.; Ullah, I.; Prevost, J.; Tolbert, W. D.; Symmes, K.; Ding, S.; Benlarbi, M.; **Gong, S. Y.**; Tauzin, A.; Gasser, R.; Chatterjee, D.; Vezina, D.; Goyette, G.; Richard, J.; Zhou, F.; Stamatatos, L.; McGuire, A. T.; Charest, H.; Roger, M.; Pozharski, E.; Kumar, P.; Mothes, W.; Uchil, P. D.; Pazgier, M.; Finzi, A., **A Fc-enhanced NTD-binding non-neutralizing antibody delays virus spread and synergizes with a nAb to protect mice from lethal SARS-CoV-2 infection.** *Cell Rep*. (Feb 2022)

10. Li, W.; Chen, Y.; Prévost, J.; Ullah, I.; Lu, M.; **Gong, S. Y.;** Tauzin, A.; Gasser, R.; Vézina, D.; Anand, S. P.; Goyette, G.; Chaterjee, D.; Ding, S.; Tolbert, W. D.; Grunst, M. W.; Bo, Y.; Zhang, S.; Richard, J.; Zhou, F.; Huang, R. K.; Esser, L.; Zeher, A.; Côté, M.; Kumar, P.; Sodroski, J.; Xia, D.; Uchil, P. D.; Pazgier, M.; Finzi, A.; Mothes, W., **Structural basis and mode of action for two broadly neutralizing antibodies against SARS-CoV-2 emerging variants of concern**. *Cell Rep.* (Jan 2022)

11. Chatterjee, D.; Tauzin, A.; Laumaea, A.; **Gong, S. Y.**; Bo, Y.; Guilbault, A.; Goyette, G.; Bourassa, C.; Gendron-Lepage, G.; Medjahed, H.; Richard, J.; Moreira, S.; Cote, M.; Finzi, A., **Antigenicity of the Mu (B.1.621) and A.2.5 SARS-CoV-2 Spikes**. *Viruses*. (Jan 2022)

12. Tauzin, A.; **Gong, S. Y.**; Beaudoin-Bussieres, G.; Vezina, D.; Gasser, R.; Nault, L.; Marchitto, L.; Benlarbi, M.; Chatterjee, D.; Nayrac, M.; Laumaea, A.; Prevost, J.; Boutin, M.; Sannier, G.; Nicolas, A.; Bourassa, C.; Gendron-Lepage, G.; Medjahed, H.; Goyette, G.; Bo, Y.; Perreault, J.; Gokool, L.; Morrisseau, C.; Arlotto, P.; Bazin, R.; Dube, M.; De Serres, G.; Brousseau, N.; Richard, J.; Rovito, R.; Cote, M.; Tremblay, C.; Marchetti, G. C.; Duerr, R.; Martel-Laferriere, V.; Kaufmann, D. E.; Finzi, A., **Strong humoral immune responses against SARS-CoV-2 Spike after BNT162b2 mRNA vaccination with a 16-week interval between doses.** *Cell Host Microbe.* (Jan 2022)

13. Ding, S.; Adam, D.; Beaudoin-Bussieres, G.; Tauzin, A.; **Gong, S. Y**.; Gasser, R.; Laumaea, A.; Anand, S. P.; Prive, A.; Bourassa, C.; Medjahed, H.; Prevost, J.; Charest, H.; Richard, J.; Brochiero, E.; Finzi, A., **SARS-CoV-2 Spike Expression at the Surface of Infected Primary Human Airway Epithelial Cells.** Viruses. (Dec 2021)

14. Prévost, J.; Richard, J.; Gasser, R.; Ding, S.; Fage, C.; Anand, S. P.; Adam, D.; Gupta Vergara, N.; Tauzin, A.; Benlarbi, M.; **Gong, S. Y.**; Goyette, G.; Privé, A.; Moreira, S.; Charest, H.; Roger, M.; Mothes, W.; Pazgier, M.; Brochiero, E.; Boivin, G.; Abrams, C. F.; Schön, A.; Finzi, A., **Impact of temperature on the affinity of SARS-CoV-2 Spike glycoprotein for host ACE2.** *J Biol Chem*. (Oct 2021)

15. Anand, S. P.; Prevost, J.; Nayrac, M.; Beaudoin-Bussieres, G.; Benlarbi, M.; Gasser, R.; Brassard, N.; Laumaea, A.; **Gong, S. Y.**; Bourassa, C.; Brunet-Ratnasingham, E.; Medjahed, H.; Gendron-Lepage, G.; Goyette, G.; Gokool, L.; Morrisseau, C.; Begin, P.; Martel-Laferriere, V.; Tremblay, C.; Richard, J.; Bazin, R.; Duerr, R.; Kaufmann, D. E.; Finzi, A., **Longitudinal analysis of humoral immunity against SARS-CoV-2 Spike in convalescent individuals up to 8 months post-symptom onset**. *Cell Rep Med.* (Jun 2021)

16. Richard, J.; Nguyen, D. N.; Tolbert, W. D.; Gasser, R.; Ding, S.; Vezina, D.; **Yu Gong, S.**; Prevost, J.; Gendron-Lepage, G.; Medjahed, H.; Gottumukkala, S.; Finzi, A.; Pazgier, M., **Across Functional Boundaries: Making Nonneutralizing Antibodies To Neutralize HIV-1 and Mediate Fc-Mediated Effector Killing of Infected Cells.** *mBio.* (Oct 2021)

17. Vezina, D.; **Gong, S. Y.**; Tolbert, W. D.; Ding, S.; Nguyen, D.; Richard, J.; Gendron-Lepage, G.; Melillo, B., 3rd; Smith, A. B.; Pazgier, M.; Finzi, A., **Stabilizing the HIV-1 envelope glycoprotein State 2A conformation.** *J Virol.* (Dec 2020)

CONTRIBUTION OF AUTHORS

Chapter I (Introduction), Chapter IV (Discussion), and Chapter V (Conclusion):

Shang Yu Gong wrote the chapters with edits from Dr. Andrés Finzi.

Chapter II:

Contribution of single mutations to selected SARS-CoV-2 emerging variants spike antigenicity

Published in *Virology.* (Nov 2021)

Gong, S. Y.; Chatterjee, D.; Richard, J.; Prévost, J.; Tauzin, A.; Gasser, R.; Bo, Y.; Vézina, D.; Goyette, G.; Gendron-Lepage, G.; Medjahed, H.; Roger, M.; Côté, M.; Finzi, A.,

S.G., D.C., J.P. and A.F. conceived the study. S.G., J.P., J.R., and A.F. designed experimental approaches. S.G., D.C., J.R., A.T., R.G., performed, analyzed, and interpreted the experiments. S.G. and D.C., performed statistical analysis. J.P., Y.B., G.G., H.M., G.G.L., M.C., and A.F. contributed unique reagents. S.D., J.P., J.R. and M.R., provided scientific input. S.G. D.C., and A.F wrote the manuscript with inputs from others. All authors have read and agreed to the published version of the manuscript.

Chapter III:

Temperature Influences the Interaction between SARS-CoV-2 Spike from Omicron Subvariants and Human ACE2

Published in *Viruses.* (Sept 2022)

Gong, S. Y.; Ding, S.; Benlarbi, M.; Chen, Y.; Vezina, D.; Marchitto, L.; Beaudoin-Bussieres, G.; Goyette, G.; Bourassa, C.; Bo, Y.; Medjahed, H.; Levade, I.; Pazgier, M.; Cote, M.; Richard, J.; Prevost, J.; Finzi, A.,

S.G., J.P. and A.F. conceived the study. S.G., S.D., D.V., J.P., J.R., M.P. and A.F. designed experimental approaches. S.G., S.D., D.V., H.M., M.B., L.M., G.B.-B., G.G. and C.B. performed, analyzed, and interpreted the experiments. S.G. performed statistical analysis. J.P., Y.C., G.G., M.P., M.C., Y.B. and A.F. contributed unique reagents. S.D., J.P., J.R. and I.L. provided scientific input. S.G. and A.F wrote the manuscript with inputs from others. All authors have read and agreed to the published version of the manuscript.

ABSTRACT

Since it's emergence towards the end of 2019, the SARS-CoV-2 virus, causative agent of the COVID-19 pandemic, remains a major health burden worldwide. Global collaborative efforts have rapidly developed and instituted multiple vaccination platforms, which were shown to be effective in preventing the infection of the original Wuhan-Hu-1 strain and remain effective at preventing severe outcomes for newly arising variants. The Spike glycoprotein (Spike) is exposed at the surface of viral particles and is composed of two subunits (S1 and S2). The Spike mediates the first step of the replication cycle: viral entry. Its receptor binding domain (RBD) is located in the S1 subunit and mediates attachment to the host receptor angiotensin-converting enzyme 2 (ACE2). Upon binding, the Spike is cleaved by cellular proteases at the S2' cleavage sites, leading to viral entry mediated by the fusion peptide in the S2 subunit.

By being highly exposed at the surface of viral particles and infected cells, the Spike is the main target of humoral responses elicited upon infection. Accordingly, vaccination and therapeutic interventions such as antibody-based immunotherapy target the SARS-CoV-2 Spike glycoprotein. Although the correlates of protection are unclear, some studies suggest that antibodies with neutralizing and/or Fc-effector function, in combination with a long-lasting cellular immune response, may play an important role in the protection conferred by vaccination or natural infection. Due to the strong immune pressure against the Spike, multiple variants have arisen since the first Wuhan-Hu-1, strongly dominating the subsequent waves of the pandemic. The World Health organization (WHO) denominated them Variants of Interest (VOI), or Variants of Concern (VOC) based on their transmissibility, infectivity, disease severity, and immune evasion.

During my Master studies, I first aimed to characterize how the Spike glycoproteins of VOCs interact with its receptor, ACE2, and whether this binding could be influenced by temperature, since the virus must cross a temperature gradient during its passage from the exterior environment into the human airway. Moreover, I aimed to assess the impact of single mutation on the antigenicity of the Spike. We found that antigenic profile and ACE2 binding properties of the variants cannot be predicted by single mutations. Altogether, findings from this thesis highlight the shift in antigenicity and ACE2 binding ability of SARS-CoV-2 VOI and VOC Spikes since their emergence, and the role of temperature in Spike – ACE2 interaction. Results presented in this thesis can serve to better understand the mechanisms of infection and immune evasion of this virus.

RÉSUMÉ

Depuis son apparition vers la fin de 2019, le virus SARS-CoV-2, responsable de la pandémie COVID-19, demeure un problème de santé majeur à travers le monde. Grâce aux efforts de collaboration globale, de multiples plateformes de vaccination ont rapidement été déployées à travers le monde. Il a été montré rapidement que ces vaccins étaient efficaces à prévenir l'infection par la souche originale. De plus, malgré le fait que leur efficacité à prévenir l'infection a été compromise par l'arrivée des nouveaux variants, ils restent efficaces à prévenir des complications graves par les nouveaux variants préoccupants. La glycoprotéine de Spike est exposée à la surface des particules virales et est composée de deux sous-unités (S1 et S2). La Spicule est responsable de la première étape du cycle réplicatif : l'entrée virale. Le domaine d'interaction avec le récepteur, le *receptor binding domain* (RBD), situé dans le S1, médie l'attachement au récepteur d'hôte, l'enzyme de conversion de l'angiotensine II, aussi appelé l'*angiotensin converting enzyme II* (ACE2). Suivant l'engagement RBD – ACE2, la Spicule est clivée par des protéases cellulaires aux sites de clivage, soient au S1/S2 et au S2', ce qui amène l'entrée virale par le peptide de fusion situé dans le S2.

En étant très exposée à la surface des particules virales et des cellules infectieuses, la Spike demeure la cible principale de la réponse humorale élicitée par une infection. En conséquence, la vaccination et les interventions thérapeutique telles que l'immunothérapie à base d'anticorps ciblent la Spicule glycoprotéine de SARS-CoV-2. Bien que les corrélats de protections soient incertains, des études suggèrent que des anticorps ayant une capacité neutralisante et/ou des fonctions effectrices Fc, en combinaison avec une réponse immunitaire cellulaire, peuvent jouer un rôle dans la protection accordée par la vaccination or l'infection naturelle. À cause de la forte pression immunitaire contre la Spicule, de multiples variants sont apparus depuis la première souche Wuhan-Hu-1 et dominent les vagues ultérieures de la pandémie. L'organisation mondiale de la santé (OMS), les a désigné comme des variants à suivre (VOI) ou variants préoccupants (VOC) basé sur leur transmissibilité, infectivité, gravité de symptôme et habileté d'évasion du système immunitaire.

Au cours de mes études de Maîtrise, mon objectif était d'abord caractériser l'impact des mutations simples sur le changement antigénique global d'un VOC particulier et l'impact sur sa capacité à interagir avec son récepteur. On a trouvé que le profil antigénique et la capacité d'interagir avec

ACE2 des variants ne peut pas être prédit par des mutations individuelles. La combinaison des mutations dans la Spicule de chaque VOC fournit une signature antigénique unique. Puisque le virus doit traverser un gradient de température durant son passage de l'environnement extérieur jusqu'à la voie respiratoire humaine, j'ai aussi étudié l'impact de la température sur l'affinité des Spike des VOC avec son récepteur. Ensemble, les trouvailles de cette thèse soulignent le changement d'antigénicité et la capacité d'interagir avec ACE2 des Spicules de SARS-CoV-2 VOI et VOC depuis leur émergence et du rôle que joue la température dans les interactions Spike – ACE2. Les résultats présentés dans cette thèse pourraient servir à mieux comprendre les mécanismes d'infection et de l'évasion immunitaire de ce virus.

ACKNOWLEDGEMENTS

I would like to first acknowledge Dr. Andrés Finzi, my deepest thanks for taking me in, and being such an inspiring figure in the ways of science, and for guiding me for the past 3 years. I truly admire your self-discipline and the discipline which you ask of your students. I am truly grateful for the numerous opportunities you have provided me to present and publish my research, and for expanding my horizons. I have learned so much from you. A big thank you for your patience with me and for allowing me grow. THANK YOU SO MUCH!!!

I would like to thank my co-supervisor, Dr. Chen Liang. You have been very helpful and supportive throughout my studies. As well, my advisory committee, Dr. Selena Sagan and Dr. Nicole Bernard, I am so grateful for your warm welcome for me into the science community, and for your encouragements. As well, my mentor from Win4Science – Dr. Aimee K. Ryan, for your support. Thank you for giving me time for discussions, which have always been most helpful. Importantly, big thanks to our collaborators, who provided important scientific input, reagents, assays, which allowed me to expand my projects. I would also like to thank my professors and the Department of Microbiology and Immunology at McGill, for providing me with the knowledge needed to pursue graduate studies in this enriching program. My gratitude also goes to the CRCHUM cytometry platform, for providing vital training.

As well, my dearest mentors and friends from the lab who have been so supportive of me – Dr. Jonathan Richard and Dr. Jérémie Prévost, for your helpful discussions and brilliant ideas for my projects. Dr. Sai Priya Anand and (almost Msc.) Dani, for your training, guidance, and support. Dr. Annemarie Laumaea, for our insightful discussions, be it work- or life-related. Future Dr. Benlarbi, for always being there, no matter rain or shine. Gabrielle, for being so approachable and supportive since day 1. Guillaume (soon Dr.), for our honest and lengthy conversations, and for always being a big help! Marianne (future Msc.) and Lorie (future Dr.), for your advice both on the professional and personal front. For dear Dr. Shilei, thank you for being a level-headed, good mentor, your insights are most helpful, and your positive attitude always cheer me up. Big thanks the past and present members and staff of the lab, Dr. Halima Medjahed, Catherine Bourassa, Dr. Guillaume Goyette, Dr. Alexandra Tauzin, Dr. Debashree Chatterjee, Nicolas Beeckmans and Dr. Romain Gasser, for your encouragement as well as providing much needed reagents and help for

my projects. Above all, a big THANK YOU for all the support, laugh, and tears, that we shared throughout the years!! You are the best team I could have ever asked for.

For my best friends and support network, future Dr. Solymoss and Dr. Brassard, I am so grateful for meeting you during undergrad, and for going through grad school and life with you guys! I am also thankful for my dear friends: Lucy Xiang, Sophie Deng, Jiaxuan Lin, for lending a helpful ear. My loving partner, Jimmy Wang, for being a steady presence in my life, standing by me when I most needed it. Thank you, to you and your family, for patiently and gently supporting me.

Finally, for my family near and far, for my parents Wei Gong and Ai Rong Mu, and little Viviane Gong, thank you for being my biggest supporters, for always having my back, and for all the sacrifice you've made for me to be able to stand here today. Lastly, for my grandparents 沙兰凤 & 牧春旺, for the most memorable years of my life, and for shaping me into the person I am today.

LIST OF ABBREVIATIONS

Abs	Antibodies
ACE2	Angiotensin-converting enzyme 2
ADCC	Antibody-dependent cellular cytotoxicity
Alpha	B.1.1.7
AR2G	Amine Reactive Second-Generation
Beta	B.1.351
BLI	Biolayer interferometry
BSA	Bovine serum albumin
CD16	Fcγ receptor III
CH	Central helix
COVID-19	Coronavirus disease 2019
CT	Cytoplasmic tail
CTD	C-terminal domain
Cryo-EM	Cryo-electron microscopy
D	Aspartic acid
Delta	B.1.617.2
DMEM	Dulbecco's modified Eagle's medium
DMS	Deep mutational scanning
E	SARS-CoV-2 Envelope protein
EF	Extrafollicular
Env	HIV-1 Envelope glycoprotein
Epsilno	B.1.429
ER	Endoplasmic reticulum
ERGIC	Endoplasmic reticulum-Golgi intermediate compartment
EUL	Emergency Use Listing
Fab	Antigen-binding fragment
Fc	Crystallizable fragment
FP	Fusion peptide
G	Glycine

Gamma	P.1
GC	Germinal center
GFP	Green fluorescent protein
HR1	Heptad repeat 1
HR2	Heptad repeat 2
IFN-1	Type I interferon
Ig	Immunoglobulins
IgMs	Immunoglobulins of class M
Iota	B.1.526
K_a	On-rates
Kappa	B.1.617.1
K_D	Affinity constants
K_{dis}	Off-rates
M	Membrane protein
Mabs	Monoclonal antibodies
Mabs	Monoclonal antibody
MAVS	Mitochondrial antiviral signaling protein
MERS-CoV	Middle East Respiratory Syndrome Coronavirus
MFI	Median Fluorescence intensities
MHC-1	Major histocompatibility complex class I
MMPs	Metalloproteinase
N	Nucleocapsid protein
NiRan	RdRp-associated nucleotidyltransferase
NiRan	Nucleotidyltransferase
NGS	Next generation sequencing
NK	Natural killer cells
NSP	Non-structural proteins
NTD	N-terminal domain
NTD	N-terminal domain
ORF	Open reading frame
PBS	Phosphate-buffered saline

PrEP	Pre-exposure prophylaxis
PSO	Post-symptom onset
RBD	Receptor binding domain
RBM	Receptor binding motif
RER	Rough ER
RTC	Replicase-transcriptase complex
S	Spike glycoprotein
sACE2	Soluble ACE2
SARS-CoV	Severe Acute Respiratory Syndrome Coronavirus
sgRNA	Subgenomic RNA
smFRET	Single-molecule Förster resonance energy transfer
TM	Transmembrane domain
TMPRSS2	Transmembrane protease serine 2
TNF	Tumor necrosis factor
TRS	Transcription regulatory sequence
TRS-B	TRS body
TRS-L	TRS leader
UTR	Untranslated region
VOCs	Variants of concern
VOIs	Variants of interest
VSV-G	Vesicular stomatitis virus G
WHO	World Health Organization
WT	Wild-type

LIST OF FIGURES

CHAPTER 1

Figure 1.1 Mature SARS-CoV-2 virion structure.

Figure 1.2 SARS-CoV-2 genomic organization.

Figure 1.3 SARS-CoV-2 Replication Cycle.

Figure 1.4 SARS-CoV-2 RNA synthesis.

Figure 1.5 SARS-CoV-2 Spike Sequence

Figure 1.6 Timeline of Emerging Variants of Concern (VOC), Variants of Interest (VOI), and Variants Under Surveillance (VUS).

CHAPTER 2

Figure 2.1 Evaluation hACE2 Fc binding to SARS-CoV-2 Spike variants.

Figure 2.2 Kinetic Analysis of RBD interaction to hACE2 Binding by Biolayer Interferometry

Figure 2.3 Evaluation of the impact of temperature on Spike-ACE2 interaction.

Figure 2.4 Recognition of SARS-CoV-2 Spike variants and single mutants by plasma from vaccinated SARS-CoV-2 naïve individuals.

Figure 2.5 Recognition of SARS-CoV-2 Spike variants and single mutants by plasma from vaccinated previously-infected individuals.

Figure 2.6 Neutralization of SARS-CoV-2 Spike variants by plasma from previously infected vaccinated individuals.

CHAPTER 3

Figure 3.1. Low temperature enhances Omicron subvariant Spikes' interactions with ACE2.

Figure 3.2. Low temperatures "open" Omicron subvariant Spikes.

LIST OF TABLES

Chapter 1

Table 1. List of single mutations in all VOCs.

Table 2. List of COVID-19 vaccines granted Emergency Use Listing (EUL) by the World Health Organization (WHO).

CHAPTER 1. INTRODUCTION

1.1 SARS-CoV-2 and COVID-19

Severe acute respiratory syndrome coronavirus 2 (SARS-CoV-2), responsible for causing pneumonia-like syndromes, was first reported in Wuhan, Hubei province, China in December 2019 [1]. In January, the World Health Organization (WHO) has coined the name COVID-19 to describe the disease. Since then, the virus has infected over 638 million people, and caused over 6.6 million deaths across the globe [2], and caused severe disruption of daily lives with great economic repercussions. This has led to massive investment in the development of vaccine platforms. The rapid generation of vaccines helped reduce infection cases for the original Wuhan-Hu-1 strain, and prevent severe outcomes for newly arising variants. However, the immune pressure caused by vaccination combined with the continued transmission has driven the virus to accumulate mutations which are advantageous to its transmissibility, infectivity, and/or immune evasion [3]. Therefore, it is primordial to keep studying the evolving virus in order to understand its mechanisms of disease and better prepare for future viral pandemics.

1.2 Viral Origin and Reservoir

In late December 2019, a cluster of patients with pneumonia of unknown origin was reported in Wuhan, China [4]. Investigations regarding the viral origins has found that the outbreak is tied to a wet market in Hubei, suggesting the zoonotic origins of the virus. The increased contacts between humans and wild animals due to urbanization has accelerated the spillover of such zoonotic diseases. SARS-CoV-2 was isolated in human airway epithelial cells, and subsequently identified as a novel *Betacoronavirus* in the *Nidovirale* order, of *Sarbecovirus* subgenus, from its RNA sequence [4-6]. Coronaviruses are enveloped positive RNA viruses that are commonly found in humans, other mammals, and birds. It is composed of four genera - *Alpha* and *Betacoronavirus* which mainly infect mammals, and *Gammacoronavirus* and *Deltacoronavirus* which mainly infect birds [7]. Therefore, domestic animals, livestock, and wild animals are important intermediate hosts to consider for spillover events to humans.

Prior to SARS-CoV-2, two highly pathogenic zoonotic viruses from the *Betacoronavirus* genus - severe acute respiratory syndrome coronavirus (SARS-CoV) and Middle East respiratory syndrome coronavirus (MERS-CoV) - were classified pandemic in 2002 and 2012, respectively. SARS-CoV has been found to be transmitted to humans from the intermediate host market civets [8], whereas MERS-CoV from dromedary camels [9], and both viruses were originated from bats [10,11].

Other human endemic coronaviruses include OC43, HKU1, NL63, and 229E [7]. These viruses cause mild cold syndromes in immunocompetent humans. OC43 and HKU1 are *Betacoronaviruses,* while NL63 and 229E are *Alphacoronaviruses* [12]. OC43 and HKU1 likely originated from rodents, whereas bats are progenitors of NL63 and 229E viruses [13]. Studies suggest that SARS-CoV-2 is of either horseshoe bat [6] or pangolin origins [14], with more evidence supporting its bats origins [15-17]. As well, there seem to be a lack of animal reservoir such as farmed or domestic animals for SARS-CoV-2 [18]. Work included in this thesis will focus on SARS-CoV-2, which is the most recent and very pathogenic zoonotic coronavirus.

1.3 Viral Structure and Genome Organization

SARS-CoV-2 virions are spherical shaped, enveloped particles of 100-160 nm in diameter [12], and are distinguished by their "crown-shaped" Spikes distributed throughout the surface of the virion. SARS-CoV-2 is composed of four structural proteins – Spike (S), Envelope (E), Membrane (M) and the Nucleocapsid (N) proteins (Figure 1.1). The virion is surrounded by a lipid bilayer, which carries three transmembrane proteins - the S glycoprotein and two smaller proteins: the E protein and the M protein [19]. There are between 15-40 Spike glycoproteins trimers on the surface; each trimer is composed of a surface S1 subunit and a transmembrane S2 subunit which are non-covalently bound at the prefusion conformation [20,21]. The E protein is the smallest protein, and it is less incorporated as they remain at the site of assembly, inside the host cells' endoplasmic reticulum –Golgi intermediate compartment and membranes [22]. The M protein is situated on the inner surface of the virus. It is the most abundant viral component, and interacts with all the other structural proteins (E, S, and N) for viral packing [23,24]. Inside the virus particle, the N protein encapsulates the positive-sense single-stranded RNA genome.

Other than structural proteins, the genome also encodes 11 accessory proteins: ORF3a, ORF3b, ORF3c, ORF3d, ORF6, ORF7a, ORF7b, ORF8, ORF9b, ORF9c, and ORF10 [25,26]. SARS-CoV-2 genome also encodes 16 non-structural proteins: NSP1-16, which forms the replicase-transcriptase complex (RTC), which is responsible for replication and inhibiting interferon responses by synthesizing viral proteins which counteracts the cellular immune response [27-29]. (Figure 1.2)

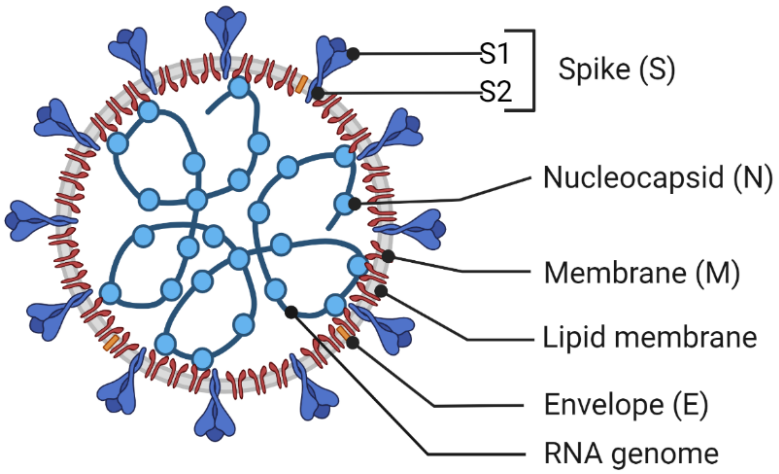

Figure 1.1 Mature SARS-CoV-2 virion structure. Schematic representation of a mature SARS-CoV-2 virion and the viral particle's structure. The SARS-CoV-2 Spike is composed of a trimeric S1-S2 heterodimers, which are embedded in the lipid membrane. The E protein interacts with the M protein during the assembly of the viral particles. The C-terminal domain (CTD) of the M protein protruding from the inside of the lipid membrane interacts with the N to ensure the structural stability of N proteins bound to the RNA genome. Diagram created with BioRender.com

The SARS-CoV-2 genome is ~30k base pairs long and comprises of 16 open reading frames (ORFs), encoding 29 gene products [30]. The SARS-CoV-2 genome consists of a single-stranded, positive-sense RNA genome, which is one of the largest genomes of RNA viruses. The novel *betacoronavirus* SARS-CoV-2 shares 79% genome sequence identity with SARS-CoV, and 50% with MERS-CoV [31]. The genome contains a 5' cap and a 3' poly(A) tail of variable length. The coding portion of the genome is flanked by a 5' untranslated region (UTR) and a 3' UTR [32]. From its 5' end, two-thirds of the genome is composed of two large open reading frames, ORF1a and ORF1b. ORF1a encoding the nsp1-11, and ORF1b encoding nsp12-16 [26,27,33]. The 3' end

of the genome, occupying one third of the genome, encode for the four structural proteins interlaced with accessory proteins (Figure 1.2) [26,27,33].

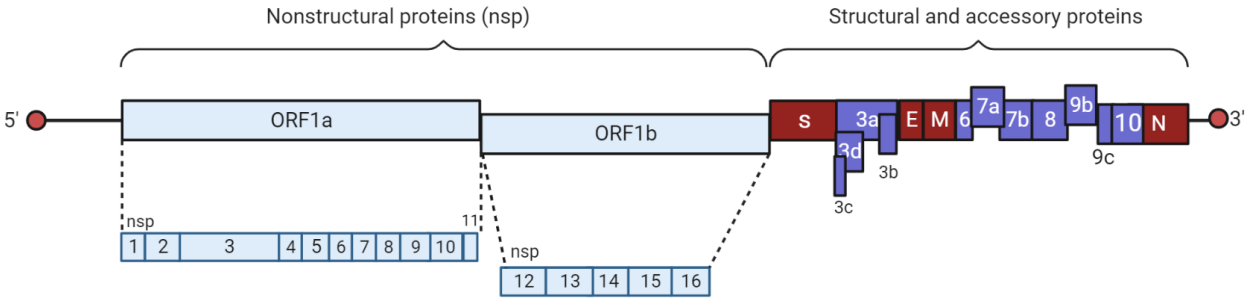

Figure 1.2 SARS-CoV-2 genomic organization. Starting from the 5'-end, the SARS-COV-2 encodes for two large open reading frames, ORF1a and ORF1b encoding non-structural proteins (nsp) nsp1-11 and nsp12-16 respectively. The structural proteins Spike (S), Envelope (E), Membrane (M), and Nucleocapsid (N) are in red and the eleven accessory proteins (ORFs 3a, 3b, 3c, 3d, 6, 7a, 7b, 8, 9b, 9c, 10) are in purple. Diagram created with BioRender.com

1.4 Replication Cycle

The SARS-CoV-2 replication cycle can be divided into three phases – entry, translation of viral proteins, and transcription of novel genetic material to incorporate into newly-made particles. (Figure 1.3).

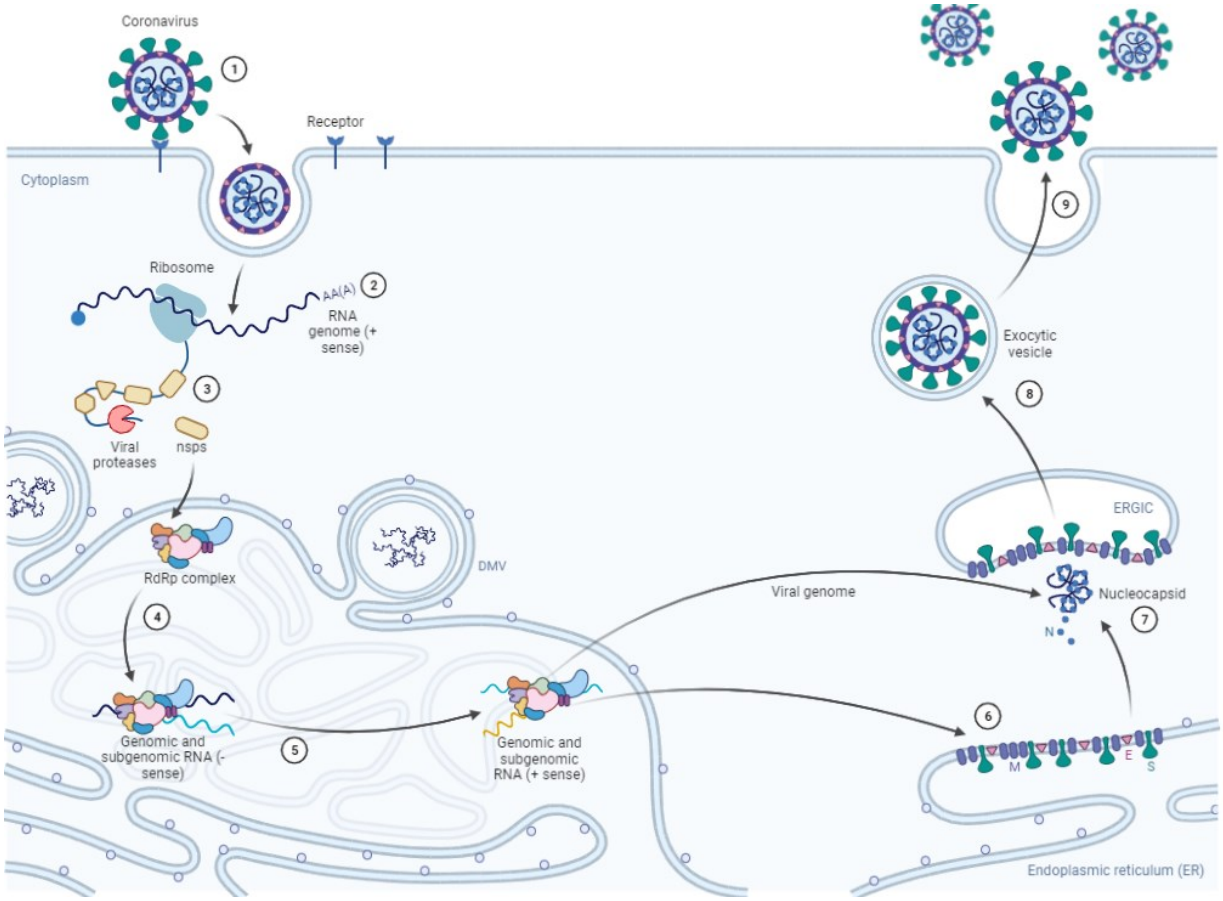

Figure 1.3 SARS-CoV-2 Replication Cycle. Schematic representation of the main stages of viral replication. 1- receptor binding and viral entry via membrane fusion or endocytosis, 2- translation of polypeptides, 3- autoproteolysis and generation of non-structural proteins (nsp), 4- negative sense subgenomic transcription and RNA replication, 5- positive sense subgenomic transcription and RNA replication, 6- translation of subgenomic mRNA and making of structural and accessory proteins, 7- nucleocapsid buds into the endoplasmic reticulum-Golgi intermediate compartment (ERGIC), 8- virion formation, 9- exocytosis. Schematic created with BioRender.com

1.4.1 Entry

The first step of the viral replication begins with the entry of the SARS-CoV-2 virus into the host cell. The Spike glycoprotein is responsible for mediating viral entry into the host cells. The receptor binding domain (RBD) situated on the S1 subunit of the Spike recognizes and binds to its

receptor, the host angiotensin converting enzyme 2 (ACE2) [34]. Therefore, SARS-CoV-2 infect cells which express ACE2 receptor, which comprises numerous tissues including human airway epithelia [35,36], gut [37], kidney[38], and heart [39,40].

The proteolytic cleavage of SARS-CoV-2 Spike by host proteases represents a crucial step prior to fusion. A special feature of the Spike is a polybasic furin cleavage site. Cleavage by furin is associated with higher infection efficiency and likely played an important role in the cross-species transmission of the virus [41]. Furthermore, the binding of Spike with ACE2 triggers conformational rearrangements of the Spike, which then exposes an additional cleavage site, the S2' site, which can be cleaved by transmembrane protease serine 2 (TMPRSS2) at the cell surface [42], or in the case of lack of TMPRSS2, clathrin-mediated endocytosis will occur and the S2' will be cleaved by cathepsin L in the late endolysosome [43,44]. A third way of entry independent of both TMPRSS2 and cathepsin is via metalloproteinase (MMPs) [45]. The cleavage of the S2' site exposes the fusion peptide and allows viral entry from either the surface or the endosome. The viral genome is then released into the host cells' cytoplasm for uncoating and the beginning of replication.

1.4.2 Translation of viral non-structural proteins

Upon entering the cell, the viral genome is released into the host cytoplasm, where the replication process begins. Since the viral genome is positive-stranded, precursor proteins ORF1a and ORF1b are seen immediately by ribosomes and can be directly translated into polyproteins pp1a and pp1ab respectively, the latter is produced following a programmed -1 ribosomal frameshift [46,47]. The polyproteins are cleaved into functional Nsps which form the replicase-transcriptase complex responsible for the genome replication and subgenomic mRNA synthesis [48]. The cysteine proteases processing cleavage of Nsps are located within the Nsp3 (papain-like protease; $PL1^{pro}$ and $PL2^{pro}$) and Nsp 5 (chymotrypsin-like protease; $3CL^{pro}$ or M^{pro}) [49]. Nsp1 will be the first to be released as it interacts with the host ribosome to shut down the host translation machinery and prevent the production of host proteins, including antiviral host factors such as interferons [48]. Nsp2-11 proteins assist in the replication process by acting as cofactors of the RTC. The main players involved in the replication are the RNA-dependent RNA polymerase encoded by Nsp12, and the helicase encoded by Nsp13, the RNA proofreading 3'-5' exonuclease Nsp14, and

methyltransferase Nsp16 [32,50]. Nsp8 is a second RdRP whose proposed function is to generate primers required for the initiation of RNA synthesis by the main RdRP – Nsp12 [50,51]. Furthermore, Nsp14 provides a 3'-5' exonuclease activity which also has RNA proofreading function to keep the genome void of mutational defects, which is important considering the size of SARS-CoV-2 genome. The SARS-CoV-2 virus also comprises a capping mechanism: the 5' cap is involved in the translation process, protecting the genome from exonuclease, and playing a role in immune evasion [32,52,53]. There are two main proposed mechanisms for the capping of the genome, one involving a four-step sequential mechanism of the RTC involving helicase nsp13, RdRp-associated nucleotidyltransferase (NiRan) domain in Nsp12, methyltransferases Nsp14 and Nsp16, and co-factor Nsp9 [54]; another proposed mechanism is fairly simple, where the capping is facilitated by NiRan in Nsp12 and cofactor Nsp9 only [55].

1.4.3 Genome Replication and Transcription

The RNA-dependent RNA synthesis include two different processes: the genome replication and the transcription of subgenomic mRNA which encode structural and accessory proteins. The virus induces double-membrane replication organelles in which viral RNA synthesis can occur [56]. The replicase proteins generated from ORF1a and ORF1b use the genome as template to generate full-length negative sense RNA and subgenomic RNA (sgRNA). The full-length negative-sense RNA subsequently serves as template to generate additional copies of the genome to make more Nsps or to be packaged into progeny viral particles.

As for the production of sgRNA, the SARS-CoV-2 transcription process is discontinuous, a feature of viruses of the order *Nidovirales* and most coronaviruses [47,57]. The genes encoding structural and accessory proteins are expressed from the sgRNAs, which are initiated at the 3'end of the negative genome and produce a set of nested, co-terminal sgRNAs with a common 5' end leader sequence long of ~70 nucleotides [47]. The 5' end leader sequence is added following the transcription termination, which is signaled by the transcription regulatory sequence (TRS) located between the ORFs. The RdRp pauses when it reaches a TRS within the genome body (TRS-B) and changes its template to the leader TRS (TRS-L). These sgRNA act as template for the production of subgenomic mRNAs, which are produced from the negative strand sgRNA (Figure 1.4).

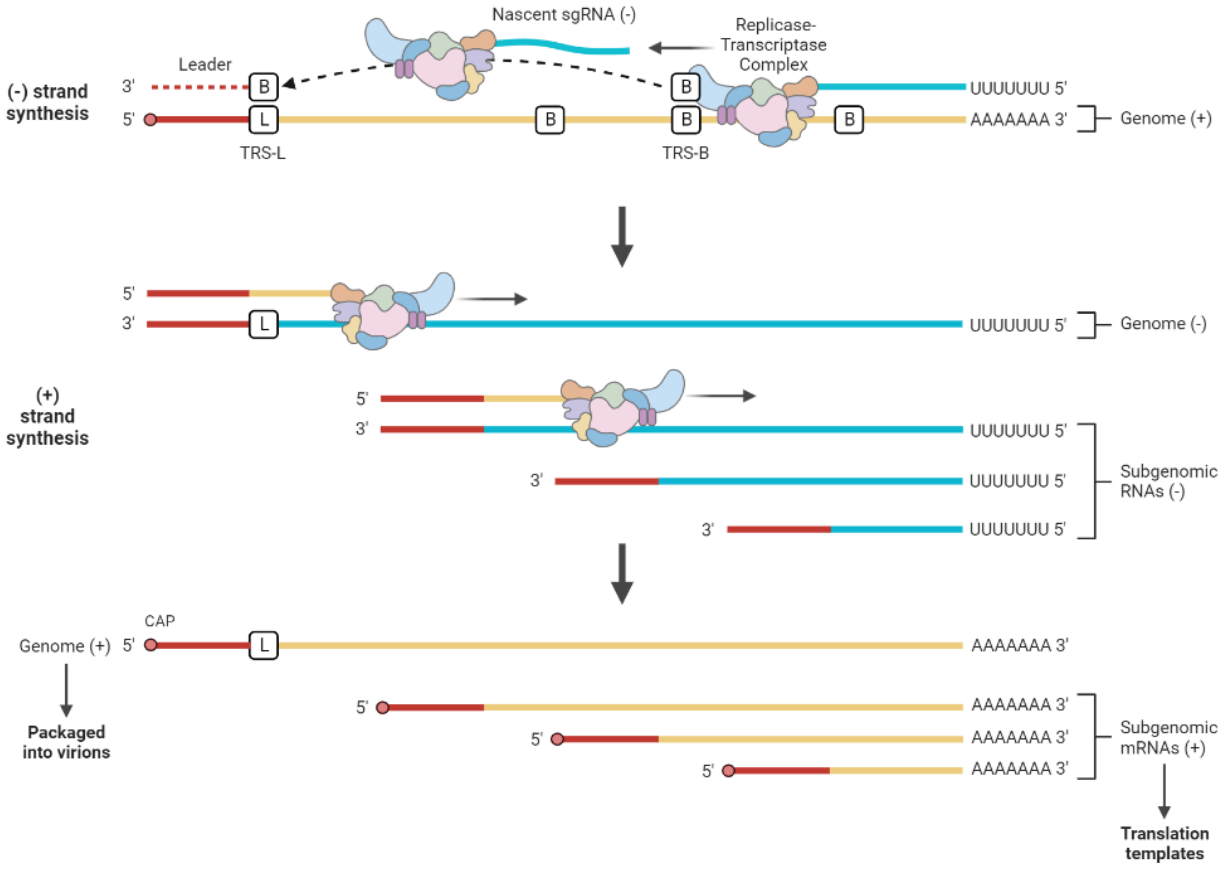

Figure 1.4 SARS-CoV-2 RNA synthesis. The positive single-stranded genomic RNA is used to produce both full-length negative strand RNA, and negative subgenomic RNA (sgRNA). Positive strand RNAs is in turquoise whereas negative strand RNAs are in yellow. To produce sgRNA, the replicase-transcriptase complex (RTC) starts off from the 3' end and pauses at a transcription regulatory sequence (TRS) between two ORFs (TRS-B), and switches to the leader TRS (TRS-L) to be capped. The negative sgRNA are then used to produce subgenomic mRNA for the translation of structural and accessory proteins. Schematic created with BioRender.com

1.4.4 Viral Assembly and Budding

The viral proteins N, E, M, and S proteins are first synthesized into the endoplasmic reticulum (ER), and shuttled towards the ER-Golgi intermediate compartment (ERGIC), where they are further processed for cleavage and/or glycosylation [58], and the misfolded proteins are retained at the Golgi. The newly assembled virions, formed by the structural proteins S, M, E, and S, bud at the membranes of the ERGIC and Golgi [59], and are released by exocytosis.

1.5 Structural proteins

1.5.1 Spike Glycoproteins

The Spike Glycoprotein is involved in the first step of viral entry, and it is highly immunogenic. The Spike is a type I membrane protein stemming from the viral membrane [60]. It has a characteristic "crown-shape" from which the name coronavirus is derived from [20,61]. It is first produced as a precursor and is then cleaved into a surface S1 and a transmembrane S2 subunit, which are linked together by non-covalent interactions. The S1 subunit is responsible for binding its receptor ACE2 whereas the S2 subunit is responsible for membrane fusion. The Spike is proteolytically cleaved at the S1/S2 junction by furin and later at the S2' junction to expose the fusion peptide and permit membrane fusion. As S1 binds the ACE2 receptor, the Spike is cleaved at the S2' junction by host proteases TMPRSS2 or cathepsin L, inducing S1 shedding and exposure of the fusion protein in the S2 subunit [42].

The Spike glycoprotein is 180-200kDa, and it is synthesized as a 1273 amino acid precursor in the rough ER (RER). The unprocessed Spike precursor contains a signal sequence, which targets it to the lumen of the ER, where it trimerizes and N-linked mannose-rich oligosaccharides side chains are added [62]. The Spike is highly glycosylated by N-linked glycans [21], which contribute to the Spike stability and evade immune detection [63,64]. The trimeric Spike glycoproteins then traffic to the Golgi complex, where the glycans are modified to more complex forms and O-linked glycosylation occurs [62,65]. Furthermore, in the trans-Golgi network, the Spike is proteolytically cleaved by cellular furin or furin-like proteases at the S1/S2 cleavage site, which is comprised of a PRRAR motif [66]. This furin-like cleavage is necessary for the cell-to-cell fusion characteristic of SARS-CoV-2 and for effective infection of lung cells and airway epithelial cells [41]. Following cleavage, the Spike accumulates near the ER-Golgi intermediate compartment (ERGIC), where it participates in viral assembly upon interaction with the M protein.

The Spike samples distinct conformations on the viral membrane [67] and its anchoring on the viral membrane is also flexible [21]. The RBD of the Spike samples the "open", or "up" conformation when it interacts with the receptor, and in the absence of ACE2 receptors, the Spike samples the "closed," or the "down" conformation. In the "closed" conformation, the RBD is packed closely against the NTD of the neighbouring protomer, and becomes more exposed in the "up" conformation. In its ground state, the Spike can spontaneously switch from RBD-down

conformation to an intermediate conformation before passing to the RBD-up conformation [67]. Due to its high antigenicity, it is a good target for humoral responses, making it a strong candidate for vaccine antigen. The protein must remain stable for the development of the vaccine, highlighting the importance of generating a stable protein trimer. The trimeric Spike used in current vaccines is stabilized by adding a disulfide bridge with a double cysteine mutant S383C (in the RBD) D985C (in the S2 subunit), which stabilizes the Spike in the down conformation [68].

The cytoplasmic tail (CT) serves to mediate cell-to-cell fusion, and multiple other functions and deletion of CT has been shown to increase the S packaging into virions, due to the deletion of the ER-retention motif KxHxx situated in the last 13 amino acids [69]. Furthermore, deletion of cytoplasmic tail is associated with increased neutralization sensitivity [70] and increased infectivity [69], suggesting that it has a role in stabilizing the Spike conformation and the exposure of the RBD [20].

The Spike can be found on the surface of infected cells, where it has been observed to cause fusion of the infected cell with the neighbouring cells, forming large multinucleated cells also known as syncytia [71,72].

Due to the immune pressure against the Spike caused by vaccination and sustained transmission within the population, there has been numerous variants which have emerged since the original strain (Wuhan-Hu-1) has been described [31]. The Spike variants will be described in its own section below.

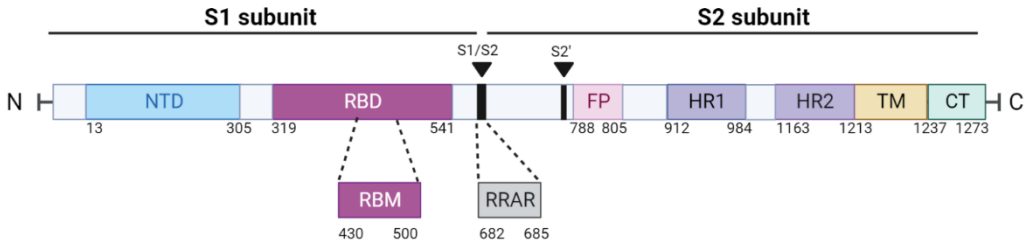

Figure 1.5 SARS-CoV-2 Spike Sequence. The Spike is comprised of an S1 subunit containing the N-terminal domain (NTD, residues 13-305), receptor binding domain (RBD, residue 319-541) within which the receptor binding motif (RBM 430-500) interacts with the human angiotensin-enzyme 2 receptor (ACE2). The S1 and S2 subunits are separated at the S1/S2 cleavage site, which presents a RRAR motif (residues 682-685). The S2 subunit harbors the fusion peptide (FP; residues 788-805), the heptad repeat 1 (HR1, 912-984) and heptad repeat 2 (HR2, 1163-1213), the transmembrane domain (TM; 1213-1237), and cytoplasmic tail (1237-1273). Schematic created with BioRender.com

1.5.2 S1 subunit

The S1 subunit of the Spike (14-684 residues) is composed of a N-terminal domain (NTD; 14-305 residues), RBD (319-541 residues) (Figure 1.5). The receptor binding motif (RBM) that is directly in contact with the receptor ACE2 is located in the RBD, from residues 437 to 507 [20,34,42].

The NTD serves as a glycan shield [73] and harbors a neutralization supersite [74] which is vastly targeted by the antibody response [75-77]. Indeed, antibodies (Abs) targeting the NTD can achieve 95-100% neutralization [74] and provide potent Fc-effector functions which have protective effects against SARS-CoV-2 in vivo [76,77].

The RBD contains two subdomains, a five-stranded antiparallel beta sheet connected the RBM, and the RBM itself [78]. The RBD is one of the most immunogenic domains of the Spike glycoprotein. The immune pressure mounted against RBD causes it to undergo several mutations, which gave rise to the multiple variants which show both immune escape and increased ACE2 binding abilities.

The CTD1 and CTD2 situated between the S1 and the S2 subunit are involved in the fusion machinery and participates in the structural rearrangements of the S glycoprotein. It touches the NTD and the S2. It is also involved in stabilizing Spike protein in the down conformation [79].

1.5.3 S2 subunit

The S2 subunit (686-1273 residues) is composed of a fusion peptide (FP; 786-806 residues), heptad repeat region 1 and 2 (HR1; 912-984 residues and HR2; 1163-1213 residues), a transmembrane domain (TM; 1213-1237 residues), and a cytoplasmic domain (1237-1273 residues) [80]. The S2 is the most conserved regions amongst variants and other *betacoronavirus* [20], as such, Abs targeting the S2 are broadly neutralizing [77,81].

In the prefusion conformation, three S2 are tightly packed around a central 3-stranded coiled-coil central helix (CH). The FP is occluded by two neighbouring Spike protomers, and upon ACE2 binding, it is projected onto the cell membrane. The HR1 and HR2 undergo large conformational rearrangements to form the six-helical bundle to bring the viral and target membrane close to each other, leading to membrane fusion [78].

1.5.4 Membrane Protein

The M protein is a 222 aa-long, dimeric, non-glycosylated protein [82]. It is the most abundant viral structural protein, and it is responsible for interacting with other structural proteins for viral assembly and for recruiting the viral genome into the virion [83]. It is highly conserved [84], and has several functions throughout the infection process: in the early stages of viral infection, M protein agglomerated in the host cell nucleus prevents the transcription and translation of host antiviral immune response to allow viral replication, transcription, and translation [85]. In the late stage of infection, M protein interacts with the other structural proteins to promote virion assembly by recruiting and interacting with S, E, and N proteins in the ERGIC [86].

1.5.5 Envelope Protein

The E protein of SARS-CoV-2 is a small (77aa) transmembrane protein. E proteins are highly conserved across betacoronaviruses [87]. One of their proposed functions is to form a cation-selective channel across the ERGIC, which is necessary for SARS-CoV-2 infection [88]. During viral replication, the E protein is expressed in the infected cell, but is not abundantly incorporated into the virion envelope. Instead, it remains at the site of viral assembly, in the ERGIC membranes [22] and participates in the assembly, budding, and trafficking of the newly-made virions [89]. Furthermore, E proteins play a role in eliciting robust host inflammatory response and induces cell death in vivo [90].

1.5.6 Nucleocapsid

The N protein (419aa) interacts with the M protein to assemble the genome by directly binding to the viral RNA and providing genome stability [91]. It is very conserved between coronaviruses, sharing 90% homology with the SARS-CoV N protein [91]. It is recruited by the Nsp3 to interact with the RTC, which is crucial for viral replication and RNA synthesis [92], multimerizes and exerts its key role of encapsidating the RNA genome [93]. Antibodies against N protein are a marker of acute infection [94] and the presence of N protein in the blood is one of the predictors of severe disease [95,96]. Serum antigen against N protein is used as diagnosis for SARS-CoV-2 infection [97].

1.6 Accessory Proteins

SARS-CoV-2 encodes for eleven accessory proteins [25]. Newly arising variants harbor mutations in a number of them, such as ORF3a, ORF6, ORF7a, ORF8, and ORF10 [98], which are suggested to be involved in the pathogenesis and transmissibility of these SARS-CoV-2 strains [26].

1.6.1 ORF3a

ORF3a is the largest accessory proteins of SARS-CoV-2, being 274 aa in length [99]. It is orthologous to the SARS-CoV ORF3a protein and shares 79% protein identity with SARS-CoV and 50% with MERS-CoV [100]. It has multiple domains, which serve multiple functions: it is involved in forming a viroporins of K+ ion channel that is essential for replication together with the E protein [99]. ORF3a is also involved in virulence, infectivity, and viral release [99,100].

1.6.2 ORF6

ORF6 is a 61aa residues protein that has been shown to be an antagonist of host cell interferon production. The orthologous ORF6 protein from SARS-CoV has been shown to inhibiting the induction of interferon pathways by blocking the nuclear import of STAT1 by interacting with nuclear import factors [101], and it has been suggested that SARS-CoV-2 ORF6 acts in a similar way to block the nuclear import and export of host mRNA from the nucleus [102]. Furthermore, it antagonizes interferon production by inhibiting the expression of the interferon promoter [103].

1.6.3 ORF7a

ORF7a is a 121aa-long accessory protein which prevents antigen presentation by downregulating major histocompatibility complex class I (MHC-I) on the surface of infected cells [104]. It does so by disrupting the peptide-loading system of MHC-1, inducing the latter to be retained in the ER [104]. ORF7 has also been suggested to also antagonizes the IFN-I response by hijacking the host ubiquitin system and by targeting the IFN to ubiquitination [105]. Other studies also show that it prevents the phosphorylation of STAT1 and/or STAT2, leading to the downstream inhibition of IFN-I response [29].

1.6.4 ORF8

ORF8 is a 121aa-long, the most variable accessory protein among coronaviruses [106]. Deletion of ORF8 has been linked to a less severe disease progression [107]. In fact, ORF8 has been shown

to interact with monocytes and NK cells and decrease their ability to perform Fc-effector functions by downregulating Fcγ receptor III (CD16) on the effector cells' surface [108]. ORF8 also contributes to pathogenesis by activating the IL-17 signaling and eliciting cytokine storm [109]. Furthermore, ORF8 is highly immunogenic, and can be secreted from infected cells. When detected from the plasma of individuals with an acute SARS-COV-2 infection, ORF8 is associated with decreased survival [110]. Due to its secretory nature, ORF8 may be used as a diagnostic tool as it elicits strong antibody response during infection [111].

1.6.5 ORF10

ORF10 is comprised of 38aa and has been described to supress the antiviral innate immune response by inhibiting the expression of type I interferon (IFN-I) genes and IFN-stimulated genes by targeting the mitochondrial antiviral signaling protein (MAVS) [112].

1.7 Variants

Due to the increased immune pressure mounted by mass vaccination and by sustained transmission, the circulating strains have undergone an antigenic drift. Since the start of the pandemic, massive, unprecedented effort has been put to the surveillance of the evolution of the genome of the virus. Next generation sequencing (NGS) – based technologies have been used to analyze samples obtained for clinical diagnostic purposes with high viral loads and wastewater, which allowed the sequencing and genome reconstruction [113]. The online database GISAID has been used for harboring SARS-CoV-2 sequences to facilitate the discovery and surveillance of newly arising variants [114]. Multiple systems of nomenclatures have been proposed to identify unique SARS-CoV-2 lineages (NextStrain [115], GISAID [114], Pango lineages [116]). Since lineages of arising variants can be named solely using their Spike sequences [116], and the Spike glycoprotein is the focus of this thesis, we will refer to different variants with regard to their Spikes using the Pango lineage nomenclature and their respective WHO labels [117].

The first variant to take over the Wuhan-Hu-1 strain is a single mutation from an aspartic acid (D) to a glycine (G) on the 614th position of the Spike (i.e. the D614G mutation) [118]. The D614G variant came into prevalence during March 2020 in Europe [119]. This mutation has been described to have higher viral loads [118,119], increased infectivity, and Spike trimer stability

[120,121]. The D614G mutation is present in variants which emerged at a later date throughout the world (Figure 1.6). Notably, the WHO created a system which separates these variants into VOC and VOI depending on their transmissibility, epidemiology, virulence, and sensitivity to diagnostic tools, vaccines and therapeutics [117]. In this section we will highlight the main VOC which circulated worldwide and mutations which contributed to their increased spread

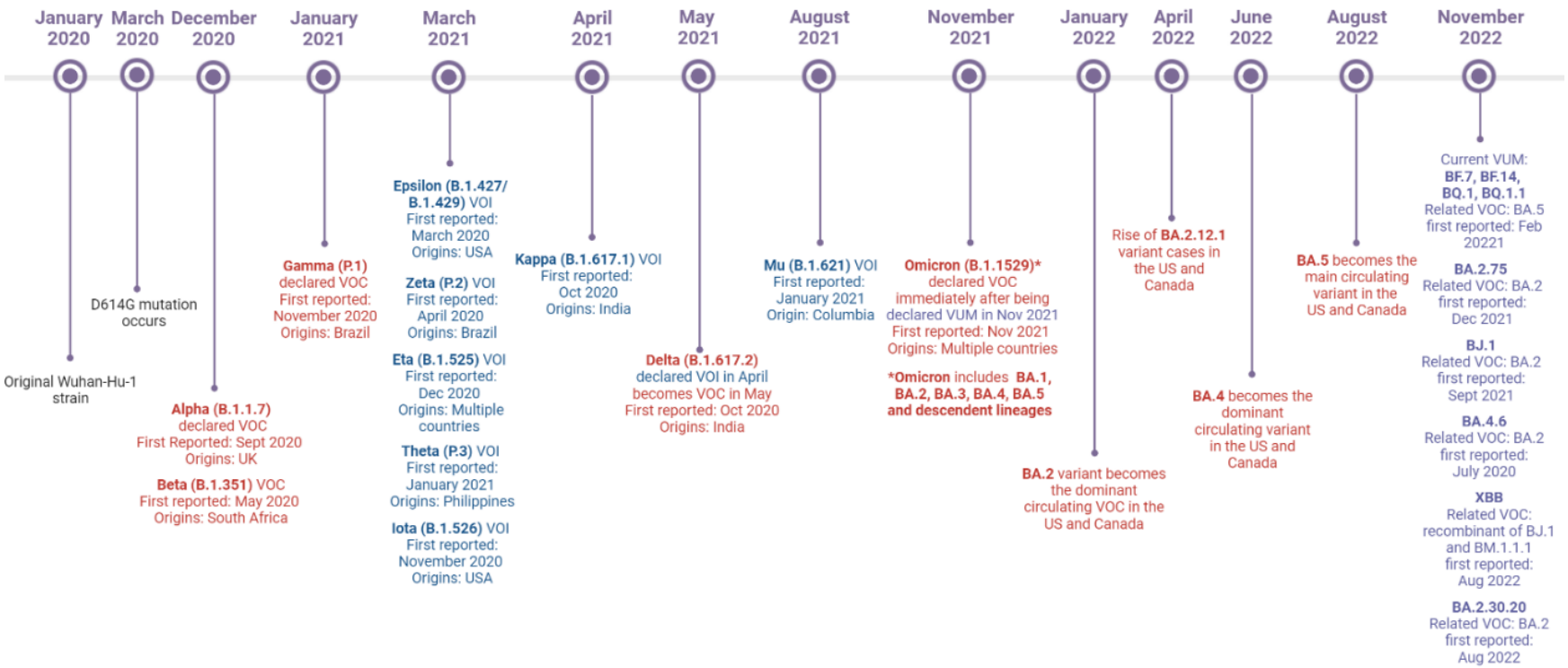

Figure 1.6: Timeline of Emerging Variants of Concern (VOC), Variants of Interest (VOI), and Variants Under Surveillance (VUS). Following the original Wuhan-Hu-1 strain, D614G, VOCs Alpha (B.1.1.7), Beta (B.1.351), and Gamma (P.1) arose from the United Kingdom, South Africa, and Brazil respectively from December 2020 to January 2021. Then, Delta (B.1.617) emerged in India towards mid 2021. Following this, Omicron subvariants (BA.1, BA.2, BA.2.12.1, BA.4, BA.4.6, BA.5) became the dominant circulating VOCs starting November 2021. Original strains Wuhan-Hu-1 and D614G are in black, VOC in red, VOI in blue, VUS in purple. Data incorporated from WHO [117], CDC [122], and Government of Canada [123]. Schematic made with BioRender.com

1.7.1 B.1.1.7 (Alpha)

The Alpha variant was first reported in UK in December 2020 [124]. Some notable mutations from this variant comprise of the deletion Δ144 in the NTD, which has immune evasion functions [76], the N501Y mutation in the RBD which shows increased ACE2 receptor binding [125,126]. Thanks to its N501Y mutation, B.1.1.7 variant has also been found to be able to bypass the temperature constraint to bind ACE2 with increased affinity [127]. The P681H mutation near the S1/S2 cleavage site increases cell surface entry by promoting cells surface route of entry, therefore confers resistance to IFN-β [128,129] and host restriction factor IFITM2, which reside in the endosomal compartments [121].

1.7.2 B.1.351 (Beta) and P.1 (Gamma)

The Beta (B.1.351) variant was first detected in South Africa in December 2020 [130], and the Gamma (P.1) variant was retraced to Brazil from a case in Japan [131]. The N501Y mutation which increases ACE2 affinity is also present in these variants [130]. Some other notable Spike mutations with the Beta variant are the K417N/T and E484K mutations, which contribute to escaping host immune response [132-134].

1.7.3 B.1.617.2 (Delta)

The Delta (B.1.617.2) variant was first described in India in late 202, and became the main circulating variant by mid-2021 [117]. It descends from the "Double mutant" B.1.617, which contained only two mutations in the Spike– the E484Q and L452R mutations [135]. The latter was first found in Epsilon (B.1.429) and was associated with increased transmission, infectivity, and neutralization [136]. This mutation has also been shown to enhance ACE2 affinity and immune escape [137,138]. Additionally, the P681R mutation situated in the S2' increases cleavage and is hypothesized to be the main driver of outstanding transmission and pathogenesis [138]. The Delta variant was also associated with increased disease severity compared to previous variant such as Beta [139].

1.7.4 B.1.1.529 (Omicron)

Omicron (B.1.1.529) variant was first reported in South Africa in November 2021 [140]. The Omicron variant contain the highest number of mutations seen in variants so far, with over 30 mutations in the Spike [141]. Omicron regroups many subvariants: BA.1, BA.1.1, BA.2,

BA.2.12.1, BA.3, BA.4, BA.4.6, BA.5, all of which have been the main circulating VOC in Canada and the US since November 2021 [122]. Compared to previous VOCs, Omicron infections cause significantly less disease severity, but were associated with higher instances of breakthrough infections [142]. Indeed, due to its numerous Spike mutations, Omicron has shown resistance to vaccine and infection-elicited antibodies [143,144], requiring the need of a booster dose in order to re-establish protection from severe disease [145,146]. Furthermore, I generated data showing that Omicron interacts better with ACE2 at lower temperatures, suggesting that Omicron Spikes have a better propensity to sample the "Up" conformation in colder conditions [147].

Table 1. List of single mutations in all VOCs.

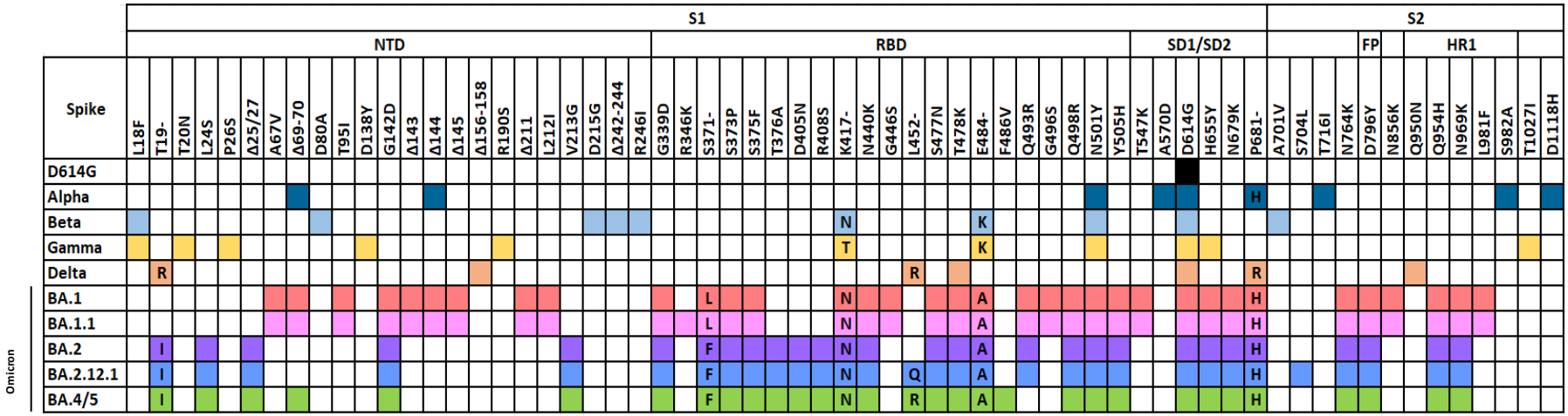

All point mutations and deletions present in circulating and past VOCs compared to D614G strain. BA.4 and BA.5 share the same Spike mutations, therefore named BA.4/5. The Spike is divided in S1 and S2 subunit. NTD: N-terminal domain; RBD: receptor binding domain; SD1/SD2: subdomain 1 and 2; FP: fusion peptide; HR1: heptad repeat region 1. Each color represents a different variant. In the case of an overlapping non-identical mutation between multiple variants, the resulting amino acid is indicated in the square. Table adapted from [147].

1.8 Pathology

The pathogenesis of COVID-19 is thought to be two-fold, divided in the early stage, where the disease is caused by SARS-CoV-2 replication, and the late stage, where disease progression is driven by the host's dysregulated immune response which leads to tissue damage. The symptoms severity ranges from asymptomatic to critical, leading to death [148,149]. Common symptoms of COVID-19 include cough, fever, dyspnea, fatigue, headache, myalgia, diarrhea, and new loss of sense of smell and taste [148,150]. Furthermore, the symptoms might last more than four months after the infection, in which case such patients are defined as people with post-COVID conditions, or long COVID [151]. The severity risk factors include but are not limited to older age (over 65), sex, immunocompromised, chronic medical conditions (cancer, kidney disease, liver disease, lung disease, diabetes, HIV infection), obesity, pregnancy, smoking, cerebrovascular disease, etc. [152,153].

Severe disease manifestation may include septic shock, where patients produce significant amounts of proinflammatory cytokines and chemokines including tumor necrosis factor (TNF) α, interleukin 1β, IL-6, granulocyte stimulating factor, interferon gamma-induced protein 10, monocyte chemoattractant protein-1, and macrophage inflammatory proteins [154-157]. Immunological profiles correlating with severe disease and mortality include presence of viral RNA in the blood, presence of immune and tissue damage markers (inflammatory cytokines, chemokines, matrix metalloproteinases), and lower levels of Spike-specific Abs and absence of Fc-effector functions such as antibody-dependent cellular cytotoxicity (ADCC) response [157-159].

1.9 Vaccine Strategies

To date, there has been 11 COVID-19 vaccines which have been approved by the WHO, representing four different vaccine platforms: protein subunit, RNA, non-replicating viral vector, and inactivated viral particles (Table 2 [160]). Here, we will focus on mRNA vaccines because they are most widely used in Québec, Canada, where we have first recruited our cohort of vaccinated naïve and previously-infected individuals.

Table 2. List of COVID-19 vaccines granted Emergency Use Listing (EUL) by the World Health Organization (WHO)*.

Platform	Manufacturer	Vaccine	Approvals
Inactivated virus	Sinopharm	Covilo	93
	Sinovac	CoronaVac	56
	Bharat Biotech	Covaxin	14
mRNA	Pfizer/BioNTech	Comirnaty (BNT162b2)	149
	Moderna	Spikevax (mRNA-1273)	88
Viral Vector	Oxford/AstraZeneca	Vaxzevria (ChAdOx1)	149
	Serum Institute of India	Covishield (ChAdOx1)	49
	Jassen / Johnson & Johnson	Jcovden (Ad26.COV2.S)	113
	CanSino	Convidecia	10
Adjuvanted Protein	Novavax	Nuvaxovid	40
	Serum Institute of India	COVOVAX (Novaxovid)	6

*Four different platforms, with ten manufactures, and nine unique vaccine products. Approvals represent the number of countries which approved the use of each vaccine. Table adapted from [161]. Source [162].

The mRNA vaccines are most widely used in developed countries in North America and Europe due to the logistics concerning their transportation, storage requirements, business priorities, etc. These concerns hinder the distribution of vaccines to countries under development, revealing the stark global health inequalities between developing and developed countries. The mRNA vaccines are composed of lipid nanoparticles which efficiently encapsulates the genetic material encoding the prefusion-stabilized Spike protein [163].

The Pfizer/BioNTech BNT162b2 and Moderna mRNA-1273 mRNA vaccines have been shown to elicit a strong antibody response after one dose, resulting in protective efficacy of 95% [164,165]. It was shown that these Abs can mediate strong Fc-effector functions in absence or poor neutralizing responses [166]. The cellular response induced by the first two doses of mRNA vaccines are more durable than the serum antibody titers, both for the maturation of B cells in the germinal center [167,168], and in the long-lasting T cell responses [169,170]. Although the initial regimen of two doses provided a good efficacy, waning of neutralizing Ab titers 6 months after vaccination [171], combined with the circulating variant at the time Delta causing increased breakthrough infection cases, hospitalization, and death [122,172], a third boosting dose has been

suggested [145]. Indeed, the protection against Delta infection was 65% after two doses, and 91% after three doses; as for Omicron infection, vaccine effectiveness was 46% after two doses and 60% after three doses [173]. Furthermore, due to the emergence of recent Omicron variants, which has been shown to be more resistant to vaccination [174-176], a bivalent vaccine containing both the stabilized Spike of original Wuhan-Hu-1 strain and Omicron strain has been proposed to the population as an alternate fourth booster to the original vaccine [177]. The latter has been shown to have a 30% protection against infection for BNT162b2 and 11% for mRNA-1273, but are more effective in preventing symptomatic disease (43% for BNT162b2 and 31% for mRNA1273) [178]. The bivalent vaccine has been reported to be more efficacious than the original booster [177,179]. Currently, the goal of vaccination against SARS-CoV-2 by mRNA vaccines is to provide protection against severe illness, hospitalization, and death against newly-arising variants.

For previously-infected individuals, the immune response elicited by a first dose of vaccine was stronger than naïve individuals, both in the levels of neutralizing Abs [180] and in their humoral immunity [181].

In immunocompromised individuals, response to vaccination is dampened in both the antibody and T-cells front; their responsiveness is dependent on the level of immunosuppression [182-184]. Extra vaccine doses are recommended for these populations [161].

Due to the circumstances in Canada where the public health prioritized vaccinating more people for their first dose, there is a unique population who have a longer interval of 16 weeks between the first and second dose [185]. The extended interval between doses elicited stronger humoral responses than a shorter interval, which converge at the third booster dose [186]. The CD4+ T cell responses of previously infected, vaccinated individuals which are initially stronger than naïve vaccinated individuals become similar after two doses of vaccine [187].

1.10 Humoral immune responses to SARS-CoV-2 infection

Humoral immune response is central to the prevention and clearing of SARS-CoV-2 infection. The humoral response can be divided into two phases – the extrafollicular (EF) phase, and the germinal center (GC) phase. During the EF phase, B cells are rapidly activated and differentiate into plasma cells outside of the follicle a few days following infection [188], producing Abs,

predominantly immunoglobulins (Ig) of class M (IgMs) which contain very few somatic hypermutations but can still have high affinities and neutralizing potency [189]. IgMs can be IgG- or IgA-switched to counter viral infections. Several days to a week following the EF phase, the GC phase begins, during which the antigen-specific B cells undergo somatic hypermutations and affinity-based selection in the GC [190]. This process lasts for months, resulting in primarily isotype-switched and high-affinity plasma cells which establish in the bone marrow in long-lived compartments [191]. It is important to note that the both EF and GC responses produce antigen-specific memory B cells which persist long after the infection is cleared [192].

The Abs can perform multiple functions, from neutralization of the antigen with their antigen-binding fragment (Fab) to effector functions, notably ADCC, which occurs when the crystallizable fragment (Fc) of Ab cross-links the FcγIIIa (CD16a) of effector cells such as natural killer (NK) cells, monocytes, or macrophages.

1.10.1. Neutralization

In the case of an infection with SARS-CoV-2, the level of antibody response correlates with disease severity [193-196]. Cross-sectional and longitudinal studies indicate that Abs level peak 3-4 weeks post-symptom onset (PSO) [193,197-200]. Further, anti-RBD and anti-Spike IgM and IgA decay rapidly, whereas IgG remain more stable [201]. The same observation can be made for IgM+ B cells, which wane rapidly compared to IgG+ B cells [201]. Neutralizing Abs levels wane faster than that of ADCC, corroborating the neutralizing activity conferred by IgM and IgA [202,203] and their rapid decline post disease clearing [193].

1.10.2 ADCC

Fc-effector function are correlated to protection in early studies in primates [204]. Furthermore, strong ADCC responses were seen in hospitalized patients [205,206], and ADCC response were associated with recovery [207]. The ADCC response peaks between 2-4 weeks, and decline gradually thereafter [201]. For vaccinated individuals, presence of Abs with both neutralizing and effector functions correlated with protection [161]. The first dose of mRNA vaccine induces high titers of IgG and IgA, which have weak neutralizing functions, but robust ADCC effects mediated by IgG [166], which is reinforced at the second dose [185].

1.10.3 Spike is the main target of Abs with neutralizing and Fc-effector functions

The Spike is a major target of the humoral response. One immunodominant site within the Spike is the RBD, with the most potent neutralizing Abs directed against the RBM [208]. Neutralizing Abs targeting the Spike can be categorized in four types according to the conformation and epitope of the RBD which they recognize : 1- neutralizing Abs which only recognize the "RBD up" conformation and block Spike – ACE2 interactions; 2- neutralizing Abs which bind adjacent RBDs in both "up" and "down" and interfere with ACE2 binding 3- neutralizing Abs which recognize outside the RBM and recognize both "RBD up" and "down" conformations; and 4- Abs which only recognize the "RBD up" conformation but does not block Spikes – ACE2 interactions [209]. Examples of potent neutralizing Ab targeting the RBD include CV3-1 (class 1) and CR3022 (class 4), which recognizes the "up" conformation of the RBD [77,210]. The NTD is another target for neutralizing and non-neutralizing Abs. A potent non-neutralizing Ab targeting the NTD is CV3-13, which shows potent ADCC resulting in protective function in SARS-CoV-2 challenged mice [76]. Abs binding outside of NTD and RBD immunogenic region may recognize the stem-helix region of S2, which is more conserved. A broadly neutralizing Ab targeting this region is CV3-25, which inhibits viral fusion [77].

1.11 Treatment options

The initial containment of the pandemic has mostly relied on non-pharmaceutical interventions such as public hygiene measures of social distancing, the use of masks, and handwashing in order to limit the spread of the infection. Currently, there are different treatments available for COVID-attained patients depending on disease severity and need for hospitalization [211,212]. Clinical management for severe COVID-19 include primarily of monoclonal antibody therapies, but also small molecules inhibitors and immunomodulators [148,212].

1.11.1 Monoclonal Abs Therapy

Monoclonal antibodies (mAbs) are used for pre-exposure prophylaxis (PrEP) for people who do not respond adequately to vaccination and those who have contraindication for the vaccines [213,214], as well, they can be used as treatments for non-hospitalized adults who are at risk of

severe disease progression. The only current PrEP approved by the FDA is Tixagevimab 150mg plus Cilgavimab 150mg (EVUSHELD™) which is an intramuscular long-acting mAbs developed by AstraZeneca [213]. These mAbs recognize non-overlapping epitopes on the RBD, and act synergistically to potently neutralize SARS-CoV-2 [215]. They are modified in the Fc to extend their half-life and to eliminate potential risk of antibody-dependent disease enhancement [216,217]. When used as PrEP or treatment for Omicron variants, it is recommended to take double dosage for each mAbs (Tixagevimab 300mg plus Cilgavimab 300mg) [213]. Other Abs include Bebtelovimab, Casirivimab, Imdevimab, Etesevimab, Sotrovimab which target the RBD [211]. Among them, Bebtelovimab was the only Ab to retain potent neutralizing activity against Omicron BA.5 [218,219]. However, with the rapid emergence of BQ.1 and BQ.1.1, the FDA has pulled its recommendation for Bebtelovimab due to its ineffectiveness against these variants [220].

1.11.2 Small Molecule inhibitors

Main strategies for preventing SARS-COV-2 proliferation involve preventing viral entry and blocking its replication. Drug repurposing has played a crucial role in the speedy identification of candidates. An example of repurposed drug targeting the Spike is VE607 [221], which has been found to be effective at inhibiting both SARS-CoV and SARS-CoV-2 infection [222]. VE607 has been shown to stabilize the RBD in its "up" conformation, inhibiting viral binding to ACE2, thus controlling infection and protecting mice from SARS-CoV-2 challenge [222].

There are currently three FDA approved drugs, all of which target viral replication – Remdesivir, Molnupiravir, and Paxlovid [211]. Remdesivir is a nucleotide analogue RNA-dependent RNA polymerase inhibitor which was first developed for Ebola [223-225]. Molnupiravir is also a nucleoside analogue [226], whereas Paxlovid is a protease inhibitor [211,227].

1.12 Experimental methods

1.12.1 Flow Cytometry

Flow cytometry is an important biological assay used in this thesis. This technique is often used for the analysis of cell surface or intracellular biomarkers [228,229]. In a fluidic system, single cells pass in front of lasers of different wavelengths, and each cell is analyzed for their light scatter

and the different fluorescence parameters [228,229]. Each cell is characterized as an "event," and the analysis of the light scatters provides information on the size, the density, and the presence or the expression of proteins of interest targeted by fluorescently labeled Abs on these cells [228,229]. In this thesis, flow cytometry is used to assess the presence of anti-Spike Abs in the plasma of infected and vaccinated individuals [134]. As well, by using Abs which recognize different regions of the Spike, we can assess the impact which a single mutation or the ensemble of mutations can have on the immune recognition of the Spike [134,147]. Finally, flow cytometry has been used to ascertain the ACE2 recognition of the mutant Spikes, both in terms of recognition and in terms of the Spike's sensitivity to conformational changes [134,147].

1.12.2 Virus Capture Assay

In this thesis, virus capture assay was used to measure the change of viral particles' Spike – ACE2 interaction in different temperatures to corroborate with our results generated by flow cytometry [147]. Briefly, in virus capture assays, proteins of interest, in this case ACE2-Fc, is immobilized on ELISA plates, then pseudoviral particles bearing SARS-CoV-2 Spikes, Vesicular stomatitis virus G (VSV-G), and luciferase gene are applied to the plate to evaluate their interactions with the proteins in different temperatures [147]. Then, SARS-CoV-2-resistant Cf2Th cells are applied to the plate, where the VSV-G expressed in the bound viral particles will be used to infect the cells, which will express luciferase. Signal is measured by the luciferase activity following 48 hours of infection [147,230].

1.12.3 Biolayer Interferometry (BLI)

Biolayer interferometry is a method which relies on optics in order to measure the binding kinetics of two proteins [231]. The reflection of light interference across two surfaces is measured: 1) the constant internal reference surface and 2) the variable surface of the ligand interacting with its receptor [231]. In this thesis, this technique was used to measure the kinetics and affinity of interaction between RBD and ACE2 [134,147]. The biosensors are coated with RBD of different SARS-CoV-2 variants and applied to increasing concentrations of sACE2 in kinetics buffer [134,147]. Information obtained from BLI may include binding kinetics (on- and off-rates), from which the affinity could be deducted [134,147].

1.13 Thesis Rationale and Objectives

Since Spike is the main player in viral entry and is targeted by both vaccines and monoclonal antibodies treatment, it is under high immune pressure to evade detection. To do so, since its emergence, SARS-CoV-2 has gone through many iterations of variants, accumulating mutations in its Spike glycoprotein, and developing ultimately the circulating VOC at the time of writing, Omicron, which is the longest circulating variant. How the mutations help the Spike avoid recognition needs to be better determined.

Objectives:

1. To assess the effect of single mutations on host recognition in
    a. Previously infected individuals
    b. Naïve-vaccinated individuals
2. To determine how individual mutations influence the variants' ability to recognize its receptor ACE2.
3. To evaluate the effect of the accumulated mutations of VOCs on ACE2 binding with respect to temperature.

CHAPTER 2. CONTRIBUTION OF SINGLE MUTATIONS TO SELECTED SARS-COV-2 EMERGING VARIANTS SPIKE ANTIGENICITY

Shang Yu Gong, Debashree Chatterjee, Jonathan Richard, Jérémie Prévost, Alexandra Tauzin, Romain Gasser, Yuxia Bo, Dani Vézina, Guillaume Goyette, Gabrielle Gendron-Lepage, Halima Medjahed, Michel Roger, Marceline Côté, and Andrés Finzi

2.1 Preface to Chapter 2

As discussed in Chapter 1, multiple variants have emerged since the ancestral Wuhan-Hu-1 strain, starting with the D614G mutation in the Spike glycoprotein, which shows increased transmissibility and infectivity [118-120]. Most importantly, the RBD is the main target of the Abs [190], as well the main player in interacting with the ACE2 receptor [210]. The virus is under high immune pressure to evade the Ab response, as well as increase ACE2 affinity [232]. Whether this immune escape and ACE2 interaction are the additive result of each single mutation, or whether it is conferred by the combination of mutations is unclear. Therefore, it is important to assess the impact which each mutation has on a given VOC. In this chapter, we dissect the contribution of each single mutation to the ACE2 binding and immune evasion of Abs elicited in infected or vaccinated individuals following one dose of vaccination.

2.2. Abstract

Towards the end of 2020, multiple variants of concern (VOCs) and variants of interest (VOIs) have arisen from the original SARS-CoV-2 Wuhan-Hu-1 strain. Mutations in the Spike protein are highly scrutinized for their impact on transmissibility, pathogenesis and vaccine efficacy. Here, we contribute to the growing body of literature on emerging variants by evaluating the impact of single mutations on the overall antigenicity of selected variants and their binding to the ACE2 receptor. We observe a differential contribution of single mutants to the global variants phenotype related to ACE2 interaction and antigenicity. Using biolayer interferometry, we observe that enhanced ACE2 interaction is mostly modulated by a decrease in off-rate. Finally, we made the interesting observation that the Spikes from tested emerging variants bind better to ACE2 at 37°C compared to the D614G variant. Whether improved ACE2 binding at higher temperature facilitates emerging variants transmission remain to be demonstrated.

2.3 Introduction

Severe Acute Respiratory Syndrome Coronavirus 2 (SARS-CoV-2), the causative agent of COVID-19, remains a major public health concern, infecting over 185 million individuals and causing over 4 million deaths worldwide [1]. The replication cycle of SARS-CoV-2 starts with viral attachment to the target cell and fusion between viral and cellular membranes. The viral entry process is mediated by the mature Spike (S) glycoprotein trimer which is composed of exterior S1 and transmembrane S2 subunits. The S1 subunit mediates attachment using its receptor-binding domain (RBD) to interact with the host protein angiotensin converting enzyme 2 (ACE2) [2-4], while the S2 subunit governs the fusion between the viral and cellular membranes [5,6].The Spike is a major target of the cellular and humoral responses elicited by natural infection. Accordingly, the antigen used in currently approved vaccines is the stabilized form of the SARS-CoV-2 S glycoprotein. These vaccines use adenoviral vectors [7,8] or mRNA vaccine platforms to express S glycoprotein [9,10]. The S glycoprotein was selected due to its high immunogenicity and safety profiles after extensive research [11-14].

Although the approval of several vaccine platforms has given us hope to end the pandemic, the asymmetric distribution of doses between rich and poor countries and the rapid emergence of SARS-CoV-2 variants is preoccupying. The Spike is under high selective pressure to evade host immune response, improve ACE2 affinity, escape antibody recognition and achieve high transmissibility [15]. The first identified D614G mutation in the Spike glycoprotein became dominant among the rapidly spreading emerging variants [16,17]. In late 2020, several other variants emerged throughout the world, including the variants of concern (VOCs) B.1.1.7 (Alpha), B.1.351 (Beta), P.1 (Gamma) and B.1.617.2 (Delta), as well as the variants of interest (VOIs) B.1.429 (Epsilon), B.1.526 (Iota), B.1.617.1 (Kappa) and B.1.617 [18-24]. Critical mutations providing a fitness increase became rapidly selected in most emerging variants. For example, the N501Y substitution that was first observed in the B.1.1.7 lineage and provides enhanced ACE2 binding [25-27], is now present in B.1.351, P.1, and P.3 lineages. Similarly, the E484K and K417N/T mutations in the RBD that were first described in the B.1.351 and P.1 lineages likely due to immune evasion from vaccine or natural infection-elicited antibodies [28,29], are now present in several other lineages [30]. Hence, it is important to closely monitor not only the emerging variants but also single mutations to better understand their contribution to replicative fitness and/or ability to evade natural or vaccine-induced immunity.

Here, by performing detailed binding and neutralization experiments with plasma from naturally infected and vaccinated individuals, we provide a comprehensive analysis of the antigenicity of the Spike from selected VOCs (B.1.1.7, B.1.351, P.1 and B.1.617.2) and VOIs (B.1.429, B.1.526, B.1.617, B.1.617.1).

2.4 Materials and Methods

Ethics Statement

All work was conducted in accordance with the Declaration of Helsinki in terms of informed consent and approval by an appropriate institutional board. Blood samples were obtained from donors who consented to participate in this research project at CHUM (19.381). Plasmas were isolated by centrifugation.

Plasmas and antibodies

Plasmas of SARS-CoV-2 naïve-vaccinated and previously infected pre- and post-first dose vaccination donors were collected, heat-inactivated for 1 hour at 56°C and stored at -80°C until use in subsequent experiments. Plasma from uninfected donors collected before the pandemic were used as negative controls in our flow cytometry and neutralization assays (not shown). The S2-specific monoclonal antibody CV3-25 [27,31] was used as a positive control and to normalize Spike expression in our flow cytometry assays. CV3-25 was extensively described [32-35]. ACE2 binding was measured using the recombinant ACE2-Fc protein, which is composed of two ACE2 ectodomains linked to the Fc portion of the human IgG [36]. Alexa Fluor-647-conjugated goat anti-human Abs (Invitrogen) were used as secondary antibodies to detect ACE2-Fc and plasma binding in flow cytometry experiments.

Cell lines

293T human embryonic kidney cells (obtained from ATCC) were maintained at 37°C under 5% CO2 in Dulbecco's modified Eagle's medium (DMEM) (Wisent) containing 5% fetal bovine serum (VWR) and 100 µg/ml of penicillin-streptomycin (Wisent). The 293T-ACE2 cell line was previously described [37] and was maintained in medium supplemented with 2 µg/mL of puromycin (Millipore Sigma).

Plasmids

The plasmid encoding B.1.1.7, B.1.351, P.1, and B.1.526 Spikes were codon-optimized and synthesized by Genscript. Plasmids encoding B.1.617, B.1.617.1, B.1.617.2 Spikes were generated by overlapping PCR using a codon-optimized wild-type SARS-CoV-2 Spike gene (GeneArt, ThermoFisher) that was synthesized (Biobasic) and cloned in pCAGGS as a template. Plasmids encoding B.1.429, D614G, other SARS-CoV-2 Spike single mutations were generated using the QuickChange II XL site-directed mutagenesis protocol (Stratagene) and the pCG1-SARS-CoV-2-S plasmid kindly provided by Stefan Pöhlmann. The plasmid encoding for the recombinant RBD (residues 319-541) fused with a hexa-histidine tag was previously reported [38]. The presence of the desired mutations was determined by automated DNA sequencing.

Protein expression and purification

FreeStyle 293F cells (Invitrogen) were grown in FreeStyle 293F medium (Invitrogen) to a density of 1 x 106 cells/mL at 37°C with 8 % CO2 with regular agitation (150 rpm). Cells were transfected with a plasmid coding for SARS-CoV-2 S RBD using ExpiFectamine 293 transfection reagent, as directed by the manufacturer (Invitrogen). One week later, cells were pelleted and discarded. Supernatants were filtered using a 0.22 µm filter (Thermo Fisher Scientific). The recombinant RBD proteins were purified by nickel affinity columns, as directed by the manufacturer (Invitrogen). The RBD preparations were dialyzed against phosphate-buffered saline (PBS) and stored in aliquots at -80°C until further use. To assess purity, recombinant proteins were loaded on SDS-PAGE gels and stained with Coomassie Blue.

Virus neutralization assay

293T cells were transfected with the lentiviral vector pNL4.3 R-E- Luc (NIH AIDS Reagent Program) and a plasmid encoding for the indicated Spike glycoprotein (D614G, B.1.1.7, P.1, B.1.351, B.1.429, B.1.526, B.1.617, B.1.617.1, B.1.617.2) at a ratio of 10:1. Two days post-transfection, cell supernatants were harvested and stored at -80°C until use. 293T-ACE2 target cells were seeded at a density of 1×104 cells/well in 96-well luminometer-compatible tissue culture plates (Perkin Elmer) 24h before infection. Pseudoviral particles were incubated with the indicated plasma dilutions (1/50; 1/250; 1/1250; 1/6250; 1/31250) for 1h at 37°C and were then added to the

target cells followed by incubation for 48h at 37°C. Then, cells were lysed by the addition of 30 µL of passive lysis buffer (Promega) followed by one freeze-thaw cycle. An LB942 TriStar luminometer (Berthold Technologies) was used to measure the luciferase activity of each well after the addition of 100 µL of luciferin buffer (15mM MgSO4, 15mM KPO4 [pH 7.8], 1mM ATP, and 1mM dithiothreitol) and 50 µL of 1mM d-luciferin potassium salt (Prolume). The neutralization half-maximal inhibitory dilution (ID50) represents the plasma dilution to inhibit 50% of the infection of 293T-ACE2 cells by SARS-CoV-2 pseudoviruses.

Cell surface staining and flow cytometry analysis

293T were transfected with full length SARS-CoV-2 Spikes and a green fluorescent protein (GFP) expressor (pIRES2-eGFP; Clontech) using the calcium-phosphate method. Two days post-transfection, 293T-Spike cells were stained with the CV3-25 Ab, ACE2-Fc or plasma from SARS-CoV-2-naïve or recovered donors. Briefly, 5 µg/mL CV3-25 or 20 µg/mL ACE2-Fc were incubated with cells at 37ºC or 4 ºC for 45 min. Plasma from SARS-CoV-2 naïve or convalescent donors were incubated with cells at 37ºC. The percentage of Spike-expressing cells (GFP+ cells) was determined by gating the living cell population based on viability dye staining (Aqua Vivid, Invitrogen). Samples were acquired on a LSRII cytometer (BD Biosciences), and data analysis was performed using FlowJo v10.7.1 (Tree Star). The conformational-independent, S2-targeting mAb CV3-25 [27] was used to normalize Spike expression. CV3-25 was shown to be effective against all Spike variants [35]. The Median Fluorescence intensities (MFI) obtained with ACE2-Fc or plasma Abs were normalized to the MFI obtained with CV3-25 and presented as ratio of the CV3-25-normalized values obtained with the D614G Spike. .

Biolayer Interferometry

Binding kinetics were performed on an Octet RED96e system (FortéBio) at 25°C with shaking at 1,000 RPM. Amine Reactive Second-Generation (AR2G) biosensors were hydrated in water, then activated for 300 s with an S-NHS/EDC solution (Fortébio) prior to amine coupling. SARS-CoV-2 RBD proteins were loaded into AR2G biosensor at 12.5 µg/mL in 10mM acetate solution pH5 (Fortébio) for 600 s and then quenched into 1M ethanolamine solution pH8.5 (Fortébio) for 300 s. Baseline equilibration was collected for 120 s in 10X kinetics buffer. Association of sACE2 (in 10X kinetics buffer) to the different RBD proteins was carried out for 180 s at various

concentrations in a two-fold dilution series from 500nM to 31.25nM prior to dissociation for 300s. The data were baseline subtracted prior to fitting performed using a 1:1 binding model and the FortéBio data analysis software. Calculation of on-rates (K_a), off-rates (K_{dis}), and affinity constants (K_D) was computed using a global fit applied to all data.

2.5 Results

ACE2 recognition by SARS-CoV-2 single mutants and full Spike variants

Since the SARS-CoV-2 Spike is under strong selective pressure and is responsible for interacting with the ACE2 receptor, we measured the ability of the Spike from emerging variants to interact with ACE2 and the contribution of each single mutations toward this binding. Plasmids expressing the SARS-CoV-2 full Spike harboring single or combined mutations from emerging variants were transfected into HEK 293T cells. Spike expression was normalized with the conformational-independent, S2-specific CV3-25 monoclonal antibody (mAb) [34,35]. ACE2 binding was measured using the recombinant ACE2-Fc protein, which is composed of two ACE2 ectodomains linked to the Fc portion of the human IgG [36]. Alexa Fluor 647-conjugated secondary Ab was then used to detect ACE2-Fc binding to cell-surface Spike by flow cytometry. At the time of writing, B.1.617, B.1.617.1 and B.1.617.2 came into importance and only the full Spikes from these variants were synthesized, not the single mutations. When compared to the D614G Spike, all tested Spike variants, with the exception of B.1.617.1, presented significantly higher ACE2 binding (Fig 2.1A).

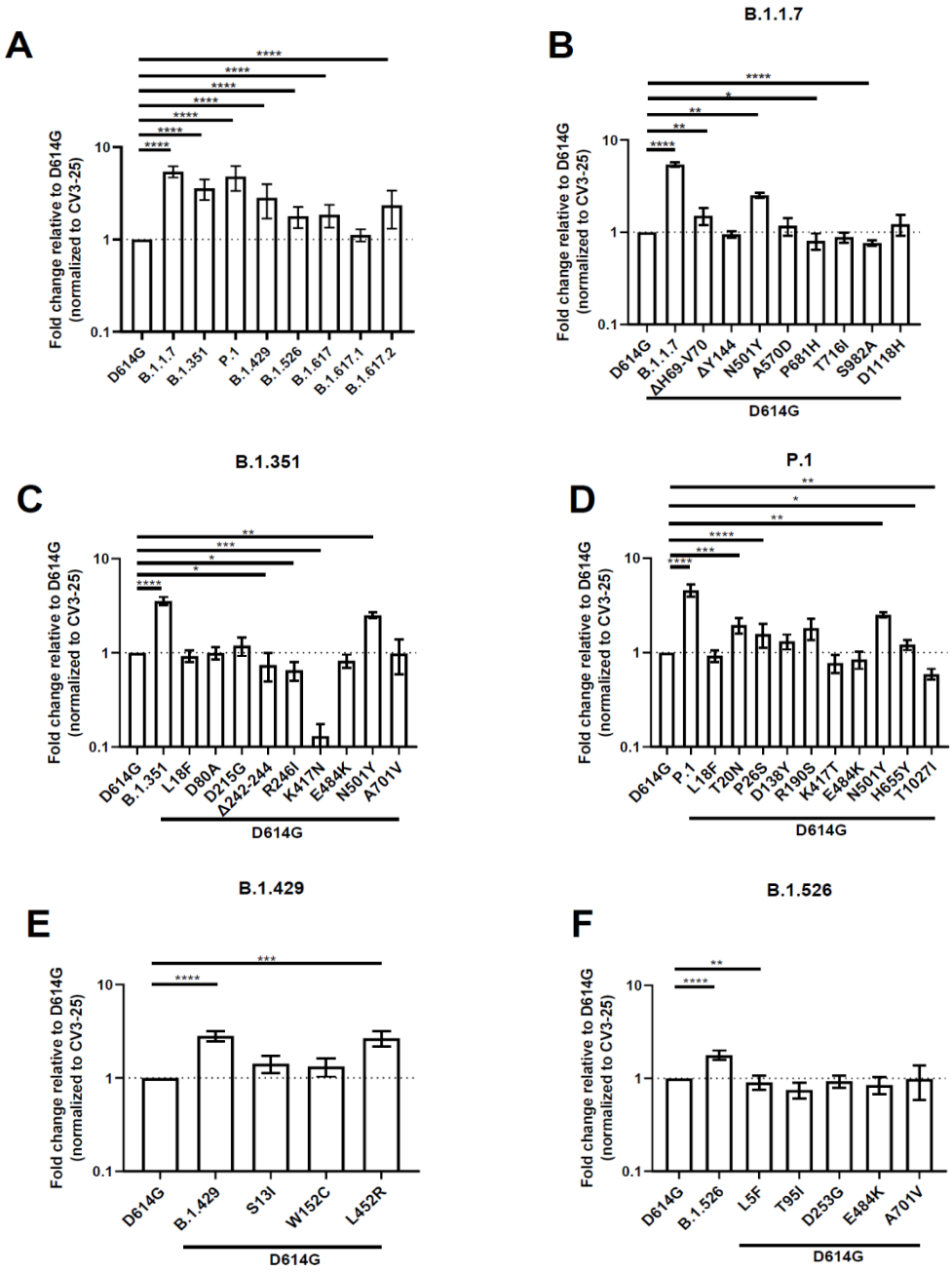

Figure 2.1 Evaluation hACE2 Fc binding to SARS-CoV-2 Spike variants

HEK 293T cells were transfected to express the indicated SARS-CoV-2 Spike variants. Two days post transfection, cells were stained with ACE2-Fc or with CV3-25 Ab as Spike expression control and analyzed by flow cytometry. ACE2-Fc binding to (A) full Spikes variants or the (B) B.1.1.7, (C) B.1.351, (D) P.1, (E) B.1.429, and (F) B.1.526 Spike and its corresponding single mutations are presented as a ratio of ACE2 binding to D614G Spike normalized to CV3-25 binding. Error bars indicate means ± SEM. Statistical significance has been performed using Mann-Whitney U test according to normality analysis (*p < 0.05; **p < 0.01; ***p < 0.001; ****p < 0.0001).

We then determined the contribution of individual Spike mutations on ACE2 binding to discern the ones contributing to the heightened receptor affinity of emerging variants. The B.1.1.7 Spike presented the highest ACE2-Fc interaction amongst all tested Spikes, which is a 5.43-fold increase in ACE2-Fc binding compared to D614G (Fig 2.1A-B). The mutations that likely contribute to this phenotype are ΔH69-V70 in the N terminal domain (NTD) and N501Y in the RBD that enhanced binding by ~1.51 and ~2.52 folds, respectively (Fig 2.1B).

The Spike from B.1.351 also presented significantly higher ACE2-Fc binding compared to D614G. Similarly to B.1.1.7, the N501Y mutation likely plays an important role in this phenotype (Fig. 2.1C). Interestingly, three mutations/deletion in this VOC decreased the interaction with ACE2-Fc, namely R246I and Δ242-244 in the NTD, as well as K417N in the RBD. The NTD substitution R246I decreased ACE2-Fc binding by ~1.52 folds, the Δ242-244 deletion by ~1.35 folds, whereas K417N had a greater impact with a decreased binding of ~7.7 folds relative to D614G (Fig 2.1C). Of note, the E484K mutation, also found in the RBD of other emerging variants (P.1 and B.1.526) did not significantly impact the ACE2-Fc interaction.

The Spike from P.1 presented a ~4.24-fold increase in binding compared to D614G (Fig 2.1D). Few NTD mutations, namely T20N, P26S, D138Y, and R190S, likely contributed to the increase in ACE2 binding, with ~2, ~1.6, ~1.3 and ~1.8-fold increase compared to D614G, respectively. Like the above-mentioned VOCs, N501Y also likely played a role in enhanced ACE2-Fc interaction. Interestingly, the RBD mutation K417T and the S2 mutation T1027I decreased the ACE2-Fc by ~1.3 and ~1.7 folds respectively. The H655Y mutation, near the S1/S2 cleavage site, also slightly increased ACE2 interaction by ~1.2 folds (Fig 2.1D).

The Spike from B.1.429 augmented ACE2-Fc interaction by ~2.8 folds (Fig 2.1E). This VOI has two NTD mutations, S13I and W152C, both of which did not significantly impact this interaction. On the other hand, its RBD mutation, L452R, increased ACE2-Fc binding by ~2.7 fold, suggesting its major contribution to the phenotype of this variant (Fig 2.1E).

Lastly, the Spike from B.1.526 showed a ~1.8-fold increase over D614G (Fig 2.1F). None of the mutation appears to explain the phenotype observed with the full variant.

While our results identified some key mutations enhancing ACE2 interaction (i.e., N501Y, L452R and mutation/deletion in the NTD), the overall increased ACE2 affinity from any given variant

appears to result from more than the sum of the effect of individual mutations composing this variant.

Impact of selected mutations on the affinity of Spike RBD for ACE2

Next, we used biolayer interferometry (BLI) to measure the binding kinetics of selected RBD mutants to soluble ACE2 (sACE2). Biosensors were coated with recombinant RBD and put in contact with increasing concentration of sACE2 (Fig 2.2). In agreement with previous reports [25,27], the N501Y mutation present in B.1.1.7, B.1.351, and P.1 significantly decreased the off-rate (Kdis) (from 6.88×10-3 to 1.49×10-3 1/s), presenting a 3.88-fold increase in K_D compared to its wild-type counterpart (Fig 2.2A-B). Substitution at position K417 (either N or T) present in B.1.351 or P.1 lineages accelerated the off-rate kinetics, resulting in a 0.75- and 0.66-fold decrease in binding affinity (Fig 2.2C-D). Although both K417N and K417T presented a modest increase in the on-rate kinetic by ~1.56 and ~ 1.11 folds, the accelerated off-rate kinetics dictated the overall decrease affinity of these mutants. No major changes were observed for the E484K mutation (Fig 2.2F). Interestingly, the L452R mutant did not have a major impact in ACE2 affinity when tested in the context of recombinant monomeric RBD (Fig 2.2G) but presented enhanced binding within the context of full-length membrane anchored Spike (Fig 2.1E), indicating that the overall phenotype of a mutant (in this case enhanced binding) cannot always be recapitulated with the RBD alone. Altogether, our results show that at least for the RBD mutants tested here, ACE2 affinity is mostly dictated by the dissociation kinetics.

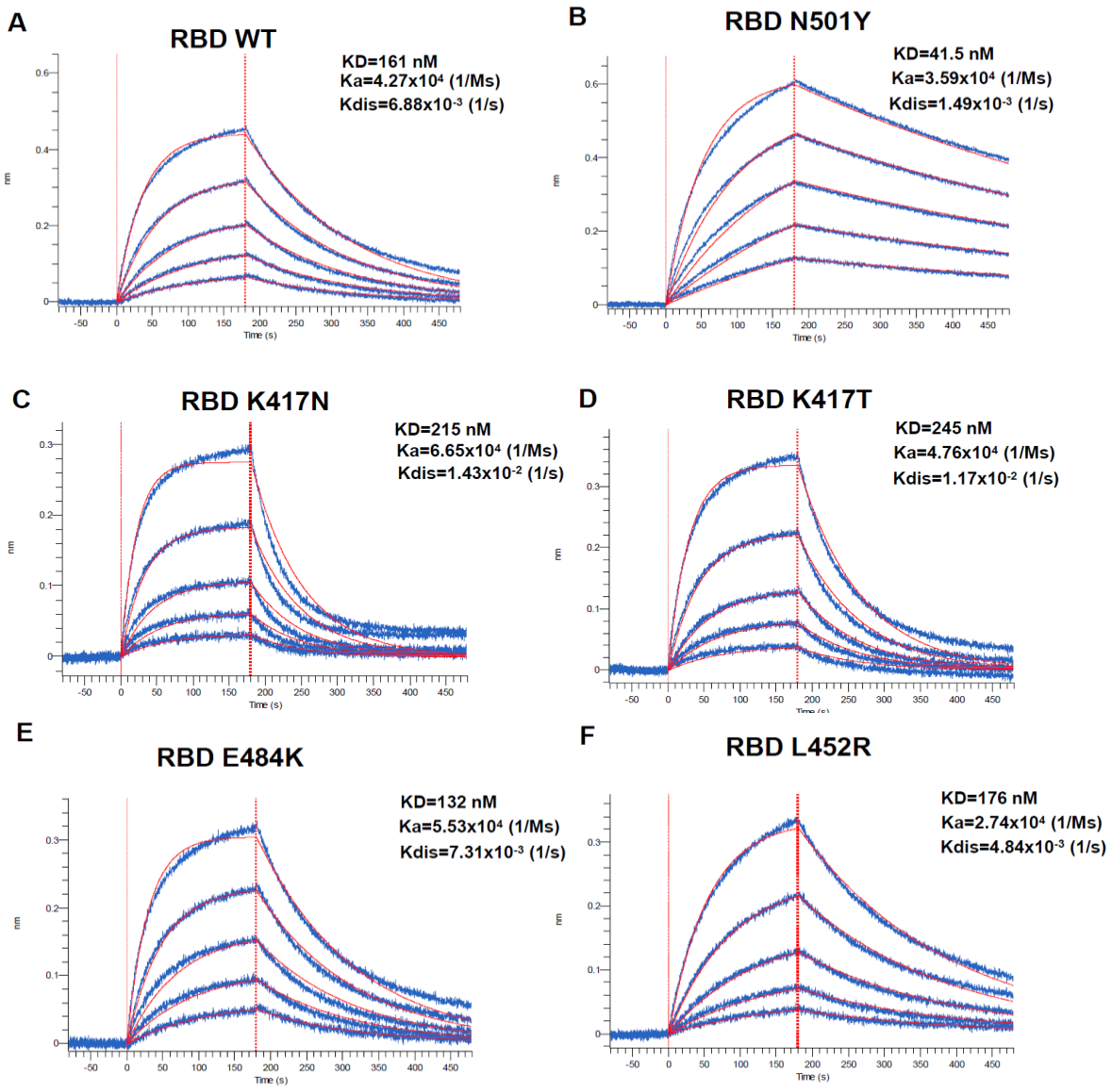

Figure 2.2 Kinetic Analysis of RBD interaction to hACE2 Binding by Biolayer Interferometry

Association of the different RBD proteins to sACE2 was carried out for 180s at various concentrations in a two-fold dilution series from 500nM to 31.25nM prior to dissociation for 300s for (A) WT, (B) N501Y, (C) K417N, (D) K417T, (E) E484K, and (F) L452R. Curve fitting was performed using a 1:1 binding model in the ForteBio data analysis software. Calculation of on-rates (K_a), off-rates (K_{dis}), and affinity constants (K_D) was computed using a global fit applied to all data. Raw data are presented in blue and fitting models are in red.

Effect of temperature on full variants Spike recognition of ACE2

It was recently shown that the affinity of Spike for ACE2 increases at low temperatures [27]. Interestingly, Prévost et al. also showed that the Spike from B.1.1.7 or harboring the N501Y mutation present better ACE2 binding at higher temperatures compared to the D614G strain [27]. To evaluate whether the Spikes from the emerging variants tested here also shared this phenotype, Spike-expressing cells were incubated at either 4ºC or 37ºC, and their ACE2-Fc binding was measured by flow cytometry, as described [27]. Of note, the conformational independent S2-specific CV3-25 antibody was used to normalize expression levels of the different Spikes since its binding is not affected by temperature [27]. As presented in Fig 2.3, the binding of ACE2-Fc to cell surface Spike was higher at cold temperature (4°C) compared to warm temperature (37°C) for all the variants. The impact of cold temperature on ACE2 binding was, however, more pronounced for the D614G Spike (3.62-fold increase) comparatively to Spikes from emerging variants (1.57 - 3.08 -fold increase). While ACE2 displayed higher binding for the different emerging variants Spikes at 37ºC, similar level of binding could only be achieved for the D614G Spike when decreasing the temperature to 4°C. This suggests that Spikes from emerging variants are able to bypass the temperature restraint to achieve high ACE2 binding. Interestingly, variants harboring the N501Y mutation (B.1.1.7, B.1.351 and P.1) exhibited an increase in ACE2 binding compared to D614G Spike at both 4ºC and 37ºC, while this phenotype was only observed at 4ºC with Spike from the other variants. This indicate that the cold temperature and the N501Y mutation significantly impact Spike-ACE2 interaction.

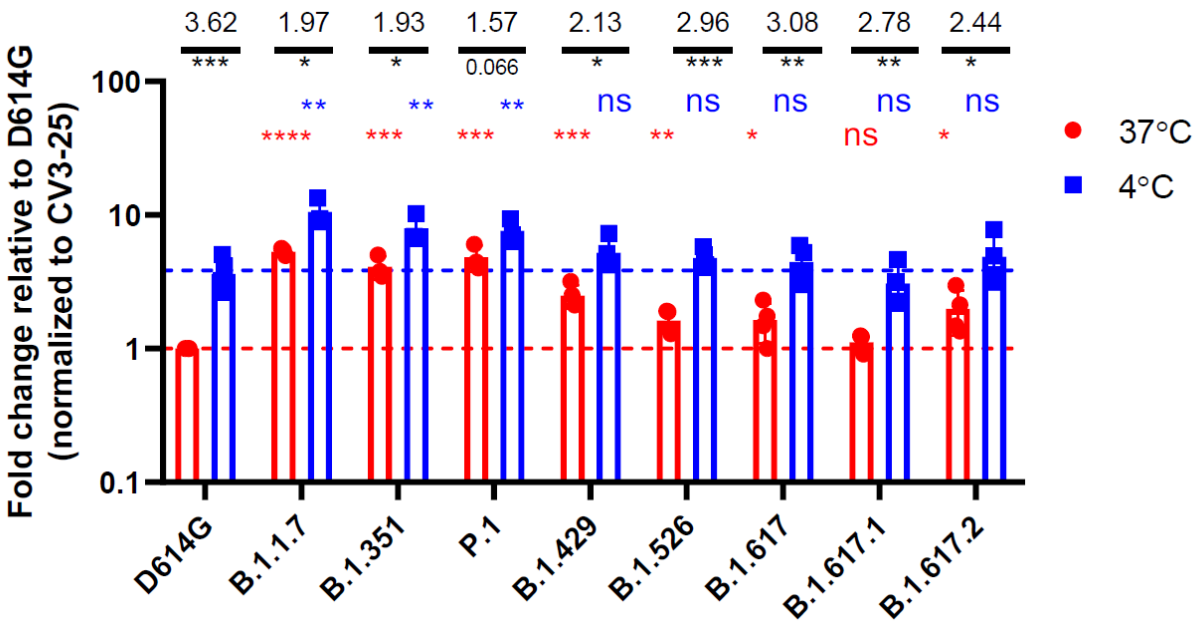

Figure 2.3 Evaluation of the impact of temperature on Spike-ACE2 interaction.
HEK 293T cells were transfected with the indicated SARS-CoV-2 Spike variants. Two days post-transfection, cells were stained with ACE2-Fc or with CV3-25 Ab as Spike expression control at 4ºC or 37ºC and analyzed by flow cytometry. ACE2-Fc binding to the different Spike variants are presented as a ratio of ACE2 binding to D614G Spik, normalized to CV3-25 binding at 37ºC (red) or at 4ºC (blue). Statistical analyses were used to compare each Spike at 4ºC vs 37ºC (black) or to compare variants Spike to D614G at 37ºC (red) or at 4ºC (blue). Fold changes of ACE2 binding at 4ºC vs 37ºC for each Spike is shown in black. Error bars indicate means ± SEM. Statistical significance has been performed using Mann-Whitney U test (*p < 0.05; **p < 0.01; ***p < 0.001; ****p < 0.0001, ns; non-significant).

Recognition of Spike variants by plasma from vaccinated individuals

To gain information related to the antigenic profile of each emerging variants Spike and their single mutants, we used plasma collected three weeks post BNT162b2 vaccination from SARS-CoV-2 naïve (Fig. 2.4) or previously-infected individuals (Fig. 2.5) [32]. HEK 293T cells were transfected with Spike from emerging variants or their individual mutants and plasma binding was evaluated by flow cytometry, as previously reported [32,37-40]. When compared to D614G, Spike from B.1.1.7, P.1 and the recently emerged B.1.617.1 and B.1.617.2 variants were significantly less recognized by the plasma from SARS-CoV-2 naïve individuals (Fig 2.4A).

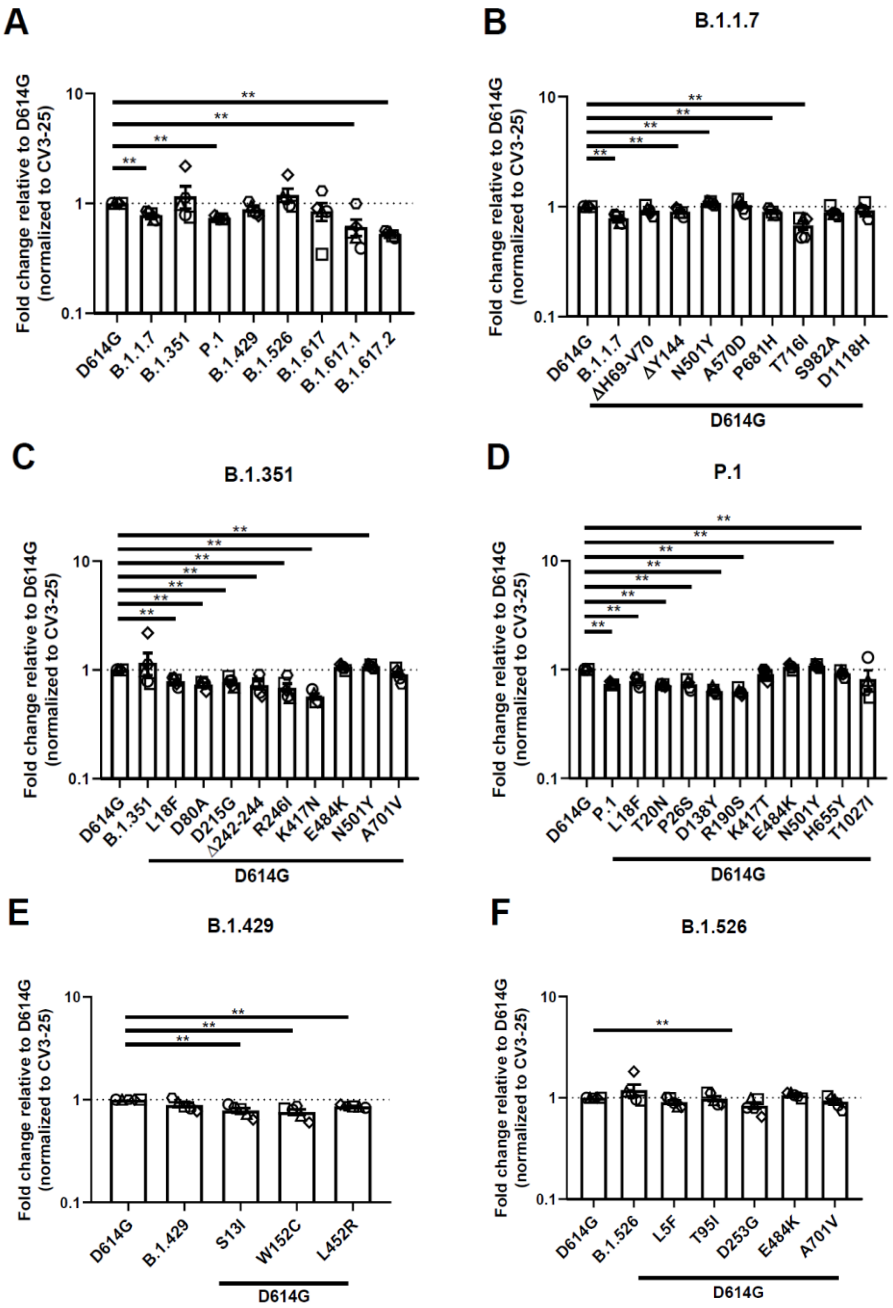

Figure 2.4 Recognition of SARS-CoV-2 Spike variants and single mutants by plasma from vaccinated SARS-CoV-2 naïve individuals.

HEK 293T cells were transfected with the indicated SARS-CoV-2 spike variants. Two days post transfection, cells were stained with 1:250 dilution of plasma collected from naïve-vaccinated individuals (n=3-5) or with CV3-25 Ab as control and analyzed by flow cytometry. Plasma recognition of (A) full Spike variants, (B) B.1.1.7, (C) B.1.351, (D)P.1, (E) B.1.429, (F) B.1.526 Spike and variant-specific Spike single mutations are presented as ratio of plasma binding to D614G Spike normalized CV3-25 binding. Error bars indicate means ± SEM. Statistical significance has been performed using Mann-Whitney U test (*$p < 0.05$; **$p < 0.01$; ***$p < 0.001$; ****$p < 0.0001$).

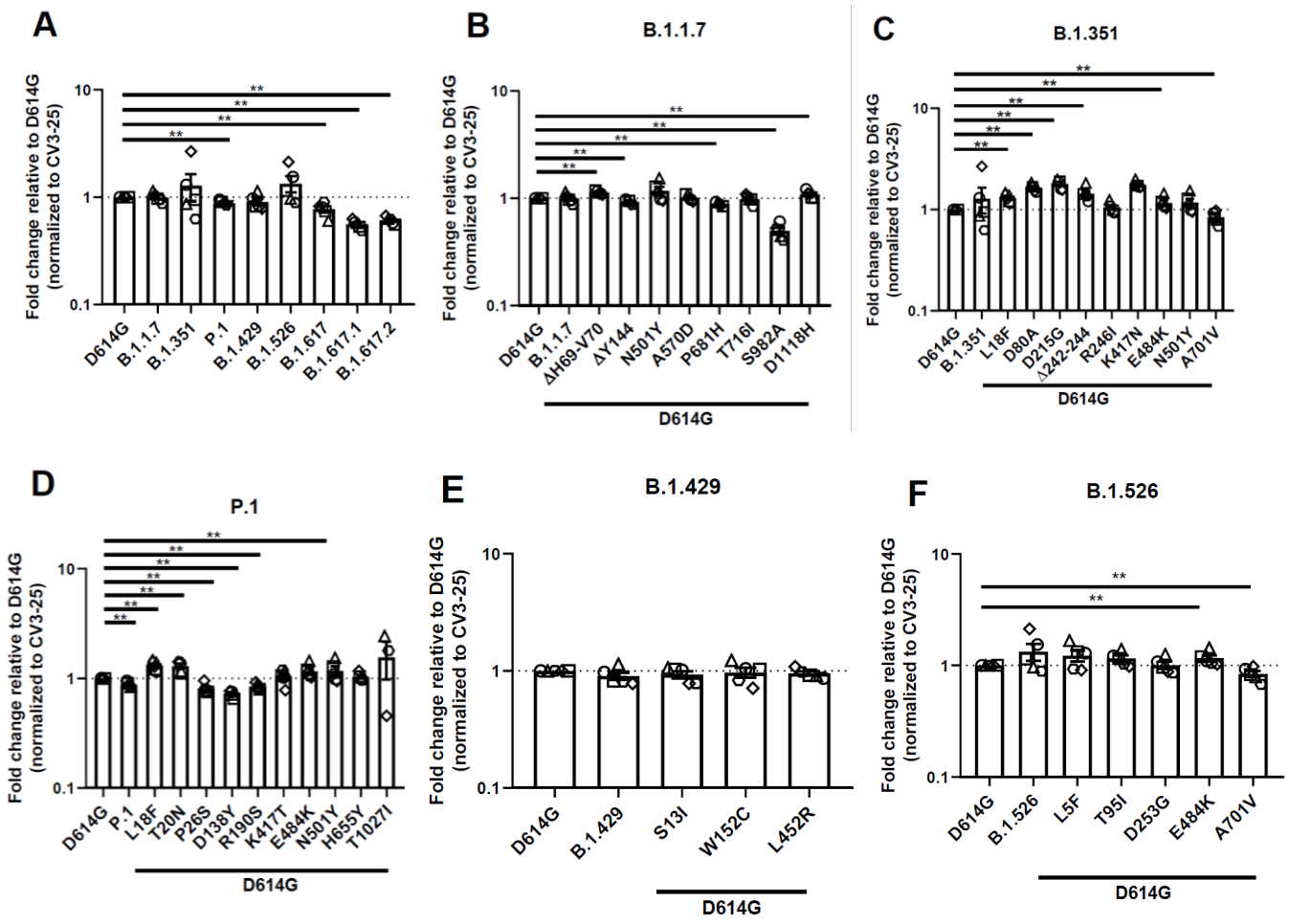

Figure 2.5 Recognition of SARS-CoV-2 Spike variants and single mutants by plasma from vaccinated previously-infected individuals.
HEK 293T cells were transfected with SARS-CoV-2 full Spike variants and stained with plasma collected 3 weeks post-first dose vaccinated previously infected individuals (n=3-5) or with CV3-25 Ab and analyzed by flow cytometry. Plasma recognition of (A) full Spike variants or the (B) B.1.1.7, (C) B.1.351, (D) P.1, (E) B.1.429, (F) B.1.526 Spikes and Spikes with their corresponding single mutations are presented as a ratio of plasma binding to D614G Spike normalized with CV3-25 binding. Error bars indicate means ± SEM. Statistical significance has been performed using Mann-Whitney U test (*p < 0.05; **p < 0.01; ***p < 0.001; ****p < 0.0001).

Mutations apparently contributing to the reduction of plasma recognition of the B.1.1.7 Spike are the ΔY144 deletion in the NTD, P681H and T716I near the S1/S2 cleavage site (Fig 2.4B). The N501Y substitution, also present in other emerging variants (B1.351 and P.1), is the only mutation that increased plasma recognition.

While we did not observe a significant decrease in plasma recognition of the B.1.351 Spike, most single mutants of this VOC (L18F, D80A, D215G, Δ242-244, R246I in the NTD, and K417N in the RBD) exhibit decreased binding. Of note, the K417N mutation that reduced ACE2 binding (Fig 2.1C), also significantly impacted plasma recognition by ~1.75 fold compared to D614G (Fig 2.4C).

Polyclonal recognition of the P.1 Spike was reduced by ~1.33 folds (Fig 2.4D). Our results show that all the NTD mutations, namely L18F, T20N, P26S, D138Y and R190S, attenuated the binding of naïve-vaccinated plasma Abs (Fig 2.4D). Furthermore, H655Y also contributed to the immuno-evasive phenotype of the full Spike (Fig 2.4D). Again, N501Y is the only mutation that increased plasma recognition, indicating its major role amongst all the mutations of this variant.

Although the full B.1.429 Spike did not show a significant evasion of plasma recognition, all of its mutations presented a significant decrease in plasma binding (Fig 2.4E). Both its NTD mutations, S13I and W152C, were less efficiently recognized by plasma compared to D614G (Fig 2.4E). The RBD mutation L452R also presented a minor ~1.16-fold decrease in recognition by plasma from vaccinated individuals. Lastly, the B.1.526 full Spike variant did not significantly affect vaccine-elicited plasma recognition. The same phenotype is applicable to most of its mutations, with the exception of D253G substitution in the NTD, which showed a modest ~1.2-fold decrease in binding (Fig 2.4F).

We then evaluated the recognition of our panel of Spikes (VOC, VOI and single mutants) by plasma from previously-infected vaccinated individuals (plasma recovered three weeks post vaccination), as recently described [32]. When comparing all Spikes from emerging variants, the convalescent plasma pre- and post-first dose vaccination both effectively recognized all tested Spikes (Fig 2.5A). Previously-infected vaccinated individuals developed Abs that were able to robustly recognize and bind to the emerging variants B.1.1.7, B.1.351, B.1.429 and B.1.526 at a similar level than D614G. Binding was decreased by ~ 1.14 folds for P.1, ~1.3 folds for B.1.617 and by ~ 1.8 and ~1.64 folds for B.1.617.1 and B.1.617.2 Spikes, respectively (Fig 2.5A).

Examining each variant and their single mutations more closely, though full B.1.1.7 Spike did not significantly reduce plasma binding in previously-infected vaccinated individuals, three of its single mutations, ΔY144, P681H, and S982A significantly affected plasma recognition. Substitution S982A in the S2 showed the most important reduction, by ~2 folds compared to

D614G (Fig 2.5B). Inversely, the deletion ΔH69-V70 and the substitution D1118H slightly enhanced the recognition of this Spike by plasma from previously-infected vaccinated individuals. However, combined together, the B.1.1.7 was recognized similarly to its D614G counterpart by these plasmas.

The B.1.351 Spike was efficiently recognized by plasma from previously-infected vaccinated individuals with a single mutation presenting lower detection (A701V) (Fig 2.5C). In the P.1 Spike we observed mutations in the NTD that decreased recognition (P26S, D138Y, and R190S) (Fig 2.5D). The Spikes from B.1.429 and B.1.526 were also efficiently recognized. Only the A701V substitution present in the B.1.526 reduced plasma binding (Fig 2.5F). Among all tested emerging variants, the Spikes from B.1.617.1 and B.1.617.2 presented the most important decrease in recognition by ~1.8 and ~1.64 folds compared to D614G (Figure 2.5A)

Altogether, our results highlight the difficulty in predicting the phenotype of a particular variant based on the phenotype of its individual mutations.

Neutralization of Spike variants by plasma from vaccinated individuals

We then determined the neutralization profile of the different emerging variants Spikes using a pseudoviral neutralization assay [37-41]. For this assay we used plasma from five individuals previously infected with SARS-CoV-2 (on average 8 months post-symptom onset) after one dose of the Pfizer/BioNTech BNT162b2 vaccine (samples were collected 22 days after immunization) [32]. Since we recently showed that plasma from vaccinated naïve individuals have only weak neutralizing activity three weeks post vaccination [32], we didn't include them in this assay. As we described previously [32], we incubated serial dilutions of plasma with pseudoviruses bearing the different Spikes before adding to HEK 293T target cells stably expressing the human ACE2 receptor [32]. We obtained robust neutralization for all pseudoviral particles, with a modest, but significant decrease in neutralization against pseudoviruses bearing the Spike from B.1.351, B.1.526 and B.1.617.2 lineages, indicating that plasma from previously-infected individuals following a single dose have a relatively good neutralizing activity against emerging variants (Fig 2.6).

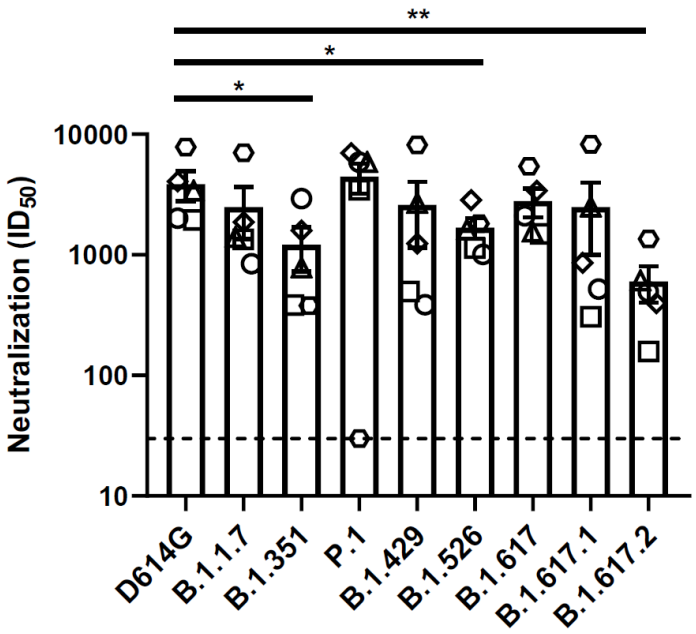

Figure 2.6 Neutralization of SARS-CoV-2 Spike variants by plasma from previously infected vaccinated individuals

Neutralizing activity of previously infected vaccinated individuals against pseudoviruses bearing the SARS-CoV-2 Spike variants were assessed. Pseudoviruses with serial dilutions of plasma were incubated for 1 h at 37°C before infecting 293T-ACE2 cells. ID_{50} against pseudoviruses were calculated by a normalized non-linear regression using GraphPad Prism software. Detection limit is indicated in the graph (ID_{50}=50). Statistical significance has been performed using Mann-Whitney U test (*$p < 0.05$).

2.6 Discussion

In our study, we offer a comparative view examining the ACE2 binding properties of selected circulating variants, and the impact of their single mutations on plasma binding. We observed that Spikes from B.1.1.7, B.1.351, P.1, B.1.429, B.1.526, B.1.617, and B.1.617.2 lineages present increased ACE2 interaction. Consistent with previous reports [26,42,43], the N501Y mutation shared by B.1.1.7, B.1.351, and P.1 variants presented a significant increase for ACE2-Fc binding. While N501Y plays a major role in enhanced transmissibility and infectivity [44], variants which do not share this mutation have also gained the increased ACE2 binding by harboring other mutations, such as in the B.1.429 lineage, where the L452R showed higher ACE2 binding.

We also analyzed the impact of temperature in modulating the capacity of Spikes from emerging variants to interact with the viral receptor ACE2. For almost all tested Spikes, we observed a

significant increase in ACE2 binding at cold temperature (4 ºC). As recently reported, this could be explained by favorable thermodynamics changes allowing the stabilization of the RBD-ACE2 interface and by modulating the Spike trimer conformation [27]. While the D614G Spike necessitates lower temperature for optimal ACE2 interaction, Spikes from the different VOCs and VOIs seem to bypass this requirement to efficiently interact with ACE2 at higher temperature (37 ºC). However, whether improved ACE2 binding at higher temperature facilitates emerging variants transmission and propagation remain to be demonstrated. Interestingly, variants harboring the N501Y mutation displayed improve ACE2 interaction compared to the D614G Spike, independently of the temperature, highlighting the critical impact of this substitution in improving Spike – ACE2 interaction. This reveals the importance of closely monitoring the appearance of this mutation among the current and future emerging variants. The appearance of this substitution could potentially impact the transmission and propagation of recent rapidly spreading emerging variants (such as the B.1.617.2 lineage) that do not harbor this mutation, by enhancing the affinity of their Spike for the ACE2 receptor at cold and warm temperatures.

We also found that plasma from vaccinated SARS-CoV-2 naïve and previously-infected individuals efficiently recognized the Spikes from emerging variants. However, as previously shown, plasma from vaccinated previously-infected individuals presented a higher and more robust recognition of all tested Spikes [32,45]. Interestingly, and in agreement with previous observations [41], we found that binding to the Spike doesn't necessarily translate into neutralization, as observed here for B.1.351. Nevertheless, plasma from previously-infected individuals presented some levels of neutralizing activity against pseudoviral particles bearing different emerging variants Spikes, further highlighting the resilience of the deployed vaccines, which were based on the original Wuhan strain.

2.7 Conclusions

Altogether, our results highlight the difficulty in predicting the phenotype of an emerging variant's Spike, either related to ACE2 interaction, antigenic profile, infectivity, and transmission based on the sum of the phenotype of single mutants making that particular Spike. Antigenic drift has been and remains a concern of the current pandemic [15, 46] and therefore, closely monitoring the

functional properties of emerging variants remains of the utmost importance for vaccine design and to inform public health authorities to better manage the epidemic by implementing preventive interventions to control the spread of highly transmissible virus, and tailoring vaccination campaign .

Acknowledgements

The authors thank the CRCHUM BSL3 and Flow Cytometry Platforms for their technical assistance and Dr Sandrine Moreira (Laboratoire de Santé Publique du Québec) for helpful discussions. We thank Dr. Stefan Pöhlmann and Dr. Markus Hoffmann (Georg-August University) for the plasmids coding for SARS-CoV-2 WT Spike (Wuhan-Hu-1 strain) and Dr Jason McLellan for the plasmid coding for sACE2 expressor. The CV3-25 antibody was produced using the pTT vector kindly provided by the Canada Research Council.

The authors declare that they have no known competing financial interests or personal relationships that could have appeared to influence the work reported in this paper.

2.8 References

1. Dong, E.; Du, H.; Gardner, L. An interactive web-based dashboard to track COVID-19 in real time. *The Lancet Infectious Diseases* **2020**, *20*, 533-534, doi:10.1016/S1473-3099(20)30120-1.
2. Hoffmann, M.; Kleine-Weber, H.; Schroeder, S.; Kruger, N.; Herrler, T.; Erichsen, S.; Schiergens, T.S.; Herrler, G.; Wu, N.H.; Nitsche, A.; et al. SARS-CoV-2 Cell Entry Depends on ACE2 and TMPRSS2 and Is Blocked by a Clinically Proven Protease Inhibitor. *Cell* **2020**, *181*, 271-280 e278, doi:10.1016/j.cell.2020.02.052.
3. Shang, J.; Ye, G.; Shi, K.; Wan, Y.; Luo, C.; Aihara, H.; Geng, Q.; Auerbach, A.; Li, F. Structural basis of receptor recognition by SARS-CoV-2. *Nature* **2020**, *581*, 221-224, doi:10.1038/s41586-020-2179-y.
4. Walls, A.C.; Xiong, X.; Park, Y.J.; Tortorici, M.A.; Snijder, J.; Quispe, J.; Cameroni, E.; Gopal, R.; Dai, M.; Lanzavecchia, A.; et al. Unexpected Receptor Functional Mimicry Elucidates Activation of Coronavirus Fusion. *Cell* **2019**, *176*, 1026-1039.e1015, doi:10.1016/j.cell.2018.12.028.
5. Walls, A.C.; Park, Y.J.; Tortorici, M.A.; Wall, A.; McGuire, A.T.; Veesler, D. Structure, Function, and Antigenicity of the SARS-CoV-2 Spike Glycoprotein. *Cell* **2020**, *181*, 281-292.e286, doi:10.1016/j.cell.2020.02.058.
6. Wrapp, D.; Wang, N.; Corbett, K.S.; Goldsmith, J.A.; Hsieh, C.L.; Abiona, O.; Graham, B.S.; McLellan, J.S. Cryo-EM structure of the 2019-nCoV spike in the prefusion conformation. *Science* **2020**, *367*, 1260-1263, doi:10.1126/science.abb2507.
7. Voysey, M.; Clemens, S.A.C.; Madhi, S.A.; Weckx, L.Y.; Folegatti, P.M.; Aley, P.K.; Angus, B.; Baillie, V.L.; Barnabas, S.L.; Bhorat, Q.E.; et al. Safety and efficacy of the ChAdOx1 nCoV-19 vaccine (AZD1222) against SARS-CoV-2: an interim analysis of four randomised controlled trials in Brazil, South Africa, and the UK. *The Lancet* **2021**, *397*, 99-111, doi:10.1016/S0140-6736(20)32661-1.
8. Sadoff, J.; Gray, G.; Vandebosch, A.; Cárdenas, V.; Shukarev, G.; Grinsztejn, B.; Goepfert, P.A.; Truyers, C.; Fennema, H.; Spiessens, B.; et al. Safety and Efficacy of Single-Dose Ad26.COV2.S Vaccine against Covid-19. *New England Journal of Medicine* **2021**, *384*, 2187-2201, doi:10.1056/NEJMoa2101544.
9. Baden, L.R.; El Sahly, H.M.; Essink, B.; Kotloff, K.; Frey, S.; Novak, R.; Diemert, D.; Spector, S.A.; Rouphael, N.; Creech, C.B.; et al. Efficacy and Safety of the mRNA-1273 SARS-CoV-2 Vaccine. *New England Journal of Medicine* **2020**, *384*, 403-416, doi:10.1056/NEJMoa2035389.
10. Polack, F.P.; Thomas, S.J.; Kitchin, N.; Absalon, J.; Gurtman, A.; Lockhart, S.; Perez, J.L.; Pérez Marc, G.; Moreira, E.D.; Zerbini, C.; et al. Safety and Efficacy of the BNT162b2 mRNA Covid-19 Vaccine. *New England Journal of Medicine* **2020**, *383*, 2603-2615, doi:10.1056/NEJMoa2034577.
11. Krammer, F. SARS-CoV-2 vaccines in development. *Nature* **2020**, *586*, 516-527, doi:10.1038/s41586-020-2798-3.
12. Sadoff, J.; Le Gars, M.; Shukarev, G.; Heerwegh, D.; Truyers, C.; de Groot, A.M.; Stoop, J.; Tete, S.; Van Damme, W.; Leroux-Roels, I.; et al. Interim Results of a Phase 1–2a Trial of Ad26.COV2.S Covid-19 Vaccine. *New England Journal of Medicine* **2021**, doi:10.1056/NEJMoa2034201.
13. Mulligan, M.J.; Lyke, K.E.; Kitchin, N.; Absalon, J.; Gurtman, A.; Lockhart, S.; Neuzil, K.; Raabe, V.; Bailey, R.; Swanson, K.A.; et al. Phase I/II study of COVID-19 RNA

vaccine BNT162b1 in adults. *Nature* **2020**, *586*, 589-593, doi:10.1038/s41586-020-2639-4.
14. Jackson, L.A.; Anderson, E.J.; Rouphael, N.G.; Roberts, P.C.; Makhene, M.; Coler, R.N.; McCullough, M.P.; Chappell, J.D.; Denison, M.R.; Stevens, L.J.; et al. An mRNA Vaccine against SARS-CoV-2 — Preliminary Report. *New England Journal of Medicine* **2020**, *383*, 1920-1931, doi:10.1056/NEJMoa2022483.
15. Prévost, J.; Finzi, A. The great escape? SARS-CoV-2 variants evading neutralizing responses. *Cell Host Microbe* **2021**, *29*, 322-324, doi:10.1016/j.chom.2021.02.010.
16. Plante, J.A.; Liu, Y.; Liu, J.; Xia, H.; Johnson, B.A.; Lokugamage, K.G.; Zhang, X.; Muruato, A.E.; Zou, J.; Fontes-Garfias, C.R.; et al. Spike mutation D614G alters SARS-CoV-2 fitness. *Nature* **2021**, *592*, 116-121, doi:10.1038/s41586-020-2895-3.
17. Korber, B.; Fischer, W.M.; Gnanakaran, S.; Yoon, H.; Theiler, J.; Abfalterer, W.; Hengartner, N.; Giorgi, E.E.; Bhattacharya, T.; Foley, B.; et al. Tracking Changes in SARS-CoV-2 Spike: Evidence that D614G Increases Infectivity of the COVID-19 Virus. *Cell* **2020**, *182*, 812-827.e819, doi:10.1016/j.cell.2020.06.043.
18. CDC. SARS-CoV-2 Variant Classifications and Definitions. Available online: https://www.cdc.gov/coronavirus/2019-ncov/variants/variant-info.html#print (accessed on
19. Mwenda M, S.N., Sinyange N, et al. *Detection of B.1.351 SARS-CoV-2 Variant Strain - Zambia, December 2020*; CDC: 2021.
20. Deng, X.; Garcia-Knight, M.A.; Khalid, M.M.; Servellita, V.; Wang, C.; Morris, M.K.; Sotomayor-González, A.; Glasner, D.R.; Reyes, K.R.; Gliwa, A.S.; et al. Transmission, infectivity, and neutralization of a spike L452R SARS-CoV-2 variant. *Cell* **2021**, doi:10.1016/j.cell.2021.04.025.
21. Ferreira, I.; Datir, R.; Kemp, S.; Papa, G.; Rakshit, P.; Singh, S.; Meng, B.; Pandey, R.; Ponnusamy, K.; Radhakrishnan, V.S.; et al. SARS-CoV-2 B.1.617 emergence and sensitivity to vaccine-elicited antibodies. *bioRxiv* **2021**, 2021.2005.2008.443253, doi:10.1101/2021.05.08.443253.
22. West, A.P.; Wertheim, J.O.; Wang, J.C.; Vasylyeva, T.I.; Havens, J.L.; Chowdhury, M.A.; Gonzalez, E.; Fang, C.E.; Di Lonardo, S.S.; Hughes, S.; et al. Detection and characterization of the SARS-CoV-2 lineage B.1.526 in New York. *bioRxiv* **2021**, 2021.2002.2014.431043, doi:10.1101/2021.02.14.431043.
23. ECDC. *Rapid increase of a SARS-CoV-2 variant with multiple spike protein mutations observed in the United Kingdom*; 20 December 2020 2020.
24. ECDC. *Emergence of SARS-CoV-2 B.1.617 variants in India and situation in the EU/EEA*; 11 May 2021 2021.
25. Zhu, X.; Mannar, D.; Srivastava, S.S.; Berezuk, A.M.; Demers, J.P.; Saville, J.W.; Leopold, K.; Li, W.; Dimitrov, D.S.; Tuttle, K.S.; et al. Cryo-electron microscopy structures of the N501Y SARS-CoV-2 spike protein in complex with ACE2 and 2 potent neutralizing antibodies. *PLoS Biol* **2021**, *19*, e3001237, doi:10.1371/journal.pbio.3001237.
26. Starr, T.N.; Greaney, A.J.; Hilton, S.K.; Ellis, D.; Crawford, K.H.D.; Dingens, A.S.; Navarro, M.J.; Bowen, J.E.; Tortorici, M.A.; Walls, A.C.; et al. Deep Mutational Scanning of SARS-CoV-2 Receptor Binding Domain Reveals Constraints on Folding and ACE2 Binding. *Cell* **2020**, *182*, 1295-1310.e1220, doi:10.1016/j.cell.2020.08.012.
27. Prévost, J.; Richard, J.; Gasser, R.; Ding, S.; Fage, C.; Anand, S.P.; Adam, D.; Gupta Vergara, N.; Tauzin, A.; Benlarbi, M.; et al. Impact of temperature on the affinity of SARS-

CoV-2 Spike glycoprotein for host ACE2. *J Biol Chem* **2021**, *297*, 101151, doi:10.1016/j.jbc.2021.101151.
28. Wang, P.; Nair, M.S.; Liu, L.; Iketani, S.; Luo, Y.; Guo, Y.; Wang, M.; Yu, J.; Zhang, B.; Kwong, P.D.; et al. Antibody resistance of SARS-CoV-2 variants B.1.351 and B.1.1.7. *Nature* **2021**, *593*, 130-135, doi:10.1038/s41586-021-03398-2.
29. Amanat, F.; Thapa, M.; Lei, T.; Ahmed, S.M.S.; Adelsberg, D.C.; Carreño, J.M.; Strohmeier, S.; Schmitz, A.J.; Zafar, S.; Zhou, J.Q.; et al. SARS-CoV-2 mRNA vaccination induces functionally diverse antibodies to NTD, RBD, and S2. *Cell* **2021**, doi:10.1016/j.cell.2021.06.005.
30. Rambaut, A.; Holmes, E.C.; O'Toole, Á.; Hill, V.; McCrone, J.T.; Ruis, C.; du Plessis, L.; Pybus, O.G. A dynamic nomenclature proposal for SARS-CoV-2 lineages to assist genomic epidemiology. *Nature Microbiology* **2020**, *5*, 1403-1407, doi:10.1038/s41564-020-0770-5.
31. Li, W.; Chen, Y.; Prévost, J.; Ullah, I.; Lu, M.; Gong, S.Y.; Tauzin, A.; Gasser, R.; Vézina, D.; Anand, S.P.; et al. Structural basis and mode of action for two broadly neutralizing antibodies against SARS-CoV-2 emerging variants of concern. *Cell Rep* **2021**, *38*, 110210, doi:10.1016/j.celrep.2021.110210.
32. Tauzin, A.; Nayrac, M.; Benlarbi, M.; Gong, S.Y.; Gasser, R.; Beaudoin-Bussières, G.; Brassard, N.; Laumaea, A.; Vézina, D.; Prévost, J.; et al. A single dose of the SARS-CoV-2 vaccine BNT162b2 elicits Fc-mediated antibody effector functions and T cell responses. *Cell Host Microbe* **2021**, *29*, 1137-1150.e1136, doi:10.1016/j.chom.2021.06.001.
33. Jennewein, M.F.; MacCamy, A.J.; Akins, N.R.; Feng, J.; Homad, L.J.; Hurlburt, N.K.; Seydoux, E.; Wan, Y.-H.; Stuart, A.B.; Edara, V.V.; et al. Isolation and characterization of cross-neutralizing coronavirus antibodies from COVID-19+ subjects. *Cell Reports* **2021**, *36*, 109353, doi:https://doi.org/10.1016/j.celrep.2021.109353.
34. Ullah, I.; Prévost, J.; Ladinsky, M.S.; Stone, H.; Lu, M.; Anand, S.P.; Beaudoin-Bussières, G.; Benlarbi, M.; Ding, S.; Gasser, R.; et al. Live imaging of SARS-CoV-2 infection in mice reveals neutralizing antibodies require Fc function for optimal efficacy. *bioRxiv* **2021**, doi:10.1101/2021.03.22.436337.
35. Mothes, W.; Li, W.; Chen, Y.; Prevost, J.; Ullah, I.; Lu, M.; Gong, S.Y.; Tauzin, A.; Gasser, R.; Vezina, D.; et al. Structural Basis and Mode of Action for Two Broadly Neutralizing Antibodies Against SARS-CoV-2 Emerging Variants of Concern. *bioRxiv* **2021**, 2021.2008.2002.454546, doi:10.1101/2021.08.02.454546.
36. Anand, S.P.; Chen, Y.; Prévost, J.; Gasser, R.; Beaudoin-Bussières, G.; Abrams, C.F.; Pazgier, M.; Finzi, A. Interaction of Human ACE2 to Membrane-Bound SARS-CoV-1 and SARS-CoV-2 S Glycoproteins. *Viruses* **2020**, *12*, doi:10.3390/v12101104.
37. Prevost, J.; Gasser, R.; Beaudoin-Bussieres, G.; Richard, J.; Duerr, R.; Laumaea, A.; Anand, S.P.; Goyette, G.; Benlarbi, M.; Ding, S.; et al. Cross-Sectional Evaluation of Humoral Responses against SARS-CoV-2 Spike. *Cell Rep Med* **2020**, *1*, 100126, doi:10.1016/j.xcrm.2020.100126.
38. Beaudoin-Bussières, G.; Laumaea, A.; Anand Sai, P.; Prévost, J.; Gasser, R.; Goyette, G.; Medjahed, H.; Perreault, J.; Tremblay, T.; Lewin, A.; et al. Decline of Humoral Responses against SARS-CoV-2 Spike in Convalescent Individuals. *mBio* **2020**, *11*, e02590-02520, doi:10.1128/mBio.02590-20.
39. Anand, S.P.; Prévost, J.; Nayrac, M.; Beaudoin-Bussières, G.; Benlarbi, M.; Gasser, R.; Brassard, N.; Laumaea, A.; Gong, S.Y.; Bourassa, C.; et al. Longitudinal analysis of

humoral immunity against SARS-CoV-2 Spike in convalescent individuals up to 8 months post-symptom onset. *Cell Rep Med* **2021**, *2*, 100290, doi:10.1016/j.xcrm.2021.100290.
40. Gasser, R.; Cloutier, M.; Prévost, J.; Fink, C.; Ducas, É.; Ding, S.; Dussault, N.; Landry, P.; Tremblay, T.; Laforce-Lavoie, A.; et al. Major role of IgM in the neutralizing activity of convalescent plasma against SARS-CoV-2. *Cell Rep* **2021**, *34*, 108790, doi:10.1016/j.celrep.2021.108790.
41. Ding, S.; Laumaea, A.; Benlarbi, M.; Beaudoin-Bussières, G.; Gasser, R.; Medjahed, H.; Pancera, M.; Stamatatos, L.; McGuire, A.T.; Bazin, R.; et al. Antibody Binding to SARS-CoV-2 S Glycoprotein Correlates with but Does Not Predict Neutralization. *Viruses* **2020**, *12*, doi:10.3390/v12111214.
42. Leung, K.; Shum, M.H.; Leung, G.M.; Lam, T.T.; Wu, J.T. Early transmissibility assessment of the N501Y mutant strains of SARS-CoV-2 in the United Kingdom, October to November 2020. *Eurosurveillance* **2021**, *26*, 2002106, doi:doi:https://doi.org/10.2807/1560-7917.ES.2020.26.1.2002106.
43. Washington, N.L.; Gangavarapu, K.; Zeller, M.; Bolze, A.; Cirulli, E.T.; Schiabor Barrett, K.M.; Larsen, B.B.; Anderson, C.; White, S.; Cassens, T.; et al. Emergence and rapid transmission of SARS-CoV-2 B.1.1.7 in the United States. *Cell* **2021**, *184*, 2587-2594.e2587, doi:10.1016/j.cell.2021.03.052.
44. Liu, Y.; Liu, J.; Plante, K.S.; Plante, J.A.; Xie, X.; Zhang, X.; Ku, Z.; An, Z.; Scharton, D.; Schindewolf, C.; et al. The N501Y spike substitution enhances SARS-CoV-2 transmission. *bioRxiv : the preprint server for biology* **2021**, 2021.2003.2008.434499, doi:10.1101/2021.03.08.434499.
45. Lucas, C.; Vogels, C.B.F.; Yildirim, I.; Rothman, J.; Lu, P.; Monteiro, V.; Gelhausen, J.R.; Campbell, M.; Silva, J.; Tabachikova, A.; et al. Impact of circulating SARS-CoV-2 variants on mRNA vaccine-induced immunity in uninfected and previously infected individuals. *medRxiv* **2021**, 2021.2007.2014.21260307, doi:10.1101/2021.07.14.21260307.
46. Callaway, E. Fast-spreading COVID variant can elude immune responses. *Nature* **2021**, *589*, 500-501, doi:10.1038/d41586-021-00121-z.

CHAPTER 3. TEMPERATURE INFLUENCES THE INTERACTION BETWEEN SARS-COV-2 SPIKE FROM OMICRON SUBVARIANTS AND HUMAN ACE2

Shang Yu Gong, Shilei Ding, Mehdi Benlarbi, Yaozong Chen, Dani Vézina, Lorie Marchitto, Guillaume Beaudoin-Bussières, Guillaume Goyette, Catherine Bourassa, Yuxia Bo, Halima Medjahed, Inès Levade, Marzena Pazgier, Marceline Côté, Jonathan Richard, Jérémie Prévost and Andrés Finzi

3.1 Preface

Omicron has taken over the previous circulating VOC, Delta, since November 2021, and one year later, in December 2022, Omicron subvariants remain the main circulating VOCs. Previous studies by Prévost *et al.* as well as findings in Chapter 2 highlight the main contributing mutations by which past VOCs overcome temperature barrier in order to interact with the ACE2 receptor with increased affinity [127,134]. As shown in Chapter 1, Omicron subvariants contain the highest number of mutations observed in all VOCs, most of which in the RBD, which could impact their ability to interact with the ACE2 receptor. In this chapter, we will evaluate how their mutations impact their ability to interact with ACE2 at different temperatures.

3.2 Abstract

SARS-CoV-2 continues to infect millions of people worldwide. The subvariants arising from the variant-of-concern (VOC) Omicron include BA.1, BA.1.1, BA.2, BA.2.12.1, BA.4, and BA.5. All possess multiple mutations in their Spike glycoprotein, notably in its immunogenic receptor-binding domain (RBD), and present enhanced viral transmission. The highly mutated Spike glycoproteins from these subvariants present different degrees of resistance to recognition and cross-neutralisation by plasma from previously infected and/or vaccinated individuals. We have recently shown that the temperature affects the interaction between the Spike and its receptor, the angiotensin converting enzyme 2 (ACE2). The affinity of RBD for ACE2 is significantly increased at lower temperatures. However, whether this is also observed with the Spike of Omicron and sub-lineages is not known. Here we show that, similar to other variants, Spikes from Omicron sub-lineages bind better the ACE2 receptor at lower temperatures. Whether this translates into enhanced transmission during the fall and winter seasons remains to be determined.

3.3 Introduction

Severe acute respiratory syndrome coronavirus 2 (SARS-CoV-2) is the causative agent of the coronavirus disease 2019 (COVID-19) pandemic, which still looms over populations worldwide. Since the start of the pandemic, strategies such as vaccination or therapeutic interventions using monoclonal antibodies or antivirals have been used to prevent and control the infection [1]. Amongst them, vaccination remains the only preventative measure and has been proven effective against SARS-CoV-2 infection from earlier variants [2-4] and remains effective at protecting from severe outcomes caused by newly emerged Variants of Concern (VOCs) [5-7]. Currently approved vaccines target predominantly the Spike glycoprotein (S), which is responsible for viral entry. The Spike is a trimer comprised of three surface S1 and three transmembrane S2 subunits. The S1 subunit uses its highly immunogenic receptor-binding domain (RBD) to interact with the human angiotensin-converting enzyme 2 (ACE2), following which the S2 subunit mediates viral fusion with the host membrane [8-12]. The structure of the S glycoprotein has been solved by cryo-electron microscopy and X-ray crystallography [9, 12-15], and its dynamic conformational landscape studied by single-molecule Förster resonance energy transfer (smFRET) [16-22].

Variants of concern (VOCs) denominated by the World Health Organization (WHO) harbour mutations in different regions of the virus, notably in the S glycoprotein since it is under high selective pressure to evade host immune response [23]. The most recent VOC, Omicron (B.1.1.529) and its sub-lineages (BA.1, BA.1.1, BA.2, BA.2.12.1, BA.2.75, BA.4, BA.5), possess over 30 mutations compared to S from ancestral strains and share over 20 mutations between them [24-29]. Omicron and its sub-variants show enhanced transmissibility and immune evasion from antibodies elicited in vaccinated and previously infected individuals, causing global concern over vaccine failure and immune escape [28-35].

One of the many factors influencing transmissibility appears to be linked to the capacity of the different VOC Spikes to interact with the ACE2 receptor [36, 37]. Previous work has shown that this interaction is influenced by temperature [38]. Here, by combining an array of biochemical and biological assays, including flow cytometry, virus capture assay, and biolayer interferometry, we report on the impact that temperature has on the capacity of Omicron subvariant Spikes to interact with human ACE2.

3.4 Materials and methods

Plasmids

The plasmids expressing SARS-CoV-2 Spike D614G and SARS-CoV-2 S RBD (residues 319–541) fused with a hexahistidine tag were previously described [39]. The plasmids encoding the SARS-CoV-2 S RBD from the B.1.1.529-BA.2 lineage was synthesised commercially by Genscript (Piscataway, NJ, USA). The RBD sequence (encoding for residues 319–541) fused to a C-terminal hexa-histidine tag was cloned into the pcDNA3.1(+) expression vector. The plasmids encoding the full-length spike from the B.1.617.2 (Delta), B.1.1.529 (Omicron) BA.1, BA.1.1, BA.2, BA.2.12.1, BA.4/5 lineages were generated by overlapping PCR using a codon-optimised wild-type SARS-CoV-2 spike gene that was synthesised (Biobasic, Markham, ON, Canada) and cloned in pCAGGS as a template [16,17,40]. All constructs were validated by Sanger sequencing. The plasmid encoding for soluble human ACE2 (residues 1–615) fused with an 8xHisTag was reported elsewhere [12]. The plasmid encoding for the ACE2-Fc chimeric protein, a protein composed of an ACE2 ectodomain (1–615) linked to an Fc segment of human IgG1, was previously reported [41]. The lentiviral vector pNL4.3 R-E− Luc was obtained from the NIH AIDS Reagent Program. The vesicular stomatitis virus G (VSV-G)-encoding plasmid was previously described [42].

Cell lines

HEK 293T cells (obtained from the American Type Culture Collection [ATCC]) were derived from 293 cells, into which the simian virus 40 T-antigen was inserted. Cf2Th cells (ATCC) are canine thymocytes resistant to SARS-CoV-2 entry and were used as target cells in the virus capture assay. 293T cells and Cf2Th were maintained at 37°C under 5% CO2 in Dulbecco's modified Eagle's medium (DMEM) (Wisent, St. Bru-no, QC, Canada), supplemented with 5% fetal bovine serum (FBS) (VWR, Radnor, PA, USA) and 100 U/mL penicillin/streptomycin (Wisent).

Protein expression and purification

FreeStyle 293F cells (Invitrogen, Waltham, MA, USA) were grown in FreeStyle 293F medium (Invitrogen) to a density of 1 × 106 cells/mL at 37°C with 8% CO2 with regular agitation (150 rpm). Cells were transfected with a plasmid coding for SARS-CoV-2 Omicron BA.2 S RBD (319-

537), soluble ACE2 (sACE2, 1-615), or ACE2-Fc (1-615), using ExpiFectamine 293 transfection reagent, as directed by the manufacturer (Invitrogen). One week later, cells were pelleted and discarded. Supernatants were filered using a 0.22 μm filter (Thermo Fisher Scientific). The recombinant sACE2 protein and RBD proteins were purified by nickel affinity columns, as directed by the manu-facturer (Invitrogen) and ACE2-Fc was purified using a protein A affinity column (Cytiva, Marlborough, MA, USA), as directed by the manufacturer. The protein preparations were dialysed against phosphate-buffered saline (PBS) and stored at -80°C in aliquots until further use. To assess purity, recombinant proteins were loaded on SDS-PAGE gels and stained with Coomassie Blue. Purified proteins were >95% pure after size-exclusion chromatography as verified by SDS-PAGE and Coomassie blue staining.

Flow cytometry analysis of cell-surface staining

Using the standard calcium phosphate method, 10 μg of spike expressor and 2 μg of a green fluorescent protein (GFP) expressor (pIRES2-GFP, Clontech) were transfected into 2 × 106 293T cells. At 48 h post transfection, 293T cells were stained with anti-Spike monoclonal antibodies CV3-25 (5 μg/mL) or using the ACE2-Fc chimeric protein (20 μg/mL) for 45 min at 37℃, 22℃, or 4℃. Alternatively, to determine the Hill coefficients, cells were preincubated with increasing concentrations of sACE2 (0 to 665 nM) at 37°C or 4°C. sACE2 binding was detected using a polyclonal goat anti-ACE2 (RND systems, Minneapolis, MN, USA). AlexaFluor-647-conjugated goat anti-human IgG (H+L) Ab (Invitrogen) and AlexaFluor-647-conjugated donkey anti-goat IgG (H+L) Ab (Invitrogen) were used as secondary antibodies to stain cells for 30 min at room temperature. The percentage of transfected cells (GFP+ cells) was determined by gating the living cell population based on viability dye staining (Aqua Vivid, Invitrogen). Samples were acquired on an LSRII cytometer (BD Biosciences, Mississauga, ON, Canada) and data analysis was performed using FlowJo v10.3 (Tree Star, Ashland, OR, USA). Hill coefficient analyses were done using GraphPad Prism version 8.0.1 (GraphPad, San Diego, CA, USA).

Virus capture assay

The SARS-CoV-2 virus capture assay was previously reported [43]. Pseudoviral particles were produced by transfecting 2 × 106 293T cells with pNL4.3 R-E- Luc (3.5 μg), plasmids encoding for SARS-CoV-2 Spike (1 μg) proteins and VSV-G (1 μg) using the standard calcium phosphate

method. Forty-eight hours later, virus-containing supernatants were collected, and cell debris were removed through centrifugation (1500 rpm for 10 min). The CV3-25 antibody or ACE2-Fc protein was immobilised on white MaxiSorp ELISA plates (Thermo Fisher Scientific) at a concentration of 5 μg/mL in 100 μL of PBS overnight at 4°C. Unbound proteins were removed by washing the plates twice with PBS. Plates were subsequently blocked with 3% bovine serum albumin (BSA) in PBS for 1 hour at room temperature, followed by 1 hour incubation at 37℃, 22°C, or 4℃. Meanwhile, virus-containing supernatants were pre-tempered at 37°C, 22°C, or 4°C for 1 hour. After washing plates twice with PBS, 200 μL of virus-containing supernatant were added to the wells. After 30 min of incubation at 37°C, 22°C, or 4°C, respectively, supernatants were discarded, and the wells were washed with PBS three times. Virus capture was visualised by adding 1×104 SARS-CoV-2-resistant Cf2Th cells per well in complete DMEM. Forty-eight hours post-infection, cells were lysed by the addition of 30 μL of passive lysis buffer (Promega, Madison, WI, USA) and one freeze–thaw cycle. An LB942 TriStar luminometer (Berthold Technologies, Bad Wildbad, Germany) was used to measure the luciferase activity of each well after the addition of 100 μL of luciferin buffer (15 mM MgSO4, 15 mM KH2PO4 [pH 7.8], 1 mM ATP, and 1 mM dithiothreitol) and 50 μL of 1 mM D-luciferin potassium salt (Prolume, Randolph, VT, USA).

Biolayer interferometry

Binding kinetics were performed with an Octet RED96e system (ForteBio, Fremont, CA, USA) at different temperatures (10°C, 25°C, and 35°C), shaking at 1000 RPM. Amine-reactive second-generation (AR2G) biosensors (Sartorius, Göttingen, Germany) were hydrated in water, then activated for 300 s with a solution of 5 mM sulfo-NHS and 10 mM EDC (Sartorius) prior to amine coupling. Either SARS-CoV-2 RBD WT or BA.2 were loaded into the AR2G biosensor at 12.5 μg/mL at 25°C in 10 mM acetate solution pH 5 for 600 s then quenched into 1 M ethanolamine solution pH 8.5 (Sartorius) for 300 s. Loaded biosensor were placed in a 10X kinetics buffer (Sartorius) for 120 s for baseline equilibration. Association of sACE2 (in the 10X kinetics buffer) to the different RBD proteins was carried out for 180 s at various concentrations in a twofold dilution series from 500 nM to 31.25 nM prior to dissociation for 300 s. The data were baseline subtracted prior to fitting being performed using a 1:1 binding model and the ForteBio data

analysis software. Calculation of on rates (k_{on}), off rates (k_{off}), and affinity constants (K_D) was computed using a global fit applied to all data.

Statistical analysis

Statistical analyses were done using GraphPad Prism version 8.0.1 (GraphPad). Every dataset was tested for statistical normality and this information was used to ap-ply the appropriate (parametric or nonparametric) statistical analysis. Difference in ACE2-Fc recognition and viral entry by VOC full Spikes were analyzed using Mann–Whitney U tests. Outliers were ruled out by Rout's outlier test (Rout Q = 10%). P values < 0.05 were considered significant; significance values are indicated as * $p < 0.05$, ** $p < 0.01$, *** $p < 0.001$, and **** $p < 0.0001$.

3.5 Results

Spike changes in Delta and Omicron subvariants compared to the ancestral D614G strain

Omicron (B.1.1.529) subvariants (BA.1, BA.1.1, BA.2, BA.2.12.1, BA.4, and BA.5) Spikes accumulated the larger number of mutations amongst all VOCs to date. They share 20 mutations between them (Figure 3.1A). We compared the ACE2-binding capacity of different Omicron subvariant Spikes with the ancestral strain D614G and the previous Delta (B.1.617.2) VOC Spike. The original Omicron BA.1 has 13 unique mutations, and its sub-lineage BA.1.1 differs from BA.1 by one mutation (R346K). Compared to BA.1, the BA2 subvariant has eight unique mutations, and harbours entirely different NTD mutations (T19I, L24S, Δ25/27, V213G), sharing only the G142D substitution. In the RBD, BA.2 shares 12 mutations with BA.1 but shows one different substitution at residue 371 (S371F; S371L in BA.1) and three extra mutations, T376A, D405N, and R408S. The BA.2.12.1 sub-lineage harbours the same 29 mutations than BA.2, with two extra mutations, L452Q in the RBD and S704L in the S2 subunit. The BA.4 and BA.5 subvariants are derived from BA.2, differing by one deletion (Δ69-70), one reversion (R493Q), and two additional mutations (L452R and F486V). The RBD of the Omicron strains have over 14 extra mutations compared to the VOC with the highest ACE2 affinity, Alpha (B.1.1.7), which had only one RBD mutation (N501Y) [44]. The T478K mutation is shared between the Delta variant and all Omicron subvariants. BA.4/5 shares the L452R mutation with Delta, a mutation that enhances ACE2 interaction [44].

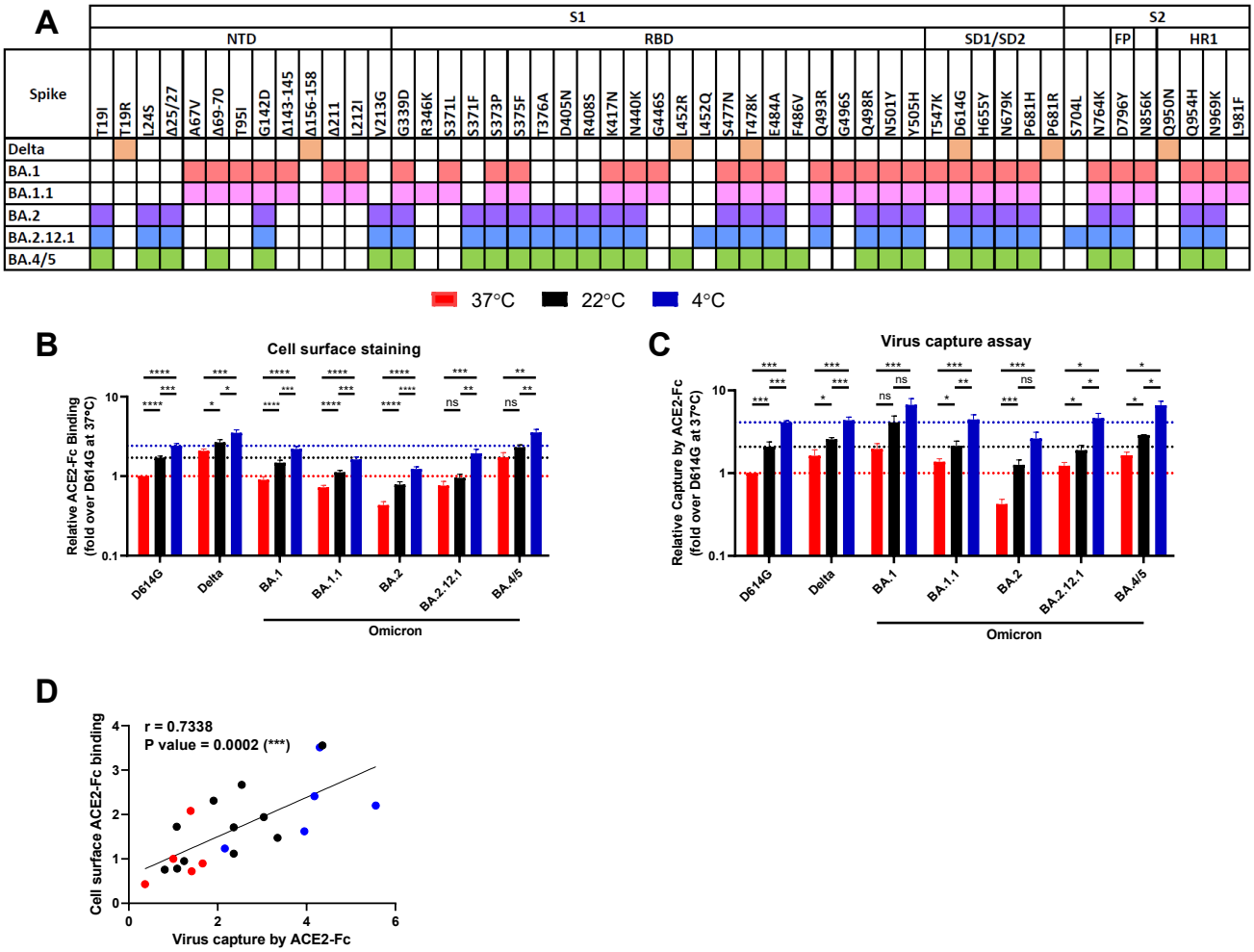

Figure 3.1. Low temperature enhances Omicron subvariant Spikes' interactions with ACE2. (**A**) List of point mutations and deletions in the Spike amino acid sequence from Delta variant and Omicron subvariants compared to the D614G ancestral strain. NTD: N-terminal domain; RBD: receptor binding domain; SD1/SD2: subdomains 1 and 2; FP: fusion peptide; HR1: heptad repeat region 1. (**B-C**) Cell surface staining of transfected 293T cells and virus capture assay of Omicron and subvariant Spikes at 37°C (red), 22°C (black), and 4°C (blue). **(B)** ACE2-Fc recognition is presented as a ratio of ACE2 binding to D614G Spike obtained at 37°C. (**C**) Pseudoviruses encoding the luciferase gene (Luc+) and expressing the SARS-CoV-2 Spike D614G, Delta or from Omicron subvariants (BA.1, BA.1.1, BA.2, BA.2.12.1, BA.4/5) were tested for viral capture by ACE2-Fc at the respective temperatures. Relative light units (RLU) obtained using ACE2-Fc was normalised to the signal obtained with the temperature-independent CV3-25 mAb and presented as a ratio of ACE2 capture to D614G obtained at 37°C. (**D**) Correlation between virus capture and cell surface binding of Spike by ACE2-Fc is depicted for the three temperatures tested. These results represent at least three independent experiments showing means ± SEM. Statistical significance was tested using (**B-D**) the Mann–Whitney U test or (**E**) Spearman rank correlation test (*p<0.05; **p<0.01; ***p<0.001, ****p<0.0001, ns: non-significant).

Temperature modulation of D614G, Delta and Omicron Spikes interaction with ACE2

We first measured ACE2 recognition of Omicron subvariants using a flow cytometry assay, as described [38,44]. Briefly, plasmids expressing the full-length SARS-CoV-2 Spike of the ancestral strain D614G, the previously prominent VOC Delta, and current Omicron subvariants were transfected in HEK 293T cells. ACE2 inter-action was determined by using the chimeric ACE2-Fc protein, which is composed of two ACE2 ectodomains linked to the Fc portion of human IgG [41].

To ensure that any differential recognition was not linked to a temperature-dependent variation in Spike levels, we used the conformational- and temperature-independent S2-targeting monoclonal antibody (mAb) CV3-25 as an experimental control [19,38,40,45]. Compared to the ancestral D614G Spike, the Delta and BA.4/5 Spikes presented an increase in ACE2-Fc interaction at 37°C whereas BA.1.1, BA.2, and BA.2.12.1 bound ACE2 less efficiently (Figure 3.1B). At this temperature, we observed no differences with BA.1.

Previous studies have reported that lower temperatures enhance RBD affinity for ACE2 and favour the adoption of the "up" conformation, therefore enhancing the capacity of the trimeric Spike to interact with ACE2 [38,44,45]. We therefore evaluated whether this was the case for the Omicron Spike and its subvariants. Forty-eight hours post-transfection, Spike-expressing cells were incubated at different temperatures (37°C, 22°C, and 4°C) before measuring ACE2-Fc binding by flow cytometry, as described above. We observed a gradual increase in ACE2-Fc binding concomitant with the temperature decrease for all Spikes tested (Figure 3.1B), validating a temperature-dependent interaction between Spike and ACE2 [38,44].

We then evaluated whether the observed increase in Spike–ACE2 interaction at low temperature was maintained when the Spike was expressed at the surface of pseudoviral particles. To this end, we used a previously described virus capture assay [43] that uses pseudoviral particles bearing the different SARS-CoV-2 Spikes and evaluated their ability to interact with ACE2-Fc immobilised on ELISA plates. In agreement with a better interaction with ACE2 at lower temperatures, we observed a stepwise increase in viral capture at colder temperatures for all Spikes tested (Figure 3.1C), which significantly correlated with the cell-based binding assay (Figure 3.1D). Thus, our findings indicate that the Spike–ACE2 interaction is similarly modulated by temperature independently of whether the Spike is expressed on viral particles or cell membranes.

Temperature modulates ACE2 binding cooperativity and affinity for Omicron Spikes

The Spike interacts with its ACE2 receptor in its "up" conformation [46]. However, the Spike trimer of Omicron BA.1 and subvariant BA.2 was reported to assume more the RBD "down" conformation that is stabilised by a strong network of inter-protomer contacts leading to its higher thermostability [47,48]. Therefore, we studied the sensitivity of the Spike subvariants to conformational changes in response to ACE2. To do so, we calculated the Hill coefficient (h), which is the degree of binding cooperativity between the protomers of the trimeric Spike and monomeric ACE2 molecules in a concentration-response manner. The h values are calculated from the steepness of dose-response curves generated upon incubation of Spike-expressing cells with increasing concentrations of sACE2, as previously described [38]. Briefly, HEK293T cells were transfected with full-length Spikes from the D614G ancestral strain, the Delta VOC or the Omicron subvariants. With the exception of BA.4/ 5, all other Spikes tested presented a negative cooperativity (h value <1) at 37°C (Figure 3.2A, red lines). This is consistent with previous observations suggesting an energetic barrier to engage additional ACE2 molecules at high temperatures [38]. The Spike from BA.4/5 presented a positive Hill coefficient (h=1.256) at 37°C, thus suggesting a coordinated Spike opening at warmer temperatures (Figure 3.2A). Interestingly, sACE2 binding cooperativity was improved in all Spikes at low temperature (4°C), confirming that low temperatures facilitate ACE2-induced Spike opening (Figure 2A, blue lines). Interestingly, the ACE2 binding cooperativity with BA.4/5 Spike at 37°C (h=1.256) was found to be similar to its parental BA.2 lineage at 4°C (h=1.163), suggesting a lesser reliability on cold temperatures to expose RBD in the "up" conformation.

To assess the temperature's role in modulating binding kinetics between Omicron RBD and ACE2, we performed biolayer interferometry (BLI) experiments at different temperatures (10°C, 25°C, and 35°C) (Figure 3.2B). We observed a drastic decrease in the off rate at lower temperatures compared with its wild-type (WT, Wuhan-Hu-1 strain) counterpart. As observed previously [127,134], the affinity of the RBD with its receptor is mainly dictated by its off rate as the RBD BA.2 has a 4.5-fold decrease in K_D compared to WT at colder temperatures.

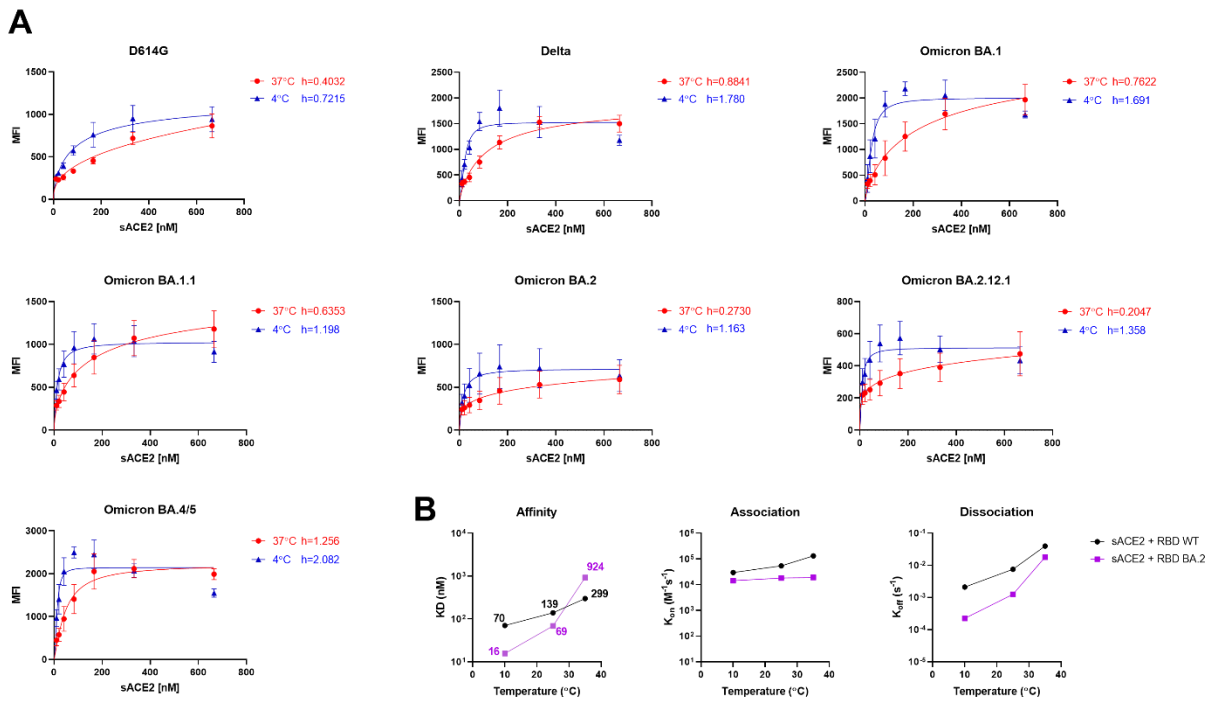

Figure 3.2. Low temperatures "open" Omicron subvariant Spikes. (**A**) The binding of sACE2 to the Spike of D614G, Delta, Omicron BA.1, BA.1.1, BA.2, BA.2.12.1, BA.4/5 expressed on the surface of 293T cells was measured by flow cytometry. Increasing concentrations of sACE2 were incubated with Spike-expressing cells in 4°C (blue) or 37°C (red). Means ± SEM derived from at least three independent experiments are shown. The Hill coefficients were calculated using GraphPad software. (**B**) Binding kinetics between SARS-CoV-2 RBD (WT or BA.2) and sACE2 assessed by biolayer interferometry at different temperatures. Graphs represent the affinity constants (K_D), on rates (K_{on}), and off rates (K_{off}) values obtained at different temperatures and calculated using a 1:1 binding model.

3.6 Discussion

Previous studies have shown that low temperature impacts the conformation of the Spike, triggering trimer opening and increasing binding to the ACE2 receptor [38,44,45]. Moreover, we have previously shown that this translates into enhanced viral attachment and infection [38]. Indeed, we observed enhanced infection at low temperatures using pseudoviral particles, as well as authentic SARS-CoV-2, the latter with primary human airway epithelial cells as target cells [38]. Since Omicron harbours 33 mutations in its Spike glycoprotein with mutations in the S2 stabilizing the RBD "down" conformation [47], we wondered whether these mutations hindered the impact of low temperature on Spike conformation and ACE2 interaction.

In this study, we investigated if temperature affects the interactions between SARS-CoV-2 Omicron subvariant Spikes and the primary receptor ACE2 in vitro with ELISA and flow cytometry assays. We have shown that the affinity and binding of Omicron subvariant Spikes to ACE2 receptors are significantly enhanced at low temperatures in cells and pseudoviral particles expressing the different Spikes. Importantly, our results show that low temperature facilitates the capacity of all Omicron subvariant Spikes to interact with their receptors, which could be explained by enhanced cooperativity between protomers upon ACE2 interaction and slower off-rate.

Our results suggest that even VOC Spikes that have a more "closed" conformation can be affected by low temperatures, enhancing binding to the ACE2 receptor. Previous VOCs such as Alpha and Delta only possess a few mutations that impact antibody recognition and ACE2 binding. However, with the widespread vaccination and infection of individuals, a stronger immune pressure over the virus emerged [23], leading to the appearance of highly mutated Spike variants [49]. Omicron and its subvariants have evolved to escape immune pressure [50,51]. However, some mutations appear to have been also selected for improved ACE2 interaction with BA.4/5 harbouring the L452R mutation, well-known to increase affinity for ACE2 while helping to evade immune responses [52].

Numerous studies offered strong evidence that temperature was a significant factor that can impact the aerosol transmission of SARS-CoV-2 [53]. How the improved Spike–ACE2 interaction at lower temperatures described in this manuscript affects viral transmission remains unknown. Further experiments in animal models will be required to address this question. However, with the constant evolution and selection of mutations leading to an increase in transmissibility and antigenic shift as seen for the Omicron lineage [54,55], it remains crucial to continue to study how these new selected mutations impact the interaction between the SARS-CoV-2 Spike and its human receptor, but also how temperature affects this interaction.

In summary, our results show that Omicron and its subvariant are sensitive to the effect of low temperature, though it is unclear whether this mechanism contributes to viral transmission or to the seasonality of VOCs. Our study indicates that the Spike–ACE2 affinity needs to be considered when evaluating the effect of temperature on SARS-CoV-2 transmission.

Acknowledgement

The authors thank the CRCHUM BSL3 and Flow Cytometry Platforms for technical assistance. We thank Stefan Pöhlmann (Georg-August University, Germany) for the plasmid coding for SARS-CoV-2 S glycoprotein and Dr. Jason McLellan for the plasmid coding for soluble ACE2. The CV3-25 mAb was produced using the pTT vector kindly provided by the Canada Research Council.

The views expressed in this manuscript are those of the authors and do not reflect the official policy or position of the Uniformed Services University, the U.S. Army, the Department of Defense, the National Institutes of Health, Department of Health and Human Services, or the U.S. Government, nor does mention of trade names, commercial products, or organisations imply endorsement by the U.S. Government.

The authors declare no competing interests.

3.7 References

1. Zhang, C.; Yang, M. Newly Emerged Antiviral Strategies for SARS-CoV-2: From Deciphering Viral Protein Structural Function to the Development of Vaccines, Antibodies, and Small Molecules. *Int J Mol Sci* **2022**, *23*, doi:10.3390/ijms23116083.
2. Polack, F.P.; Thomas, S.J.; Kitchin, N.; Absalon, J.; Gurtman, A.; Lockhart, S.; Perez, J.L.; Pérez Marc, G.; Moreira, E.D.; Zerbini, C.; et al. Safety and Efficacy of the BNT162b2 mRNA Covid-19 Vaccine. *New England Journal of Medicine* **2020**, *383*, 2603-2615, doi:10.1056/NEJMoa2034577.
3. Baden, L.R.; El Sahly, H.M.; Essink, B.; Kotloff, K.; Frey, S.; Novak, R.; Diemert, D.; Spector, S.A.; Rouphael, N.; Creech, C.B.; et al. Efficacy and Safety of the mRNA-1273 SARS-CoV-2 Vaccine. *New England Journal of Medicine* **2020**, *384*, 403-416, doi:10.1056/NEJMoa2035389.
4. Sadoff, J.; Gray, G.; Vandebosch, A.; Cárdenas, V.; Shukarev, G.; Grinsztejn, B.; Goepfert, P.A.; Truyers, C.; Fennema, H.; Spiessens, B.; et al. Safety and Efficacy of Single-Dose Ad26.COV2.S Vaccine against Covid-19. *New England Journal of Medicine* **2021**, *384*, 2187-2201, doi:10.1056/NEJMoa2101544.
5. Ionescu, I.G.; Skowronski, D.M.; Sauvageau, C.; Chuang, E.; Ouakki, M.; Kim, S.; De Serres, G. BNT162b2 effectiveness against Delta & Omicron variants in teens by dosing interval and duration. *medRxiv* **2022**, doi:10.1101/2022.06.27.22276790.
6. Kislaya, I.; Casaca, P.; Borges, V.; Sousa, C.; Ferreira, B.I.; Fernandes, E.; Dias, C.M.; Duarte, S.; Almeida, J.P.; Grenho, I.; et al. SARS-CoV-2 BA.5 vaccine breakthrough risk and severity compared with BA.2: a case-case and cohort study using Electronic Health Records in Portugal. *medRxiv* **2022**, doi:10.1101/2022.07.25.22277996.
7. Camacho, J.; Giménez, E.; Albert, E.; Zulaica, J.; Álvarez-Rodríguez, B.; Torres, I.; Rusu, L.; Burgos, J.S.; Peiró, S.; Vanaclocha, H.; et al. Cumulative incidence of SARS-CoV-2 infection in the general population of the Valencian Community (Spain) after the surge of the Omicron BA.1 variant. *medRxiv* **2022**, doi:10.1101/2022.07.19.22277747.
8. Hoffmann, M.; Kleine-Weber, H.; Schroeder, S.; Kruger, N.; Herrler, T.; Erichsen, S.; Schiergens, T.S.; Herrler, G.; Wu, N.H.; Nitsche, A.; et al. SARS-CoV-2 Cell Entry Depends on ACE2 and TMPRSS2 and Is Blocked by a Clinically Proven Protease Inhibitor. *Cell* **2020**, *181*, 271-280 e278, doi:10.1016/j.cell.2020.02.052.
9. Shang, J.; Ye, G.; Shi, K.; Wan, Y.; Luo, C.; Aihara, H.; Geng, Q.; Auerbach, A.; Li, F. Structural basis of receptor recognition by SARS-CoV-2. *Nature* **2020**, *581*, 221-224, doi:10.1038/s41586-020-2179-y.
10. Walls, A.C.; Xiong, X.; Park, Y.J.; Tortorici, M.A.; Snijder, J.; Quispe, J.; Cameroni, E.; Gopal, R.; Dai, M.; Lanzavecchia, A.; et al. Unexpected Receptor Functional Mimicry Elucidates Activation of Coronavirus Fusion. *Cell* **2019**, *176*, 1026-1039.e1015, doi:10.1016/j.cell.2018.12.028.
11. Walls, A.C.; Park, Y.J.; Tortorici, M.A.; Wall, A.; McGuire, A.T.; Veesler, D. Structure, Function, and Antigenicity of the SARS-CoV-2 Spike Glycoprotein. *Cell* **2020**, *181*, 281-292.e286, doi:10.1016/j.cell.2020.02.058.
12. Wrapp, D.; Wang, N.; Corbett, K.S.; Goldsmith, J.A.; Hsieh, C.L.; Abiona, O.; Graham, B.S.; McLellan, J.S. Cryo-EM structure of the 2019-nCoV spike in the prefusion conformation. *Science* **2020**, *367*, 1260-1263, doi:10.1126/science.abb2507.

13. Cai, Y.; Zhang, J.; Xiao, T.; Peng, H.; Sterling, S.M.; Walsh, R.M., Jr.; Rawson, S.; Rits-Volloch, S.; Chen, B. Distinct conformational states of SARS-CoV-2 spike protein. *Science* **2020**, *369*, 1586-1592, doi:10.1126/science.abd4251.
14. Lan, J.; Ge, J.; Yu, J.; Shan, S.; Zhou, H.; Fan, S.; Zhang, Q.; Shi, X.; Wang, Q.; Zhang, L.; et al. Structure of the SARS-CoV-2 spike receptor-binding domain bound to the ACE2 receptor. *Nature* **2020**, *581*, 215-220, doi:10.1038/s41586-020-2180-5.
15. Yan, R.; Zhang, Y.; Li, Y.; Xia, L.; Guo, Y.; Zhou, Q. Structural basis for the recognition of SARS-CoV-2 by full-length human ACE2. *Science* **2020**, *367*, 1444-1448, doi:10.1126/science.abb2762.
16. Li, W.; Chen, Y.; Prévost, J.; Ullah, I.; Lu, M.; Gong, S.Y.; Tauzin, A.; Gasser, R.; Vézina, D.; Anand, S.P.; et al. Structural basis and mode of action for two broadly neutralizing antibodies against SARS-CoV-2 emerging variants of concern. *Cell Rep* **2021**, *38*, 110210, doi:10.1016/j.celrep.2021.110210.
17. Ding, S.; Ullah, I.; Gong, S.Y.; Grover, J.R.; Mohammadi, M.; Chen, Y.; Vézina, D.; Beaudoin-Bussières, G.; Verma, V.T.; Goyette, G.; et al. VE607 stabilizes SARS-CoV-2 Spike in the "RBD-up" conformation and inhibits viral entry. *iScience* **2022**, *25*, 104528, doi:10.1016/j.isci.2022.104528.
18. Lu, M.; Uchil, P.D.; Li, W.; Zheng, D.; Terry, D.S.; Gorman, J.; Shi, W.; Zhang, B.; Zhou, T.; Ding, S.; et al. Real-Time Conformational Dynamics of SARS-CoV-2 Spikes on Virus Particles. *Cell Host Microbe* **2020**, *28*, 880-891.e888, doi:10.1016/j.chom.2020.11.001.
19. Ullah, I.; Prevost, J.; Ladinsky, M.S.; Stone, H.; Lu, M.; Anand, S.P.; Beaudoin-Bussieres, G.; Symmes, K.; Benlarbi, M.; Ding, S.; et al. Live imaging of SARS-CoV-2 infection in mice reveals that neutralizing antibodies require Fc function for optimal efficacy. *Immunity* **2021**, *54*, 2143-2158 e2115, doi:10.1016/j.immuni.2021.08.015.
20. Yang, Z.; Han, Y.; Ding, S.; Shi, W.; Zhou, T.; Finzi, A.; Kwong, P.D.; Mothes, W.; Lu, M. SARS-CoV-2 Variants Increase Kinetic Stability of Open Spike Conformations as an Evolutionary Strategy. *mBio* **2022**, e0322721, doi:10.1128/mbio.03227-21.
21. Guo, H.; Gao, Y.; Li, T.; Li, T.; Lu, Y.; Zheng, L.; Liu, Y.; Yang, T.; Luo, F.; Song, S.; et al. Structures of Omicron spike complexes and implications for neutralizing antibody development. *Cell Rep* **2022**, *39*, 110770, doi:10.1016/j.celrep.2022.110770.
22. Diaz-Salinas, M.A.; Li, Q.; Ejemel, M.; Yurkovetskiy, L.; Luban, J.; Shen, K.; Wang, Y.; Munro, J.B. Conformational dynamics and allosteric modulation of the SARS-CoV-2 spike. *Elife* **2022**, *11*, doi:10.7554/eLife.75433.
23. Prévost, J.; Finzi, A. The great escape? SARS-CoV-2 variants evading neutralizing responses. *Cell Host Microbe* **2021**, *29*, 322-324, doi:10.1016/j.chom.2021.02.010.
24. CDC. COVID Data Tracker - Variant Proportions.**2022**.Accessed July 6th, 2022
25. Viana, R.; Moyo, S.; Amoako, D.G.; Tegally, H.; Scheepers, C.; Althaus, C.L.; Anyaneji, U.J.; Bester, P.A.; Boni, M.F.; Chand, M.; et al. Rapid epidemic expansion of the SARS-CoV-2 Omicron variant in southern Africa. *Nature* **2022**, *603*, 679-686, doi:10.1038/s41586-022-04411-y.
26. Gangavarapu, K.; Latif, A.A.; Mullen, J.L.; Alkuzweny, M.; Hufbauer, E.; Tsueng, G.; Haag, E.; Zeller, M.; Aceves, C.M.; Zaiets, K.; et al. Outbreak.info genomic reports: scalable and dynamic surveillance of SARS-CoV-2 variants and mutations. *medRxiv* **2022**, 2022.2001.2027.22269965, doi:10.1101/2022.01.27.22269965.
27. Tsueng, G.; Mullen, J.L.; Alkuzweny, M.; Cano, M.; Rush, B.; Haag, E.; Outbreak, C.; Latif, A.A.; Zhou, X.; Qian, Z.; et al. Outbreak.info Research Library: A standardized,

searchable platform to discover and explore COVID-19 resources. *bioRxiv* **2022**, 2022.2001.2020.477133, doi:10.1101/2022.01.20.477133.
28. Bowen, J.E.; Addetia, A.; Dang, H.V.; Stewart, C.; Brown, J.T.; Sharkey, W.K.; Sprouse, K.R.; Walls, A.C.; Mazzitelli, I.G.; Logue, J.K.; et al. Omicron spike function and neutralizing activity elicited by a comprehensive panel of vaccines. *Science* **2022**, eabq0203, doi:10.1126/science.abq0203.
29. Hachmann, N.P.; Miller, J.; Collier, A.Y.; Ventura, J.D.; Yu, J.; Rowe, M.; Bondzie, E.A.; Powers, O.; Surve, N.; Hall, K.; et al. Neutralization Escape by SARS-CoV-2 Omicron Subvariants BA.2.12.1, BA.4, and BA.5. *N Engl J Med* **2022**, *387*, 86-88, doi:10.1056/NEJMc2206576.
30. Dejnirattisai, W.; Huo, J.; Zhou, D.; Zahradník, J.; Supasa, P.; Liu, C.; Duyvesteyn, H.M.E.; Ginn, H.M.; Mentzer, A.J.; Tuekprakhon, A.; et al. SARS-CoV-2 Omicron-B.1.1.529 leads to widespread escape from neutralizing antibody responses. *Cell* **2022**, *185*, 467-484.e415, doi:10.1016/j.cell.2021.12.046.
31. Gobeil, S.M.; Henderson, R.; Stalls, V.; Janowska, K.; Huang, X.; May, A.; Speakman, M.; Beaudoin, E.; Manne, K.; Li, D.; et al. Structural diversity of the SARS-CoV-2 Omicron spike. *Mol Cell* **2022**, *82*, 2050-2068.e2056, doi:10.1016/j.molcel.2022.03.028.
32. McCallum, M.; Czudnochowski, N.; Rosen Laura, E.; Zepeda Samantha, K.; Bowen John, E.; Walls Alexandra, C.; Hauser, K.; Joshi, A.; Stewart, C.; Dillen Josh, R.; et al. Structural basis of SARS-CoV-2 Omicron immune evasion and receptor engagement. *Science* **2022**, *375*, 864-868, doi:10.1126/science.abn8652.
33. Wang, Q.; Anang, S.; Iketani, S.; Guo, Y.; Liu, L.; Katsamba, P.S.; Shapiro, L.; Ho, D.D.; Sodroski, J.G. Functional properties of the spike glycoprotein of the emerging SARS-CoV-2 variant B.1.1.529. *Cell Reports* **2022**, *39*, doi:10.1016/j.celrep.2022.110924.
34. Qu, P.; Faraone, J.; Evans, J.P.; Zou, X.; Zheng, Y.M.; Carlin, C.; Bednash, J.S.; Lozanski, G.; Mallampalli, R.K.; Saif, L.J.; et al. Neutralization of the SARS-CoV-2 Omicron BA.4/5 and BA.2.12.1 Subvariants. *N Engl J Med* **2022**, *386*, 2526-2528, doi:10.1056/NEJMc2206725.
35. Evans, J.P.; Zeng, C.; Qu, P.; Faraone, J.; Zheng, Y.M.; Carlin, C.; Bednash, J.S.; Zhou, T.; Lozanski, G.; Mallampalli, R.; et al. Neutralization of SARS-CoV-2 Omicron sub-lineages BA.1, BA.1.1, and BA.2. *Cell Host Microbe* **2022**, *30*, 1093-1102.e1093, doi:10.1016/j.chom.2022.04.014.
36. Kuba, K.; Yamaguchi, T.; Penninger, J.M. Angiotensin-Converting Enzyme 2 (ACE2) in the Pathogenesis of ARDS in COVID-19. *Frontiers in Immunology* **2021**, *12*, doi:10.3389/fimmu.2021.732690.
37. Tortorici, M.A.; Veesler, D. Structural insights into coronavirus entry. *Adv Virus Res* **2019**, *105*, 93-116, doi:10.1016/bs.aivir.2019.08.002.
38. Prévost, J.; Richard, J.; Gasser, R.; Ding, S.; Fage, C.; Anand, S.P.; Adam, D.; Gupta Vergara, N.; Tauzin, A.; Benlarbi, M.; et al. Impact of temperature on the affinity of SARS-CoV-2 Spike glycoprotein for host ACE2. *J Biol Chem* **2021**, *297*, 101151, doi:10.1016/j.jbc.2021.101151.
39. Beaudoin-Bussieres, G.; Laumaea, A.; Anand, S.P.; Prevost, J.; Gasser, R.; Goyette, G.; Medjahed, H.; Perreault, J.; Tremblay, T.; Lewin, A.; et al. Decline of Humoral Responses against SARS-CoV-2 Spike in Convalescent Individuals. *mBio* **2020**, *11*, doi:10.1128/mBio.02590-20.

40. Chatterjee, D.; Tauzin, A.; Marchitto, L.; Gong, S.Y.; Boutin, M.; Bourassa, C.; Beaudoin-Bussières, G.; Bo, Y.; Ding, S.; Laumaea, A.; et al. SARS-CoV-2 Omicron Spike recognition by plasma from individuals receiving BNT162b2 mRNA vaccination with a 16-week interval between doses. *Cell Rep* **2022**, 110429, doi:10.1016/j.celrep.2022.110429.
41. Anand, S.P.; Chen, Y.; Prevost, J.; Gasser, R.; Beaudoin-Bussieres, G.; Abrams, C.F.; Pazgier, M.; Finzi, A. Interaction of Human ACE2 to Membrane-Bound SARS-CoV-1 and SARS-CoV-2 S Glycoproteins. *Viruses* **2020**, *12*, doi:10.3390/v12101104.
42. Emi, N.; Friedmann, T.; Yee, J.K. Pseudotype formation of murine leukemia virus with the G protein of vesicular stomatitis virus. *J Virol* **1991**, *65*, 1202-1207, doi:10.1128/JVI.65.3.1202-1207.1991.
43. Ding, S.; Laumaea, A.; Benlarbi, M.; Beaudoin-Bussières, G.; Gasser, R.; Medjahed, H.; Pancera, M.; Stamatatos, L.; McGuire, A.T.; Bazin, R.; et al. Antibody Binding to SARS-CoV-2 S Glycoprotein Correlates with but Does Not Predict Neutralization. *Viruses* **2020**, *12*, doi:10.3390/v12111214.
44. Gong, S.Y.; Chatterjee, D.; Richard, J.; Prévost, J.; Tauzin, A.; Gasser, R.; Bo, Y.; Vézina, D.; Goyette, G.; Gendron-Lepage, G.; et al. Contribution of single mutations to selected SARS-CoV-2 emerging variants spike antigenicity. *Virology* **2021**, *563*, 134-145, doi:https://doi.org/10.1016/j.virol.2021.09.001.
45. Costello, S.M.; Shoemaker, S.R.; Hobbs, H.T.; Nguyen, A.W.; Hsieh, C.L.; Maynard, J.A.; McLellan, J.S.; Pak, J.E.; Marqusee, S. The SARS-CoV-2 spike reversibly samples an open-trimer conformation exposing novel epitopes. *Nat Struct Mol Biol* **2022**, *29*, 229-238, doi:10.1038/s41594-022-00735-5.
46. Henderson, R.; Edwards, R.J.; Mansouri, K.; Janowska, K.; Stalls, V.; Gobeil, S.M.C.; Kopp, M.; Li, D.; Parks, R.; Hsu, A.L.; et al. Controlling the SARS-CoV-2 spike glycoprotein conformation. *Nature Structural & Molecular Biology* **2020**, *27*, 925-933, doi:10.1038/s41594-020-0479-4.
47. Stalls, V.; Lindenberger, J.; Gobeil, S.M.; Henderson, R.; Parks, R.; Barr, M.; Deyton, M.; Martin, M.; Janowska, K.; Huang, X.; et al. Cryo-EM structures of SARS-CoV-2 Omicron BA.2 spike. *Cell Rep* **2022**, *39*, 111009, doi:10.1016/j.celrep.2022.111009.
48. Zhao, Z.; Zhou, J.; Tian, M.; Huang, M.; Liu, S.; Xie, Y.; Han, P.; Bai, C.; Han, P.; Zheng, A.; et al. Omicron SARS-CoV-2 mutations stabilize spike up-RBD conformation and lead to a non-RBM-binding monoclonal antibody escape. *Nature Communications* **2022**, *13*, 4958, doi:10.1038/s41467-022-32665-7.
49. Yamasoba, D.; Kimura, I.; Nasser, H.; Morioka, Y.; Nao, N.; Ito, J.; Uriu, K.; Tsuda, M.; Zahradnik, J.; Shirakawa, K.; et al. Virological characteristics of the SARS-CoV-2 Omicron BA.2 spike. *Cell* **2022**, *185*, 2103-2115.e2119, doi:10.1016/j.cell.2022.04.035.
50. Planas, D.; Saunders, N.; Maes, P.; Guivel-Benhassine, F.; Planchais, C.; Buchrieser, J.; Bolland, W.H.; Porrot, F.; Staropoli, I.; Lemoine, F.; et al. Considerable escape of SARS-CoV-2 Omicron to antibody neutralization. *Nature* **2022**, *602*, 671-675, doi:10.1038/s41586-021-04389-z.
51. Liu, C.; Ginn, H.M.; Dejnirattisai, W.; Supasa, P.; Wang, B.; Tuekprakhon, A.; Nutalai, R.; Zhou, D.; Mentzer, A.J.; Zhao, Y.; et al. Reduced neutralization of SARS-CoV-2 B.1.617 by vaccine and convalescent serum. *Cell* **2021**, *184*, 4220-4236.e4213, doi:10.1016/j.cell.2021.06.020.

52. Deng, X.; Garcia-Knight, M.A.; Khalid, M.M.; Servellita, V.; Wang, C.; Morris, M.K.; Sotomayor-González, A.; Glasner, D.R.; Reyes, K.R.; Gliwa, A.S.; et al. Transmission, infectivity, and neutralization of a spike L452R SARS-CoV-2 variant. *Cell* **2021**, doi:10.1016/j.cell.2021.04.025.
53. Asif, Z.; Chen, Z.; Stranges, S.; Zhao, X.; Sadiq, R.; Olea-Popelka, F.; Peng, C.; Haghighat, F.; Yu, T. Dynamics of SARS-CoV-2 spreading under the influence of environmental factors and strategies to tackle the pandemic: A systematic review. *Sustainable Cities and Society* **2022**, *81*, 103840, doi:https://doi.org/10.1016/j.scs.2022.103840.
54. Shrestha, L.B.; Foster, C.; Rawlinson, W.; Tedla, N.; Bull, R.A. Evolution of the SARS-CoV-2 omicron variants BA.1 to BA.5: Implications for immune escape and transmission. *Reviews in Medical Virology* **2022**, *n/a*, e2381, doi:https://doi.org/10.1002/rmv.2381.
55. Telenti, A.; Hodcroft, E.B.; Robertson, D.L. The Evolution and Biology of SARS-CoV-2 Variants. *Cold Spring Harb Perspect Med* **2022**, *12*, doi:10.1101/cshperspect.a041390.

CHAPTER 4. DISCUSSION

4.1 Summary of findings

Since its rapid emergence towards the end of 2019, humanity has lived through numerous waves of SARS-CoV-2 variants. From the original strain, the virus has undergone numerous mutations, giving rise to variants with distinctive Spikes and unique immunogenic signatures.

In this thesis, we have first investigated the contribution of each single mutation to the Spike antigenicity of a few VOCs. We have found that single mutations cannot be used to predict the overall Spike phenotype, both in terms of the Spike – ACE2 interactions and plasma antibodies recognition. First, while plasma from vaccinated SARS-CoV-2 naïve and previously-infected individuals efficiently recognized the VOC Spikes tested, plasma from vaccinated previously-infected individuals show a more robust recognition of the Spikes compared to naïve individuals following one dose of mRNA vaccine, thus supporting the notion that hybrid immunity is superior than vaccination alone [166,185] Mutations which affect plasma Spike recognition include the Δ144 deletion, K417N/T mutation, E484K, P681H, and S982A mutations [134].

Second, while temperature has been found to play a role in aerosol transmission of SARS-CoV-2, we have found that it also affects Spike – ACE2 binding. Some notable single mutations which enhance the affinity of the Spike with the ACE2 receptor and overcame the temperature requirement include N501Y and L452R. While the transmission of SARS-CoV-2 has been suggested to be optimal at 5-15°C, enhanced ACE2 binding at warmer temperatures would suggest that the virus would be able to infect efficiently in the warm seasons, and even higher transmissibility in colder seasons.

Then, we have investigated the most recent VOC Omicron's ability to interact with the ACE2 receptor. We have found that Omicron Spikes' interactions with ACE2 are highly sensitive to colder temperatures. Visualization by Cryo-EM and single molecule Förster resonance energy transfer (smFRET) show that the Spike interacts with ACE2 in its "Up" conformation [67,78]. Therefore, increased ACE2 binding in colder conditions may suggest that SARS-CoV-2 Spikes

are more prone to adopt the "RBD up" conformation to increase interactions with its receptor in colder temperatures, despite it sampling a "down" conformation in warmer environments.

We also looked at the mechanism by which the Spike may increase its interaction with ACE2 by calculating the Hill coefficient of this interaction in both warm and cold temperatures for the Omicron subvariants in circulation at the time of writing. The Hill coefficient measures the cooperativity of a protein binding to its ligand. A positive cooperativity is translated to a Hill coefficient that is above 1. Our results suggest that in warm temperatures, Omicron Spikes are not prone to bind the ACE2 receptor no matter the concentration of ACE2 it is exposed to. However, at cold temperatures, Omicron subvariant Spikes all became more sensitive to increasing ACE2 concentrations, creating a steep dose-response curve, which would suggest that each individual protomer binding would trigger the others to bind (i.e., positive cooperativity). Therefore, the sensitivity of Omicron to colder temperatures can be speculated to be derived from its facility to change conformations once one of the three protomers is bound to an ACE2 receptor.

4.2 Contribution to knowledge

SARS-CoV-2 Spike draws many similarities to the HIV-1 Envelope (Env) – they are both heavily glycosylated, both can sample multiple conformations, both harbour numerous mutations which can make them favor different conformational states. However, as opposed to HIV, vaccines against SARS-CoV-2 elicit effective non-neutralizing Abs after a single dose of mRNA vaccines in non-immunocompromised individuals [166], and neutralizing Abs after two doses [164]. In vaccine efficacy trials, the protective capacities conferred by SARS-CoV-2 vaccines are massively superior to any of the HIV vaccine candidates, with the highest protection rate (RV144 trial, 31.2%) [233], – even considering the emergence of variants. One reason for this is due to the antigenic profile of the vaccine – whereas the Spike presented in SARS-CoV-2 vaccines is stabilized in the prefusion state, Env examined for HIV-1 vaccines pre-clinical trials are stabilized in a conformation which is not in its ground state [234-237], but rather a downstream conformation which is not readily exposed [234]. With SARS-CoV-2, the goal of a vaccine was first to prevent the infection, however it has now evolved into preventing severe disease due to the emergence of numerous variants which have high immune evasion capacities. However, the caveat with a

vaccine that only protects against severe disease remains that the vaccinated individual may still transmit the virus, allowing sustained spread within populations [178].

Since the emergence of the first D614G single mutation, increasing fitness, infectivity, and viral production, antigenic drift has been and remains a concern [232,238]. Natural infection and/or vaccination against SARS-CoV-2 elicit both cellular and humoral immune responses. The cellular immune response can be stimulated starting from a single dose of the mRNA vaccine [166] and memory T and B cells form following two doses of vaccines [187]. In the case of an infection, an insufficient T cell response is associated with severe disease and death [157], and T cells can successfully clear out the virus in the absence of antibodies [239]. On the other hand, the humoral immune response includes production of neutralizing and non-neutralizing antibodies, some of which mediating Fc-effector functions. Antibodies elicited by vaccination against SARS-CoV-2 are vastly neutralizing and most target the RBD of the Spike glycoprotein, with some targeting the NTD and others the S2 subunit [164,165,240-242]. The sustained transmission as well as immune pressure against the Spike has selected numerous adaptive mutations which favored the virus to stay undetected by the host immune system. Some mutations contributing to the immune evasion ability include the RBD mutations K417N/T, L452R, and E484K, in accordance with previous reports [132]. Additionally, the NTD is a highly variable site which differs from variant to variant, and multiple mutations present in the NTD can efficiently evade Abs recognition by both naturally infected and naïve vaccinated individuals [134]. With a large portion of the population receiving two or three doses of the SARS-CoV-2 mRNA vaccines which contains the ancestral Wuhan strain, the most recent variant Omicron harbor a large number of mutations which have been characterized to evade Abs recognition and decrease sustainability of a humoral response induced by vaccination [186].

Another positive selection of mutations permits the improvement of the virus' affinity to its primary receptor ACE2. In fact, the N501Y mutation which appeared in the first VOC, Alpha, has been shared by subsequent VOCs Beta and Gamma, and is still present in all current VOC Omicron subvariants [147,243]. The only variant that does not share this mutation is Delta, which possesses in turn the L452R mutation, which has been shown to increase affinity for ACE2 and evade immune responses [136]. This leads us to the question – what is the ultimate hallmark of a

competitive variant? In other words, how can we predict which is the next VOC which will be highly transmissible within the human population? A recent study highlights the importance of compensatory epistasis which results from the interaction of multiple mutations [244]. Compensatory epistasis could be summarized as adaptative interactions between genes which make up the loss of a given phenotype. It has been observed in other RNA viruses such as VSV, where deleterious mutations were met with compensatory mutations which allowed the reversion to WT or a higher fitness variant [245]. In the case of SARS-CoV-2, according to Moulana *et al.*, escape mutations in the RBD which decrease binding affinity to ACE2 can be rescued by the N501Y mutation, inducing even stronger ACE2 binding in some cases (e.g. N501Y combined with Q498R) [244]. This would highlight that selection for a competitive virus includes – high levels of immune evasion, and unaffected or improved affinity to ACE2 recognition and affinity. With now several waves of variants, the recurring mutations which are observed once and again such as D614G, K417N, L452R, E484K, and N501Y seem to contribute to the "winning" formula of the emerging variants, as illustrated by the long-reigning Omicron subvariants, which harbor all the aforementioned mutations [147].

As to the role which temperature plays in the conformation of the Spike glycoprotein, previous studies have shown that colder temperature may enhance the propensity of the Spike to sample the "Up" conformation, but the addition of the N501Y mutation could overcome the temperature requirement [127]. As for Omicron, several studies have shown that its numerous mutations stabilize the RBD in the "down" conformation [74,246-248], but our project suggests that the Spike remains very sensitive to ACE2 at low temperatures [147]. This could be explained by improved protomer cooperativity upon ACE2 interaction and more stable binding of the RBD to its receptor.

SARS-CoV-2 transmission conditions has been suggested to be optimal in temperatures ranging from 5-15°C [249]. A variant which can overcome the low temperature requirements to bind ACE2 with higher affinity in high temperatures would suggest that it could overtake another which is not able to do so in warmer climates. Further, in the human body, SARS-CoV-2 is confronted to a temperature gradient from the outside environment across the human airway during airway transmission. The temperature is around 30 to 32°C in the mucosa, but increases to 32°C in the

upper trachea then to 36°C in the bronchi [250,251]. Since SARS-CoV-2 has been shown to have better replication in cells at 33°C than at 37°C [252], and high temperature impedes viral replication, the fact that the Spike adapts to have increased interactions with ACE2 at higher temperature means that it may have higher transmissibility at higher temperatures too, while the implications for lower temperature remains that the chances of increased transmissibility and replication are even further enhanced.

4.3 Significance

4.3.1 The importance of single mutations

In Chapter 2, we studied the impact of single mutations in ACE2 binding and immune evasion of vaccinated SARS-CoV-2 naïve and previously infected individuals. While they are not completely predictable of the full Spike phenotype, they remain very informative about the Ab binding capacity [77,132], neutralization effect [209], the Fc-effector functions associated with them [76], and their ACE2 interactions [134].

Strikingly, we can observe a convergence in the incorporation of single mutations – despite being extremely divergent from Delta and all previous VOCs, Omicron carries a multitude of recurrent mutations, such as K417N from Beta; BA4/5 and BA2.12.1 carry L452R first seen in Epsilon then in Delta; T478K from Delta; E484A, previously E484K in Beta and Gamma; N501Y from Alpha, Beta and Gamma; and interestingly, P681H mutation from Alpha as well [243]. All these aforementioned recurring mutations have been characterized to have exceptional functions in one of the following areas: immune evasion (K417N, L452R, T478K, E484A, P681H) [129,132,135,253], enhanced ACE2 binding (L452R, N501Y) [127,136], increased transmission, stability and infectivity (D614G) [118,119], and cleavage (P681H) [244,254]. For a variant with such a high number of mutations such as Omicron, the existing body of literature on single mutations has been greatly helpful in contributing to the understanding of the phenotype of this variant. However, one caveat remains that single mutations do not encompass the compensatory effects of mutations with one another when they appear in newly formed clusters.

Interestingly, all the tested Omicron subvariants Spikes, with the exception of BA.4/5, did not show increased ACE2 binding at warmer temperatures compared to D614G [147]. However, newly emerging subvariants following BA.5 such as BQ1.1 and XBB.1 showed increased immune evasion capacities [255] despite not having enhanced ACE2 interactions compared to BA.5 [256]. At the time of the thesis revision, XBB.1.5 is the main circulating variant in the United States and Canada [122,123]. With a single major mutation change (S486P) compared to its predecessor XBB.1, XBB.1.5 Spikes have shown increased ACE2 interactions, with even higher immune evasion capacities than the previous variants [256,257]. These trends would once again indicate that increased transmission and propagation is strongly linked to both enhanced ACE2 affinity and immune evasion.

Conversely, for the non-overlapping, unique mutations in the RBD, which are highly variable between VOCs, one can observe that their primary function would be to exert immune evasion. Interestingly, Omicron's unique RBD mutations which reduce ACE2 binding in favor of Ab escape, such as Q493R, G496S, Q498R [258], have been shown to be rescued thanks to compensatory epistasis, phenomenon which occurs when two mutations in proximity to each other interact with each other, resulting in strong positive effect for ACE2 binding. In the case of Omicron, a combination of four RBD mutations: Q498R, G496S, N501Y, and Y505H, has been suggested to result in an increase in ACE2 interaction [244]. Some other mutations unique to Omicron include S371L, S373P, and S375F, which have been shown to stabilize the Spike tightly in a "RBD down" conformation [246]. These mutations would prevent Abs from recognizing the RBD, since the "down" conformation is occluded by a glycan shield [259].

As well, studying the effect of single mutations could be used to help the development of methodologies such as deep mutational scanning (DMS), which is a high-throughput method using computational analyses that can be applied to measure the functional effects of single mutations in proteins [132,260]. The *in vitro* studies of single mutations can contribute to the library of variants which are used to study the phenotypes of protein which harbor any combination of such mutations [260]. Further, the results from *in vitro* functional data may be used to confirm the phenotype for the accuracy of the predictions generated by DMS.

4.3.2 Implications for increased Spike—ACE2 cooperativity in the cold

By determining the Spike – ACE2 cooperativity by measuring the Hill coefficient, we have shown that Spike Omicron subvariants bind ACE2 better at colder temperatures [147]. This would suggest that the functionality of these variants could be enhanced at low temperature. Our results offer unique insight as to how ACE2 – Spike interactions may be improved in colder environments.

4.4 Experimental Limitations

In this thesis, we measured the interaction of the Spike with the ACE2 receptor mostly by using Flow Cytometry and BLI. From ACE2-Fc or sACE2 antibodies binding to the Spike, we could infer that the Spike is more prone to sampling the "up" conformation, since Spike interacts with ACE2 in this state [61,68]. However, a main limitation of flow cytometry is that we do not directly show the conformational dynamics changes of the Spike in varying temperatures. Furthermore, virus capture assay, another method used in this thesis, uses virus-like particles and not real virus. Both of these techniques' limitations can be overcome by further visualization experiments such as Cryo-electron microscopy (cryo-EM) and/or smFRET. These techniques could be used in order to show the effect of cold temperatures on the conformation of the Spike with or without the presence of ACE2. Cryo-EM would allow a direct visualization of the Spike through imaging [61] and smFRET would give us more information on the conformational dynamics of the Spike on the surface of virions [67].

4.5 Next Steps

Since we have shown earlier that low temperatures increase the Omicron Spike – ACE2 interactions, the next step would be to quantify by the molecular mechanism behind this phenotype. To do this, we could measure the entropy of the RBD – receptor binding. It has been recently shown that N501Y mutation in the RBD creates an enthalpic compensation, by creating less favorable enthalpy for binding and more favorable entropy for binding which results in increased binding overall affinity (low K_{dis}) and bypassing the decrease in binding affinity in warmer temperatures [261]. Mechanistically, this would suggest that the N501Y mutation makes the Spike more flexible – prone to conformational changes [261]. Since Omicron RBD also harbors

N501Y mutation, it would be interesting to examine the interaction of Omicron subvariants RBD with ACE2 in order to ascertain the cooperativity of the Spike with ACE2 from an entropic standpoint.

Furthermore, as mentioned above, it would be interesting to visualize how the Spike conformation on lentiviral particles changes in different temperatures. To do so, we could use smFRET, a technique which has previously been used to distinguish conformational states on viral surfaces [67]. SmFRET involves measuring the real-time conformational transitions of a protein by measuring the energy transferred between a donor and an acceptor fluorophore on a single molecule [262]. To set up the experiment, we would need to have viral particles which express a single Spike on its surface expressing the donor and acceptor fluorophores before and after the RBM [67]. Then, we would measure the frequency of state occupancy over time of the RBM in cold and warm temperatures, in the presence or absence of ACE2 ligand. Results resulting from such experiment would inform us of whether the SARS-CoV-2 Omicron subvariants Spikes would be more prone to sample the "Up" conformation.

4.6 Outstanding Questions

Previous studies have demonstrated that temperature had an effect on aerosol transmission of SARS-CoV-2 [263]. As well, the longest circulating variant Omicron has been shown to be sensitive to colder temperatures [147]. However, whether this mechanism contribute to viral transmission in the population, or the seasonality of VOCs remain unanswered. One way to study this mechanism would be to continue monitoring the emerging variants, and study the correlation of temperature in response to the variant Spike – ACE2 affinity using modelling based on the retrospective trends of infection [264]. Another way of inspecting whether enhanced Spike – ACE2 interaction plays a role in transmission would be to use animal models. Due to its nature as a zoonotic virus, numerous animals are permissive to SARS-CoV-2 infection [265,266]. A proposed model to study transmission would be ferrets, since ferrets allow for the transmission of SARS-CoV-2 through direct contact and through airborne transmission [267]. As well, SARS-CoV-2 viral load can be detected from nasal and oropharyngeal swabs [267]. In order to optimally detect transmission of SARS-CoV-2 from infected ferrets to healthy ferrets and assess the impact

of temperature on transmission, one would first infect two groups of ferrets with the variant of interest, Omicron, and the second group with Wuhan strain. Then, we would expose two groups of healthy ferrets for each infection conditions – one in warm temperatures and one in colder temperatures. By counting the number of ferrets which become infected by each strain, we would be able to detect whether increased ACE2 sensitivity in cold temperatures can really translate to increased transmissibility.

Another question would be whether SARS-CoV-2 will become a seasonal respiratory virus. There have been studies suggesting that SARS-CoV-2 is on its way to becoming an endemic virus [268], joining the ranks of influenza and other coronaviruses [269]. Characteristics of an endemic virus include seasonality, which allows them to avoid herd immunity from sustained transmission, efficient person-to-person infectivity, global spread, and limited severity [269]. However, with the insertion of the N501Y mutation which can overcome the low temperature requirement for the optimal engagement of ACE2 to Spike [127], it is possible that SARS-CoV-2 might not have a seasonality. Further, seasonality of a virus also depends on human behavior and as well as environmental factors such as humidity and temperature. Therefore, the only way to know whether SARS-CoV-2 will become seasonal would be to face the pandemic and continue monitoring the emerging variants.

CONCLUSION

Altogether, this thesis examined the phenotype of SARS-CoV-2 VOCs and VOIs with regard to their single mutations in terms of ACE2 interaction, antigenic profile, and infectivity. We first assessed the ability of single mutations' contribution to the interaction of the full VOC/VOI Spike with the ACE2 receptor. We found that single mutations cannot fully predict the phenotype of the full Spike in relation to their receptor binding and Ab recognition by plasma of infected and vaccinated individuals. In light of the Omicron subvariants, we then examined the ability of the different Omicron subvariant Spikes to interact with the ACE2 receptor, and found that despite harboring several mutations which have been shown to affect ACE2 binding, the Spikes become highly cooperative to ACE2 binding in colder temperatures.

To summarize, the Spike – ACE2 interaction of SARS-CoV-2 virus plays a crucial role in both the evolution of the virus, and in its infection process. Variants would find different ways to improve the ACE2 binding capacity – be it increasing the cooperativity to the receptor, or by increasing the affinity to it. Taken together, findings from this thesis highlight the importance of closely monitoring the functional properties of emerging variants with regards to their functional properties such as ACE2 binding and antibody evasion, and taking into account how temperature may affect these phenotypes. With the loosening of preventative measures, and the colder climate leading to increased human contacts, it is foreseeable that Omicron, or its subvariant, stay in circulation. The application of the research presented in this thesis has informed public health agencies and will hopefully contribute to understanding the mechanisms behind SARS-CoV-2 transmission to allow better prevention for future VOCs.

REFERENCES

1. Huang, C.; Wang, Y.; Li, X.; Ren, L.; Zhao, J.; Hu, Y.; Zhang, L.; Fan, G.; Xu, J.; Gu, X.; et al. Clinical features of patients infected with 2019 novel coronavirus in Wuhan, China. *Lancet* **2020**, *395*, 497-506, doi:10.1016/S0140-6736(20)30183-5.
2. WHO. WHO COVID-19 Dashboard. Available online: https://covid19.who.int (accessed on 13 October 2022).
3. Van Egeren, D.; Novokhodko, A.; Stoddard, M.; Tran, U.; Zetter, B.; Rogers, M.; Pentelute, B.L.; Carlson, J.M.; Hixon, M.; Joseph-McCarthy, D.; et al. Risk of rapid evolutionary escape from biomedical interventions targeting SARS-CoV-2 spike protein. *PLoS One* **2021**, *16*, e0250780, doi:10.1371/journal.pone.0250780.
4. Zhu, N.; Zhang, D.; Wang, W.; Li, X.; Yang, B.; Song, J.; Zhao, X.; Huang, B.; Shi, W.; Lu, R.; et al. A Novel Coronavirus from Patients with Pneumonia in China, 2019. *N Engl J Med* **2020**, *382*, 727-733, doi:10.1056/NEJMoa2001017.
5. Wu, F.; Zhao, S.; Yu, B.; Chen, Y.M.; Wang, W.; Song, Z.G.; Hu, Y.; Tao, Z.W.; Tian, J.H.; Pei, Y.Y.; et al. A new coronavirus associated with human respiratory disease in China. *Nature* **2020**, *579*, 265-269, doi:10.1038/s41586-020-2008-3.
6. Zhou, P.; Yang, X.L.; Wang, X.G.; Hu, B.; Zhang, L.; Zhang, W.; Si, H.R.; Zhu, Y.; Li, B.; Huang, C.L.; et al. A pneumonia outbreak associated with a new coronavirus of probable bat origin. *Nature* **2020**, *579*, 270-273, doi:10.1038/s41586-020-2012-7.
7. Woo, P.C.; Lau, S.K.; Lam, C.S.; Lau, C.C.; Tsang, A.K.; Lau, J.H.; Bai, R.; Teng, J.L.; Tsang, C.C.; Wang, M.; et al. Discovery of seven novel Mammalian and avian coronaviruses in the genus deltacoronavirus supports bat coronaviruses as the gene source of alphacoronavirus and betacoronavirus and avian coronaviruses as the gene source of gammacoronavirus and deltacoronavirus. *J Virol* **2012**, *86*, 3995-4008, doi:10.1128/JVI.06540-11.
8. Kan, B.; Wang, M.; Jing, H.; Xu, H.; Jiang, X.; Yan, M.; Liang, W.; Zheng, H.; Wan, K.; Liu, Q.; et al. Molecular evolution analysis and geographic investigation of severe acute respiratory syndrome coronavirus-like virus in palm civets at an animal market and on farms. *J Virol* **2005**, *79*, 11892-11900, doi:10.1128/JVI.79.18.11892-11900.2005.
9. Zaki, A.M.; van Boheemen, S.; Bestebroer, T.M.; Osterhaus, A.D.; Fouchier, R.A. Isolation of a novel coronavirus from a man with pneumonia in Saudi Arabia. *N Engl J Med* **2012**, *367*, 1814-1820, doi:10.1056/NEJMoa1211721.
10. Hon, C.C.; Lam, T.Y.; Shi, Z.L.; Drummond, A.J.; Yip, C.W.; Zeng, F.; Lam, P.Y.; Leung, F.C. Evidence of the recombinant origin of a bat severe acute respiratory syndrome (SARS)-like coronavirus and its implications on the direct ancestor of SARS coronavirus. *J Virol* **2008**, *82*, 1819-1826, doi:10.1128/JVI.01926-07.
11. Shi, Z.; Hu, Z. A review of studies on animal reservoirs of the SARS coronavirus. *Virus Res* **2008**, *133*, 74-87, doi:10.1016/j.virusres.2007.03.012.
12. Cui, J.; Li, F.; Shi, Z.L. Origin and evolution of pathogenic coronaviruses. *Nat Rev Microbiol* **2019**, *17*, 181-192, doi:10.1038/s41579-018-0118-9.
13. Su, S.; Wong, G.; Shi, W.; Liu, J.; Lai, A.C.K.; Zhou, J.; Liu, W.; Bi, Y.; Gao, G.F. Epidemiology, Genetic Recombination, and Pathogenesis of Coronaviruses. *Trends Microbiol* **2016**, *24*, 490-502, doi:10.1016/j.tim.2016.03.003.

14. Lam, T.T.; Jia, N.; Zhang, Y.W.; Shum, M.H.; Jiang, J.F.; Zhu, H.C.; Tong, Y.G.; Shi, Y.X.; Ni, X.B.; Liao, Y.S.; et al. Identifying SARS-CoV-2-related coronaviruses in Malayan pangolins. *Nature* **2020**, *583*, 282-285, doi:10.1038/s41586-020-2169-0.
15. MacLean, O.A.; Lytras, S.; Weaver, S.; Singer, J.B.; Boni, M.F.; Lemey, P.; Kosakovsky Pond, S.L.; Robertson, D.L. Natural selection in the evolution of SARS-CoV-2 in bats created a generalist virus and highly capable human pathogen. *PLoS Biol* **2021**, *19*, e3001115, doi:10.1371/journal.pbio.3001115.
16. Boni, M.F.; Lemey, P.; Jiang, X.; Lam, T.T.; Perry, B.W.; Castoe, T.A.; Rambaut, A.; Robertson, D.L. Evolutionary origins of the SARS-CoV-2 sarbecovirus lineage responsible for the COVID-19 pandemic. *Nat Microbiol* **2020**, *5*, 1408-1417, doi:10.1038/s41564-020-0771-4.
17. Li, W.; Shi, Z.; Yu, M.; Ren, W.; Smith, C.; Epstein, J.H.; Wang, H.; Crameri, G.; Hu, Z.; Zhang, H.; et al. Bats are natural reservoirs of SARS-like coronaviruses. *Science* **2005**, *310*, 676-679, doi:10.1126/science.1118391.
18. Valencak, T.G.; Csiszar, A.; Szalai, G.; Podlutsky, A.; Tarantini, S.; Fazekas-Pongor, V.; Papp, M.; Ungvari, Z. Animal reservoirs of SARS-CoV-2: calculable COVID-19 risk for older adults from animal to human transmission. *Geroscience* **2021**, *43*, 2305-2320, doi:10.1007/s11357-021-00444-9.
19. Ke, Z.; Oton, J.; Qu, K.; Cortese, M.; Zila, V.; McKeane, L.; Nakane, T.; Zivanov, J.; Neufeldt, C.J.; Cerikan, B.; et al. Structures and distributions of SARS-CoV-2 spike proteins on intact virions. *Nature* **2020**, *588*, 498-502, doi:10.1038/s41586-020-2665-2.
20. Walls, A.C.; Park, Y.J.; Tortorici, M.A.; Wall, A.; McGuire, A.T.; Veesler, D. Structure, Function, and Antigenicity of the SARS-CoV-2 Spike Glycoprotein. *Cell* **2020**, *181*, 281-292.e286, doi:10.1016/j.cell.2020.02.058.
21. Turonova, B.; Sikora, M.; Schurmann, C.; Hagen, W.J.H.; Welsch, S.; Blanc, F.E.C.; von Bulow, S.; Gecht, M.; Bagola, K.; Horner, C.; et al. In situ structural analysis of SARS-CoV-2 spike reveals flexibility mediated by three hinges. *Science* **2020**, *370*, 203-208, doi:10.1126/science.abd5223.
22. Venkatagopalan, P.; Daskalova, S.M.; Lopez, L.A.; Dolezal, K.A.; Hogue, B.G. Coronavirus envelope (E) protein remains at the site of assembly. *Virology* **2015**, *478*, 75-85, doi:10.1016/j.virol.2015.02.005.
23. Hurst, K.R.; Kuo, L.; Koetzner, C.A.; Ye, R.; Hsue, B.; Masters, P.S. A major determinant for membrane protein interaction localizes to the carboxy-terminal domain of the mouse coronavirus nucleocapsid protein. *J Virol* **2005**, *79*, 13285-13297, doi:10.1128/JVI.79.21.13285-13297.2005.
24. Lu, S.; Ye, Q.; Singh, D.; Cao, Y.; Diedrich, J.K.; Yates, J.R., 3rd; Villa, E.; Cleveland, D.W.; Corbett, K.D. The SARS-CoV-2 nucleocapsid phosphoprotein forms mutually exclusive condensates with RNA and the membrane-associated M protein. *Nat Commun* **2021**, *12*, 502, doi:10.1038/s41467-020-20768-y.
25. Shang, J.; Han, N.; Chen, Z.; Peng, Y.; Li, L.; Zhou, H.; Ji, C.; Meng, J.; Jiang, T.; Wu, A. Compositional diversity and evolutionary pattern of coronavirus accessory proteins. *Brief Bioinform* **2021**, *22*, 1267-1278, doi:10.1093/bib/bbaa262.
26. Redondo, N.; Zaldivar-Lopez, S.; Garrido, J.J.; Montoya, M. SARS-CoV-2 Accessory Proteins in Viral Pathogenesis: Knowns and Unknowns. *Front Immunol* **2021**, *12*, 708264, doi:10.3389/fimmu.2021.708264.

27. Gordon, D.E.; Jang, G.M.; Bouhaddou, M.; Xu, J.; Obernier, K.; White, K.M.; O'Meara, M.J.; Rezelj, V.V.; Guo, J.Z.; Swaney, D.L.; et al. A SARS-CoV-2 protein interaction map reveals targets for drug repurposing. *Nature* **2020**, *583*, 459-468, doi:10.1038/s41586-020-2286-9.
28. Kim, Y.M.; Shin, E.C. Type I and III interferon responses in SARS-CoV-2 infection. *Exp Mol Med* **2021**, *53*, 750-760, doi:10.1038/s12276-021-00592-0.
29. Xia, H.; Cao, Z.; Xie, X.; Zhang, X.; Chen, J.Y.; Wang, H.; Menachery, V.D.; Rajsbaum, R.; Shi, P.Y. Evasion of Type I Interferon by SARS-CoV-2. *Cell Rep* **2020**, *33*, 108234, doi:10.1016/j.celrep.2020.108234.
30. Fernandes, J.D.; Hinrichs, A.S.; Clawson, H.; Gonzalez, J.N.; Lee, B.T.; Nassar, L.R.; Raney, B.J.; Rosenbloom, K.R.; Nerli, S.; Rao, A.A.; et al. The UCSC SARS-CoV-2 Genome Browser. *Nat Genet* **2020**, *52*, 991-998, doi:10.1038/s41588-020-0700-8.
31. Lu, R.; Zhao, X.; Li, J.; Niu, P.; Yang, B.; Wu, H.; Wang, W.; Song, H.; Huang, B.; Zhu, N.; et al. Genomic characterisation and epidemiology of 2019 novel coronavirus: implications for virus origins and receptor binding. *Lancet* **2020**, *395*, 565-574, doi:10.1016/S0140-6736(20)30251-8.
32. Malone, B.; Urakova, N.; Snijder, E.J.; Campbell, E.A. Structures and functions of coronavirus replication-transcription complexes and their relevance for SARS-CoV-2 drug design. *Nat Rev Mol Cell Biol* **2022**, *23*, 21-39, doi:10.1038/s41580-021-00432-z.
33. Jungreis, I.; Sealfon, R.; Kellis, M. SARS-CoV-2 gene content and COVID-19 mutation impact by comparing 44 Sarbecovirus genomes. *Nat Commun* **2021**, *12*, 2642, doi:10.1038/s41467-021-22905-7.
34. Shang, J.; Ye, G.; Shi, K.; Wan, Y.; Luo, C.; Aihara, H.; Geng, Q.; Auerbach, A.; Li, F. Structural basis of receptor recognition by SARS-CoV-2. *Nature* **2020**, *581*, 221-224, doi:10.1038/s41586-020-2179-y.
35. Jia, H.P.; Look, D.C.; Shi, L.; Hickey, M.; Pewe, L.; Netland, J.; Farzan, M.; Wohlford-Lenane, C.; Perlman, S.; McCray, P.B., Jr. ACE2 receptor expression and severe acute respiratory syndrome coronavirus infection depend on differentiation of human airway epithelia. *J Virol* **2005**, *79*, 14614-14621, doi:10.1128/JVI.79.23.14614-14621.2005.
36. Sungnak, W.; Huang, N.; Becavin, C.; Berg, M.; Queen, R.; Litvinukova, M.; Talavera-Lopez, C.; Maatz, H.; Reichart, D.; Sampaziotis, F.; et al. SARS-CoV-2 entry factors are highly expressed in nasal epithelial cells together with innate immune genes. *Nat Med* **2020**, *26*, 681-687, doi:10.1038/s41591-020-0868-6.
37. Harmer, D.; Gilbert, M.; Borman, R.; Clark, K.L. Quantitative mRNA expression profiling of ACE 2, a novel homologue of angiotensin converting enzyme. *FEBS Lett* **2002**, *532*, 107-110, doi:10.1016/s0014-5793(02)03640-2.
38. Jansen, J.; Reimer, K.C.; Nagai, J.S.; Varghese, F.S.; Overheul, G.J.; de Beer, M.; Roverts, R.; Daviran, D.; Fermin, L.A.S.; Willemsen, B.; et al. SARS-CoV-2 infects the human kidney and drives fibrosis in kidney organoids. *Cell Stem Cell* **2022**, *29*, 217-231 e218, doi:10.1016/j.stem.2021.12.010.
39. Donoghue, M.; Hsieh, F.; Baronas, E.; Godbout, K.; Gosselin, M.; Stagliano, N.; Donovan, M.; Woolf, B.; Robison, K.; Jeyaseelan, R.; et al. A novel angiotensin-converting enzyme-related carboxypeptidase (ACE2) converts angiotensin I to angiotensin 1-9. *Circ Res* **2000**, *87*, E1-9, doi:10.1161/01.res.87.5.e1.
40. Crackower, M.A.; Sarao, R.; Oudit, G.Y.; Yagil, C.; Kozieradzki, I.; Scanga, S.E.; Oliveira-dos-Santos, A.J.; da Costa, J.; Zhang, L.; Pei, Y.; et al. Angiotensin-converting

enzyme 2 is an essential regulator of heart function. *Nature* **2002**, *417*, 822-828, doi:10.1038/nature00786.
41. Hoffmann, M.; Kleine-Weber, H.; Pohlmann, S. A Multibasic Cleavage Site in the Spike Protein of SARS-CoV-2 Is Essential for Infection of Human Lung Cells. *Mol Cell* **2020**, *78*, 779-784 e775, doi:10.1016/j.molcel.2020.04.022.
42. Hoffmann, M.; Kleine-Weber, H.; Schroeder, S.; Kruger, N.; Herrler, T.; Erichsen, S.; Schiergens, T.S.; Herrler, G.; Wu, N.H.; Nitsche, A.; et al. SARS-CoV-2 Cell Entry Depends on ACE2 and TMPRSS2 and Is Blocked by a Clinically Proven Protease Inhibitor. *Cell* **2020**, *181*, 271-280 e278, doi:10.1016/j.cell.2020.02.052.
43. Bayati, A.; Kumar, R.; Francis, V.; McPherson, P.S. SARS-CoV-2 infects cells after viral entry via clathrin-mediated endocytosis. *J Biol Chem* **2021**, *296*, 100306, doi:10.1016/j.jbc.2021.100306.
44. Inoue, Y.; Tanaka, N.; Tanaka, Y.; Inoue, S.; Morita, K.; Zhuang, M.; Hattori, T.; Sugamura, K. Clathrin-dependent entry of severe acute respiratory syndrome coronavirus into target cells expressing ACE2 with the cytoplasmic tail deleted. *J Virol* **2007**, *81*, 8722-8729, doi:10.1128/JVI.00253-07.
45. Benlarbi, M.; Laroche, G.; Fink, C.; Fu, K.; Mulloy, R.P.; Phan, A.; Ariana, A.; Stewart, C.M.; Prevost, J.; Beaudoin-Bussieres, G.; et al. Identification and differential usage of a host metalloproteinase entry pathway by SARS-CoV-2 Delta and Omicron. *iScience* **2022**, *25*, 105316, doi:10.1016/j.isci.2022.105316.
46. Finkel, Y.; Mizrahi, O.; Nachshon, A.; Weingarten-Gabbay, S.; Morgenstern, D.; Yahalom-Ronen, Y.; Tamir, H.; Achdout, H.; Stein, D.; Israeli, O.; et al. The coding capacity of SARS-CoV-2. *Nature* **2021**, *589*, 125-130, doi:10.1038/s41586-020-2739-1.
47. Sola, I.; Almazan, F.; Zuniga, S.; Enjuanes, L. Continuous and Discontinuous RNA Synthesis in Coronaviruses. *Annu Rev Virol* **2015**, *2*, 265-288, doi:10.1146/annurev-virology-100114-055218.
48. Thoms, M.; Buschauer, R.; Ameismeier, M.; Koepke, L.; Denk, T.; Hirschenberger, M.; Kratzat, H.; Hayn, M.; Mackens-Kiani, T.; Cheng, J.; et al. Structural basis for translational shutdown and immune evasion by the Nsp1 protein of SARS-CoV-2. *Science* **2020**, *369*, 1249-1255, doi:10.1126/science.abc8665.
49. V'Kovski, P.; Kratzel, A.; Steiner, S.; Stalder, H.; Thiel, V. Coronavirus biology and replication: implications for SARS-CoV-2. *Nat Rev Microbiol* **2021**, *19*, 155-170, doi:10.1038/s41579-020-00468-6.
50. Perlman, S.; Netland, J. Coronaviruses post-SARS: update on replication and pathogenesis. *Nat Rev Microbiol* **2009**, *7*, 439-450, doi:10.1038/nrmicro2147.
51. Gao, Y.; Yan, L.; Huang, Y.; Liu, F.; Zhao, Y.; Cao, L.; Wang, T.; Sun, Q.; Ming, Z.; Zhang, L.; et al. Structure of the RNA-dependent RNA polymerase from COVID-19 virus. *Science* **2020**, *368*, 779-782, doi:10.1126/science.abb7498.
52. Walker, A.P.; Fan, H.; Keown, J.R.; Knight, M.L.; Grimes, J.M.; Fodor, E. The SARS-CoV-2 RNA polymerase is a viral RNA capping enzyme. *Nucleic Acids Res* **2021**, *49*, 13019-13030, doi:10.1093/nar/gkab1160.
53. Daffis, S.; Szretter, K.J.; Schriewer, J.; Li, J.; Youn, S.; Errett, J.; Lin, T.Y.; Schneller, S.; Zust, R.; Dong, H.; et al. 2'-O methylation of the viral mRNA cap evades host restriction by IFIT family members. *Nature* **2010**, *468*, 452-456, doi:10.1038/nature09489.

54. Park, G.J.; Osinski, A.; Hernandez, G.; Eitson, J.L.; Majumdar, A.; Tonelli, M.; Henzler-Wildman, K.; Pawlowski, K.; Chen, Z.; Li, Y.; et al. The mechanism of RNA capping by SARS-CoV-2. *Nature* **2022**, *609*, 793-800, doi:10.1038/s41586-022-05185-z.
55. Yan, L.; Huang, Y.; Ge, J.; Liu, Z.; Lu, P.; Huang, B.; Gao, S.; Wang, J.; Tan, L.; Ye, S.; et al. A mechanism for SARS-CoV-2 RNA capping and its inhibition by nucleotide analog inhibitors. *Cell* **2022**, *185*, 4347-4360 e4317, doi:10.1016/j.cell.2022.09.037.
56. Snijder, E.J.; van der Meer, Y.; Zevenhoven-Dobbe, J.; Onderwater, J.J.; van der Meulen, J.; Koerten, H.K.; Mommaas, A.M. Ultrastructure and origin of membrane vesicles associated with the severe acute respiratory syndrome coronavirus replication complex. *J Virol* **2006**, *80*, 5927-5940, doi:10.1128/JVI.02501-05.
57. Sawicki, S.G.; Sawicki, D.L. Coronaviruses use discontinuous extension for synthesis of subgenome-length negative strands. *Adv Exp Med Biol* **1995**, *380*, 499-506, doi:10.1007/978-1-4615-1899-0_79.
58. Geva, Y.; Schuldiner, M. The back and forth of cargo exit from the endoplasmic reticulum. *Curr Biol* **2014**, *24*, R130-136, doi:10.1016/j.cub.2013.12.008.
59. Klein, S.; Cortese, M.; Winter, S.L.; Wachsmuth-Melm, M.; Neufeldt, C.J.; Cerikan, B.; Stanifer, M.L.; Boulant, S.; Bartenschlager, R.; Chlanda, P. SARS-CoV-2 structure and replication characterized by in situ cryo-electron tomography. *Nat Commun* **2020**, *11*, 5885, doi:10.1038/s41467-020-19619-7.
60. Bosch, B.J.; van der Zee, R.; de Haan, C.A.; Rottier, P.J. The coronavirus spike protein is a class I virus fusion protein: structural and functional characterization of the fusion core complex. *J Virol* **2003**, *77*, 8801-8811, doi:10.1128/jvi.77.16.8801-8811.2003.
61. Wrapp, D.; Wang, N.; Corbett, K.S.; Goldsmith, J.A.; Hsieh, C.L.; Abiona, O.; Graham, B.S.; McLellan, J.S. Cryo-EM structure of the 2019-nCoV spike in the prefusion conformation. *Science* **2020**, *367*, 1260-1263, doi:10.1126/science.abb2507.
62. Zhang, S.; Go, E.P.; Ding, H.; Anang, S.; Kappes, J.C.; Desaire, H.; Sodroski, J.G. Analysis of Glycosylation and Disulfide Bonding of Wild-Type SARS-CoV-2 Spike Glycoprotein. *J Virol* **2022**, *96*, e0162621, doi:10.1128/JVI.01626-21.
63. Walls, A.C.; Tortorici, M.A.; Frenz, B.; Snijder, J.; Li, W.; Rey, F.A.; DiMaio, F.; Bosch, B.J.; Veesler, D. Glycan shield and epitope masking of a coronavirus spike protein observed by cryo-electron microscopy. *Nat Struct Mol Biol* **2016**, *23*, 899-905, doi:10.1038/nsmb.3293.
64. Du, L.; Tai, W.; Yang, Y.; Zhao, G.; Zhu, Q.; Sun, S.; Liu, C.; Tao, X.; Tseng, C.K.; Perlman, S.; et al. Introduction of neutralizing immunogenicity index to the rational design of MERS coronavirus subunit vaccines. *Nat Commun* **2016**, *7*, 13473, doi:10.1038/ncomms13473.
65. Gong, Y.; Qin, S.; Dai, L.; Tian, Z. The glycosylation in SARS-CoV-2 and its receptor ACE2. *Signal Transduct Target Ther* **2021**, *6*, 396, doi:10.1038/s41392-021-00809-8.
66. Coutard, B.; Valle, C.; de Lamballerie, X.; Canard, B.; Seidah, N.G.; Decroly, E. The spike glycoprotein of the new coronavirus 2019-nCoV contains a furin-like cleavage site absent in CoV of the same clade. *Antiviral Res* **2020**, *176*, 104742, doi:10.1016/j.antiviral.2020.104742.
67. Lu, M.; Uchil, P.D.; Li, W.; Zheng, D.; Terry, D.S.; Gorman, J.; Shi, W.; Zhang, B.; Zhou, T.; Ding, S.; et al. Real-Time Conformational Dynamics of SARS-CoV-2 Spikes on Virus Particles. *Cell Host Microbe* **2020**, *28*, 880-891.e888, doi:10.1016/j.chom.2020.11.001.

68. Henderson, R.; Edwards, R.J.; Mansouri, K.; Janowska, K.; Stalls, V.; Gobeil, S.M.C.; Kopp, M.; Li, D.; Parks, R.; Hsu, A.L.; et al. Controlling the SARS-CoV-2 spike glycoprotein conformation. *Nature Structural & Molecular Biology* **2020**, *27*, 925-933, doi:10.1038/s41594-020-0479-4.
69. Yu, J.; Li, Z.; He, X.; Gebre, M.S.; Bondzie, E.A.; Wan, H.; Jacob-Dolan, C.; Martinez, D.R.; Nkolola, J.P.; Baric, R.S.; et al. Deletion of the SARS-CoV-2 Spike Cytoplasmic Tail Increases Infectivity in Pseudovirus Neutralization Assays. *J Virol* **2021**, doi:10.1128/JVI.00044-21.
70. Crawford, K.H.D.; Eguia, R.; Dingens, A.S.; Loes, A.N.; Malone, K.D.; Wolf, C.R.; Chu, H.Y.; Tortorici, M.A.; Veesler, D.; Murphy, M.; et al. Protocol and Reagents for Pseudotyping Lentiviral Particles with SARS-CoV-2 Spike Protein for Neutralization Assays. *Viruses* **2020**, *12*, doi:10.3390/v12050513.
71. Sanders, D.W.; Jumper, C.C.; Ackerman, P.J.; Bracha, D.; Donlic, A.; Kim, H.; Kenney, D.; Castello-Serrano, I.; Suzuki, S.; Tamura, T.; et al. SARS-CoV-2 requires cholesterol for viral entry and pathological syncytia formation. *Elife* **2021**, *10*, doi:10.7554/eLife.65962.
72. Buchrieser, J.; Dufloo, J.; Hubert, M.; Monel, B.; Planas, D.; Rajah, M.M.; Planchais, C.; Porrot, F.; Guivel-Benhassine, F.; Van der Werf, S.; et al. Syncytia formation by SARS-CoV-2-infected cells. *EMBO J* **2020**, *39*, e106267, doi:10.15252/embj.2020106267.
73. Watanabe, Y.; Allen, J.D.; Wrapp, D.; McLellan, J.S.; Crispin, M. Site-specific glycan analysis of the SARS-CoV-2 spike. *Science* **2020**, *369*, 330-333, doi:10.1126/science.abb9983.
74. McCallum, M.; Czudnochowski, N.; Rosen Laura, E.; Zepeda Samantha, K.; Bowen John, E.; Walls Alexandra, C.; Hauser, K.; Joshi, A.; Stewart, C.; Dillen Josh, R.; et al. Structural basis of SARS-CoV-2 Omicron immune evasion and receptor engagement. *Science* **2022**, *375*, 864-868, doi:10.1126/science.abn8652.
75. Chi, X.; Yan, R.; Zhang, J.; Zhang, G.; Zhang, Y.; Hao, M.; Zhang, Z.; Fan, P.; Dong, Y.; Yang, Y.; et al. A neutralizing human antibody binds to the N-terminal domain of the Spike protein of SARS-CoV-2. *Science* **2020**, *369*, 650-655, doi:10.1126/science.abc6952.
76. Beaudoin-Bussieres, G.; Chen, Y.; Ullah, I.; Prevost, J.; Tolbert, W.D.; Symmes, K.; Ding, S.; Benlarbi, M.; Gong, S.Y.; Tauzin, A.; et al. A Fc-enhanced NTD-binding non-neutralizing antibody delays virus spread and synergizes with a nAb to protect mice from lethal SARS-CoV-2 infection. *Cell Rep* **2022**, *38*, 110368, doi:10.1016/j.celrep.2022.110368.
77. Li, W.; Chen, Y.; Prévost, J.; Ullah, I.; Lu, M.; Gong, S.Y.; Tauzin, A.; Gasser, R.; Vézina, D.; Anand, S.P.; et al. Structural basis and mode of action for two broadly neutralizing antibodies against SARS-CoV-2 emerging variants of concern. *Cell Rep* **2021**, *38*, 110210, doi:10.1016/j.celrep.2021.110210.
78. Zhang, J.; Xiao, T.; Cai, Y.; Chen, B. Structure of SARS-CoV-2 spike protein. *Curr Opin Virol* **2021**, *50*, 173-182, doi:10.1016/j.coviro.2021.08.010.
79. Zhang, J.; Cai, Y.; Xiao, T.; Lu, J.; Peng, H.; Sterling, S.M.; Walsh, R.M., Jr.; Rits-Volloch, S.; Zhu, H.; Woosley, A.N.; et al. Structural impact on SARS-CoV-2 spike protein by D614G substitution. *Science* **2021**, *372*, 525-530, doi:10.1126/science.abf2303.
80. Huang, Y.; Yang, C.; Xu, X.F.; Xu, W.; Liu, S.W. Structural and functional properties of SARS-CoV-2 spike protein: potential antivirus drug development for COVID-19. *Acta Pharmacol Sin* **2020**, *41*, 1141-1149, doi:10.1038/s41401-020-0485-4.

81. Ng, K.W.; Faulkner, N.; Finsterbusch, K.; Wu, M.; Harvey, R.; Hussain, S.; Greco, M.; Liu, Y.; Kjaer, S.; Swanton, C.; et al. SARS-CoV-2 S2-targeted vaccination elicits broadly neutralizing antibodies. *Sci Transl Med* **2022**, *14*, eabn3715, doi:10.1126/scitranslmed.abn3715.
82. Zhang, Z.; Nomura, N.; Muramoto, Y.; Ekimoto, T.; Uemura, T.; Liu, K.; Yui, M.; Kono, N.; Aoki, J.; Ikeguchi, M.; et al. Structure of SARS-CoV-2 membrane protein essential for virus assembly. *Nat Commun* **2022**, *13*, 4399, doi:10.1038/s41467-022-32019-3.
83. Siu, Y.L.; Teoh, K.T.; Lo, J.; Chan, C.M.; Kien, F.; Escriou, N.; Tsao, S.W.; Nicholls, J.M.; Altmeyer, R.; Peiris, J.S.; et al. The M, E, and N structural proteins of the severe acute respiratory syndrome coronavirus are required for efficient assembly, trafficking, and release of virus-like particles. *J Virol* **2008**, *82*, 11318-11330, doi:10.1128/JVI.01052-08.
84. Yoshimoto, F.K. The Proteins of Severe Acute Respiratory Syndrome Coronavirus-2 (SARS CoV-2 or n-COV19), the Cause of COVID-19. *Protein J* **2020**, *39*, 198-216, doi:10.1007/s10930-020-09901-4.
85. Fu, Y.Z.; Wang, S.Y.; Zheng, Z.Q.; Yi, H.; Li, W.W.; Xu, Z.S.; Wang, Y.Y. SARS-CoV-2 membrane glycoprotein M antagonizes the MAVS-mediated innate antiviral response. *Cell Mol Immunol* **2021**, *18*, 613-620, doi:10.1038/s41423-020-00571-x.
86. Wang, Y.; Grunewald, M.; Perlman, S. Coronaviruses: An Updated Overview of Their Replication and Pathogenesis. *Methods Mol Biol* **2020**, *2203*, 1-29, doi:10.1007/978-1-0716-0900-2_1.
87. Breitinger, U.; Farag, N.S.; Sticht, H.; Breitinger, H.G. Viroporins: Structure, function, and their role in the life cycle of SARS-CoV-2. *Int J Biochem Cell Biol* **2022**, *145*, 106185, doi:10.1016/j.biocel.2022.106185.
88. Chen, X.; Cao, R.; Zhong, W. Host Calcium Channels and Pumps in Viral Infections. *Cells* **2019**, *9*, doi:10.3390/cells9010094.
89. Schoeman, D.; Fielding, B.C. Coronavirus envelope protein: current knowledge. *Virol J* **2019**, *16*, 69, doi:10.1186/s12985-019-1182-0.
90. Xia, B.; Shen, X.; He, Y.; Pan, X.; Liu, F.L.; Wang, Y.; Yang, F.; Fang, S.; Wu, Y.; Duan, Z.; et al. SARS-CoV-2 envelope protein causes acute respiratory distress syndrome (ARDS)-like pathological damages and constitutes an antiviral target. *Cell Res* **2021**, *31*, 847-860, doi:10.1038/s41422-021-00519-4.
91. Bai, Z.; Cao, Y.; Liu, W.; Li, J. The SARS-CoV-2 Nucleocapsid Protein and Its Role in Viral Structure, Biological Functions, and a Potential Target for Drug or Vaccine Mitigation. *Viruses* **2021**, *13*, doi:10.3390/v13061115.
92. Cong, Y.; Ulasli, M.; Schepers, H.; Mauthe, M.; V'Kovski, P.; Kriegenburg, F.; Thiel, V.; de Haan, C.A.M.; Reggiori, F. Nucleocapsid Protein Recruitment to Replication-Transcription Complexes Plays a Crucial Role in Coronaviral Life Cycle. *J Virol* **2020**, *94*, doi:10.1128/JVI.01925-19.
93. Masters, P.S. Coronavirus genomic RNA packaging. *Virology* **2019**, *537*, 198-207, doi:10.1016/j.virol.2019.08.031.
94. Verkerke, H.P.; Damhorst, G.L.; Graciaa, D.S.; McLendon, K.; O'Sick, W.; Robichaux, C.; Cheedarla, N.; Potlapalli, S.; Wu, S.C.; Harrington, K.R.V.; et al. Nucleocapsid Antigenemia Is a Marker of Acute SARS-CoV-2 Infection. *J Infect Dis* **2022**, *226*, 1577-1587, doi:10.1093/infdis/jiac225.
95. Sen, S.R.; Sanders, E.C.; Gabriel, K.N.; Miller, B.M.; Isoda, H.M.; Salcedo, G.S.; Garrido, J.E.; Dyer, R.P.; Nakajima, R.; Jain, A.; et al. Predicting COVID-19 Severity with a

Specific Nucleocapsid Antibody plus Disease Risk Factor Score. *mSphere* **2021**, *6*, doi:10.1128/mSphere.00203-21.
96. Chen, L.; Guan, W.J.; Qiu, Z.E.; Xu, J.B.; Bai, X.; Hou, X.C.; Sun, J.; Qu, S.; Huang, Z.X.; Lei, T.L.; et al. SARS-CoV-2 nucleocapsid protein triggers hyperinflammation via protein-protein interaction-mediated intracellular Cl(-) accumulation in respiratory epithelium. *Signal Transduct Target Ther* **2022**, *7*, 255, doi:10.1038/s41392-022-01048-1.
97. Deng, Q.; Ye, G.; Pan, Y.; Xie, W.; Yang, G.; Li, Z.; Li, Y. High Performance of SARS-Cov-2N Protein Antigen Chemiluminescence Immunoassay as Frontline Testing for Acute Phase COVID-19 Diagnosis: A Retrospective Cohort Study. *Front Med (Lausanne)* **2021**, *8*, 676560, doi:10.3389/fmed.2021.676560.
98. Hodcroft, E.B. CoVariants: SARS-CoV-2 Mutations and Variants of Interest. Available online: https://covariants.org/ (accessed on 2022-11-20).
99. Castano-Rodriguez, C.; Honrubia, J.M.; Gutierrez-Alvarez, J.; DeDiego, M.L.; Nieto-Torres, J.L.; Jimenez-Guardeno, J.M.; Regla-Nava, J.A.; Fernandez-Delgado, R.; Verdia-Baguena, C.; Queralt-Martin, M.; et al. Role of Severe Acute Respiratory Syndrome Coronavirus Viroporins E, 3a, and 8a in Replication and Pathogenesis. *mBio* **2018**, *9*, doi:10.1128/mBio.02325-17.
100. Issa, E.; Merhi, G.; Panossian, B.; Salloum, T.; Tokajian, S. SARS-CoV-2 and ORF3a: Nonsynonymous Mutations, Functional Domains, and Viral Pathogenesis. *mSystems* **2020**, *5*, doi:10.1128/mSystems.00266-20.
101. Frieman, M.; Yount, B.; Heise, M.; Kopecky-Bromberg, S.A.; Palese, P.; Baric, R.S. Severe acute respiratory syndrome coronavirus ORF6 antagonizes STAT1 function by sequestering nuclear import factors on the rough endoplasmic reticulum/Golgi membrane. *J Virol* **2007**, *81*, 9812-9824, doi:10.1128/JVI.01012-07.
102. Addetia, A.; Lieberman, N.A.P.; Phung, Q.; Hsiang, T.Y.; Xie, H.; Roychoudhury, P.; Shrestha, L.; Loprieno, M.A.; Huang, M.L.; Gale, M., Jr.; et al. SARS-CoV-2 ORF6 Disrupts Bidirectional Nucleocytoplasmic Transport through Interactions with Rae1 and Nup98. *mBio* **2021**, *12*, doi:10.1128/mBio.00065-21.
103. Kopecky-Bromberg, S.A.; Martinez-Sobrido, L.; Frieman, M.; Baric, R.A.; Palese, P. Severe acute respiratory syndrome coronavirus open reading frame (ORF) 3b, ORF 6, and nucleocapsid proteins function as interferon antagonists. *J Virol* **2007**, *81*, 548-557, doi:10.1128/JVI.01782-06.
104. Zhang, F.; Zang, T.M.; Stevenson, E.M.; Lei, X.; Copertino, D.C.; Mota, T.M.; Boucau, J.; Garcia-Beltran, W.F.; Jones, R.B.; Bieniasz, P.D. Inhibition of major histocompatibility complex-I antigen presentation by sarbecovirus ORF7a proteins. *Proc Natl Acad Sci U S A* **2022**, *119*, e2209042119, doi:10.1073/pnas.2209042119.
105. Cao, Z.; Xia, H.; Rajsbaum, R.; Xia, X.; Wang, H.; Shi, P.Y. Ubiquitination of SARS-CoV-2 ORF7a promotes antagonism of interferon response. *Cell Mol Immunol* **2021**, *18*, 746-748, doi:10.1038/s41423-020-00603-6.
106. Zinzula, L. Lost in deletion: The enigmatic ORF8 protein of SARS-CoV-2. *Biochem Biophys Res Commun* **2021**, *538*, 116-124, doi:10.1016/j.bbrc.2020.10.045.
107. Young, B.E.; Fong, S.W.; Chan, Y.H.; Mak, T.M.; Ang, L.W.; Anderson, D.E.; Lee, C.Y.; Amrun, S.N.; Lee, B.; Goh, Y.S.; et al. Effects of a major deletion in the SARS-CoV-2 genome on the severity of infection and the inflammatory response: an observational cohort study. *Lancet* **2020**, *396*, 603-611, doi:10.1016/S0140-6736(20)31757-8.

108. Beaudoin-Bussieres, G.; Arduini, A.; Bourassa, C.; Medjahed, H.; Gendron-Lepage, G.; Richard, J.; Pan, Q.; Wang, Z.; Liang, C.; Finzi, A. SARS-CoV-2 Accessory Protein ORF8 Decreases Antibody-Dependent Cellular Cytotoxicity. *Viruses* **2022**, *14*, doi:10.3390/v14061237.
109. Lin, X.; Fu, B.; Yin, S.; Li, Z.; Liu, H.; Zhang, H.; Xing, N.; Wang, Y.; Xue, W.; Xiong, Y.; et al. ORF8 contributes to cytokine storm during SARS-CoV-2 infection by activating IL-17 pathway. *iScience* **2021**, *24*, 102293, doi:10.1016/j.isci.2021.102293.
110. Matsuoka, K.; Imahashi, N.; Ohno, M.; Ode, H.; Nakata, Y.; Kubota, M.; Sugimoto, A.; Imahashi, M.; Yokomaku, Y.; Iwatani, Y. SARS-CoV-2 accessory protein ORF8 is secreted extracellularly as a glycoprotein homodimer. *J Biol Chem* **2022**, *298*, 101724, doi:10.1016/j.jbc.2022.101724.
111. Wang, X.; Lam, J.Y.; Wong, W.M.; Yuen, C.K.; Cai, J.P.; Au, S.W.; Chan, J.F.; To, K.K.W.; Kok, K.H.; Yuen, K.Y. Accurate Diagnosis of COVID-19 by a Novel Immunogenic Secreted SARS-CoV-2 orf8 Protein. *mBio* **2020**, *11*, doi:10.1128/mBio.02431-20.
112. Li, X.; Hou, P.; Ma, W.; Wang, X.; Wang, H.; Yu, Z.; Chang, H.; Wang, T.; Jin, S.; Wang, X.; et al. SARS-CoV-2 ORF10 suppresses the antiviral innate immune response by degrading MAVS through mitophagy. *Cell Mol Immunol* **2022**, *19*, 67-78, doi:10.1038/s41423-021-00807-4.
113. Chiara, M.; D'Erchia, A.M.; Gissi, C.; Manzari, C.; Parisi, A.; Resta, N.; Zambelli, F.; Picardi, E.; Pavesi, G.; Horner, D.S.; et al. Next generation sequencing of SARS-CoV-2 genomes: challenges, applications and opportunities. *Brief Bioinform* **2021**, *22*, 616-630, doi:10.1093/bib/bbaa297.
114. Shu, Y.; McCauley, J. GISAID: Global initiative on sharing all influenza data - from vision to reality. *Euro Surveill* **2017**, *22*, doi:10.2807/1560-7917.ES.2017.22.13.30494.
115. Hadfield, J.; Megill, C.; Bell, S.M.; Huddleston, J.; Potter, B.; Callender, C.; Sagulenko, P.; Bedford, T.; Neher, R.A. Nextstrain: real-time tracking of pathogen evolution. *Bioinformatics* **2018**, *34*, 4121-4123, doi:10.1093/bioinformatics/bty407.
116. O'Toole, A.; Pybus, O.G.; Abram, M.E.; Kelly, E.J.; Rambaut, A. Pango lineage designation and assignment using SARS-CoV-2 spike gene nucleotide sequences. *BMC Genomics* **2022**, *23*, 121, doi:10.1186/s12864-022-08358-2.
117. WHO. Tracking SARS-CoV-2 variants. **2022**.
118. Korber, B.; Fischer, W.M.; Gnanakaran, S.; Yoon, H.; Theiler, J.; Abfalterer, W.; Hengartner, N.; Giorgi, E.E.; Bhattacharya, T.; Foley, B.; et al. Tracking Changes in SARS-CoV-2 Spike: Evidence that D614G Increases Infectivity of the COVID-19 Virus. *Cell* **2020**, *182*, 812-827 e819, doi:10.1016/j.cell.2020.06.043.
119. Plante, J.A.; Liu, Y.; Liu, J.; Xia, H.; Johnson, B.A.; Lokugamage, K.G.; Zhang, X.; Muruato, A.E.; Zou, J.; Fontes-Garfias, C.R.; et al. Spike mutation D614G alters SARS-CoV-2 fitness. *Nature* **2021**, *592*, 116-121, doi:10.1038/s41586-020-2895-3.
120. Zhang, L.; Jackson, C.B.; Mou, H.; Ojha, A.; Peng, H.; Quinlan, B.D.; Rangarajan, E.S.; Pan, A.; Vanderheiden, A.; Suthar, M.S.; et al. SARS-CoV-2 spike-protein D614G mutation increases virion spike density and infectivity. *Nat Commun* **2020**, *11*, 6013, doi:10.1038/s41467-020-19808-4.
121. Laporte, M.; Raeymaekers, V.; Van Berwaer, R.; Vandeput, J.; Marchand-Casas, I.; Thibaut, H.J.; Van Looveren, D.; Martens, K.; Hoffmann, M.; Maes, P.; et al. The SARS-CoV-2 and other human coronavirus spike proteins are fine-tuned towards temperature and

proteases of the human airways. *PLoS Pathog* **2021**, *17*, e1009500, doi:10.1371/journal.ppat.1009500.
122. CDC. COVID Data Tracker - Variant Proportions. **2022**.
123. Canda, G.o. COVID-19 epidemiology update: Outbreaks **2022**.
124. Frampton, D.; Rampling, T.; Cross, A.; Bailey, H.; Heaney, J.; Byott, M.; Scott, R.; Sconza, R.; Price, J.; Margaritis, M.; et al. Genomic characteristics and clinical effect of the emergent SARS-CoV-2 B.1.1.7 lineage in London, UK: a whole-genome sequencing and hospital-based cohort study. *Lancet Infect Dis* **2021**, *21*, 1246-1256, doi:10.1016/S1473-3099(21)00170-5.
125. Liu, Y.; Liu, J.; Plante, K.S.; Plante, J.A.; Xie, X.; Zhang, X.; Ku, Z.; An, Z.; Scharton, D.; Schindewolf, C.; et al. The N501Y spike substitution enhances SARS-CoV-2 infection and transmission. *Nature* **2022**, *602*, 294-299, doi:10.1038/s41586-021-04245-0.
126. Tian, F.; Tong, B.; Sun, L.; Shi, S.; Zheng, B.; Wang, Z.; Dong, X.; Zheng, P. N501Y mutation of spike protein in SARS-CoV-2 strengthens its binding to receptor ACE2. *Elife* **2021**, *10*, doi:10.7554/eLife.69091.
127. Prévost, J.; Richard, J.; Gasser, R.; Ding, S.; Fage, C.; Anand, S.P.; Adam, D.; Gupta Vergara, N.; Tauzin, A.; Benlarbi, M.; et al. Impact of temperature on the affinity of SARS-CoV-2 Spike glycoprotein for host ACE2. *J Biol Chem* **2021**, *297*, 101151, doi:10.1016/j.jbc.2021.101151.
128. Winstone, H.; Lista, M.J.; Reid, A.C.; Bouton, C.; Pickering, S.; Galao, R.P.; Kerridge, C.; Doores, K.J.; Swanson, C.M.; Neil, S.J.D. The Polybasic Cleavage Site in SARS-CoV-2 Spike Modulates Viral Sensitivity to Type I Interferon and IFITM2. *J Virol* **2021**, *95*, doi:10.1128/JVI.02422-20.
129. Lista, M.J.; Winstone, H.; Wilson, H.D.; Dyer, A.; Pickering, S.; Galao, R.P.; De Lorenzo, G.; Cowton, V.M.; Furnon, W.; Suarez, N.; et al. The P681H Mutation in the Spike Glycoprotein of the Alpha Variant of SARS-CoV-2 Escapes IFITM Restriction and Is Necessary for Type I Interferon Resistance. *J Virol* **2022**, e0125022, doi:10.1128/jvi.01250-22.
130. Mwenda, M.; Saasa, N.; Sinyange, N.; Busby, G.; Chipimo, P.J.; Hendry, J.; Kapona, O.; Yingst, S.; Hines, J.Z.; Minchella, P.; et al. Detection of B.1.351 SARS-CoV-2 Variant Strain - Zambia, December 2020. *MMWR Morb Mortal Wkly Rep* **2021**, *70*, 280-282, doi:10.15585/mmwr.mm7008e2.
131. Tokyo, J.N.I.o.I.D. Brief report: new variant strain of SARS-CoV-2 identified in travelers from Brazil. **2021**.
132. Greaney, A.J.; Starr, T.N.; Gilchuk, P.; Zost, S.J.; Binshtein, E.; Loes, A.N.; Hilton, S.K.; Huddleston, J.; Eguia, R.; Crawford, K.H.D.; et al. Complete Mapping of Mutations to the SARS-CoV-2 Spike Receptor-Binding Domain that Escape Antibody Recognition. *Cell Host Microbe* **2021**, *29*, 44-57 e49, doi:10.1016/j.chom.2020.11.007.
133. Wang, P.; Nair, M.S.; Liu, L.; Iketani, S.; Luo, Y.; Guo, Y.; Wang, M.; Yu, J.; Zhang, B.; Kwong, P.D.; et al. Antibody resistance of SARS-CoV-2 variants B.1.351 and B.1.1.7. *Nature* **2021**, *593*, 130-135, doi:10.1038/s41586-021-03398-2.
134. Gong, S.Y.; Chatterjee, D.; Richard, J.; Prévost, J.; Tauzin, A.; Gasser, R.; Bo, Y.; Vézina, D.; Goyette, G.; Gendron-Lepage, G.; et al. Contribution of single mutations to selected SARS-CoV-2 emerging variants spike antigenicity. *Virology* **2021**, *563*, 134-145, doi:https://doi.org/10.1016/j.virol.2021.09.001.

135. Ferreira, I.; Kemp, S.A.; Datir, R.; Saito, A.; Meng, B.; Rakshit, P.; Takaori-Kondo, A.; Kosugi, Y.; Uriu, K.; Kimura, I.; et al. SARS-CoV-2 B.1.617 Mutations L452R and E484Q Are Not Synergistic for Antibody Evasion. *J Infect Dis* **2021**, *224*, 989-994, doi:10.1093/infdis/jiab368.
136. Deng, X.; Garcia-Knight, M.A.; Khalid, M.M.; Servellita, V.; Wang, C.; Morris, M.K.; Sotomayor-González, A.; Glasner, D.R.; Reyes, K.R.; Gliwa, A.S.; et al. Transmission, infectivity, and neutralization of a spike L452R SARS-CoV-2 variant. *Cell* **2021**, doi:10.1016/j.cell.2021.04.025.
137. Motozono, C.; Toyoda, M.; Zahradnik, J.; Saito, A.; Nasser, H.; Tan, T.S.; Ngare, I.; Kimura, I.; Uriu, K.; Kosugi, Y.; et al. SARS-CoV-2 spike L452R variant evades cellular immunity and increases infectivity. *Cell Host Microbe* **2021**, *29*, 1124-1136 e1111, doi:10.1016/j.chom.2021.06.006.
138. Mlcochova, P.; Kemp, S.A.; Dhar, M.S.; Papa, G.; Meng, B.; Ferreira, I.; Datir, R.; Collier, D.A.; Albecka, A.; Singh, S.; et al. SARS-CoV-2 B.1.617.2 Delta variant replication and immune evasion. *Nature* **2021**, *599*, 114-119, doi:10.1038/s41586-021-03944-y.
139. Butt, A.A.; Dargham, S.R.; Chemaitelly, H.; Al Khal, A.; Tang, P.; Hasan, M.R.; Coyle, P.V.; Thomas, A.G.; Borham, A.M.; Concepcion, E.G.; et al. Severity of Illness in Persons Infected With the SARS-CoV-2 Delta Variant vs Beta Variant in Qatar. *JAMA Intern Med* **2022**, *182*, 197-205, doi:10.1001/jamainternmed.2021.7949.
140. WHO. Classification of Omicron (B.1.1.529): SARS-CoV-2 Variant of Concern. **2021**.
141. CDC. Science brief: Omicron (B.1.1.529) variant. **2021**.
142. Esper, F.P.; Adhikari, T.M.; Tu, Z.J.; Cheng, Y.W.; El-Haddad, K.; Farkas, D.H.; Bosler, D.; Rhoads, D.; Procop, G.W.; Ko, J.S.; et al. Alpha to Omicron: Disease Severity and Clinical Outcomes of Major SARS-CoV-2 Variants. *J Infect Dis* **2022**, doi:10.1093/infdis/jiac411.
143. Andrews, N.; Stowe, J.; Kirsebom, F.; Toffa, S.; Rickeard, T.; Gallagher, E.; Gower, C.; Kall, M.; Groves, N.; O'Connell, A.M.; et al. Covid-19 Vaccine Effectiveness against the Omicron (B.1.1.529) Variant. *N Engl J Med* **2022**, *386*, 1532-1546, doi:10.1056/NEJMoa2119451.
144. Yu, J.; Collier, A.Y.; Rowe, M.; Mardas, F.; Ventura, J.D.; Wan, H.; Miller, J.; Powers, O.; Chung, B.; Siamatu, M.; et al. Neutralization of the SARS-CoV-2 Omicron BA.1 and BA.2 Variants. *N Engl J Med* **2022**, *386*, 1579-1580, doi:10.1056/NEJMc2201849.
145. Nemet, I.; Kliker, L.; Lustig, Y.; Zuckerman, N.; Erster, O.; Cohen, C.; Kreiss, Y.; Alroy-Preis, S.; Regev-Yochay, G.; Mendelson, E.; et al. Third BNT162b2 Vaccination Neutralization of SARS-CoV-2 Omicron Infection. *N Engl J Med* **2022**, *386*, 492-494, doi:10.1056/NEJMc2119358.
146. Cameroni, E.; Bowen, J.E.; Rosen, L.E.; Saliba, C.; Zepeda, S.K.; Culap, K.; Pinto, D.; VanBlargan, L.A.; De Marco, A.; di Iulio, J.; et al. Broadly neutralizing antibodies overcome SARS-CoV-2 Omicron antigenic shift. *Nature* **2022**, *602*, 664-670, doi:10.1038/s41586-021-04386-2.
147. Gong, S.Y.; Ding, S.; Benlarbi, M.; Chen, Y.; Vezina, D.; Marchitto, L.; Beaudoin-Bussieres, G.; Goyette, G.; Bourassa, C.; Bo, Y.; et al. Temperature Influences the Interaction between SARS-CoV-2 Spike from Omicron Subvariants and Human ACE2. *Viruses* **2022**, *14*, doi:10.3390/v14102178.
148. NIH. Coronavirus Disease 2019 (COVID-19) Treatment Guidelines.

149. Harapan, B.N.; Yoo, H.J. Neurological symptoms, manifestations, and complications associated with severe acute respiratory syndrome coronavirus 2 (SARS-CoV-2) and coronavirus disease 19 (COVID-19). *J Neurol* **2021**, *268*, 3059-3071, doi:10.1007/s00415-021-10406-y.
150. CDC. Symptoms of COVID-19. **2022**.
151. CDC. Long COVID or Post-COVID Conditions. **2022**.
152. CDC. Assessing Risk Factors for Severe COVID-19 Illness: People with Certain Medical Conditions. **2022**.
153. Ng, W.H.; Tipih, T.; Makoah, N.A.; Vermeulen, J.G.; Goedhals, D.; Sempa, J.B.; Burt, F.J.; Taylor, A.; Mahalingam, S. Comorbidities in SARS-CoV-2 Patients: a Systematic Review and Meta-Analysis. *mBio* **2021**, *12*, doi:10.1128/mBio.03647-20.
154. Li, H.; Liu, L.; Zhang, D.; Xu, J.; Dai, H.; Tang, N.; Su, X.; Cao, B. SARS-CoV-2 and viral sepsis: observations and hypotheses. *Lancet* **2020**, *395*, 1517-1520, doi:10.1016/S0140-6736(20)30920-X.
155. Liu, J.; Li, S.; Liu, J.; Liang, B.; Wang, X.; Wang, H.; Li, W.; Tong, Q.; Yi, J.; Zhao, L.; et al. Longitudinal characteristics of lymphocyte responses and cytokine profiles in the peripheral blood of SARS-CoV-2 infected patients. *EBioMedicine* **2020**, *55*, 102763, doi:10.1016/j.ebiom.2020.102763.
156. Rebillard, R.M.; Charabati, M.; Grasmuck, C.; Filali-Mouhim, A.; Tastet, O.; Brassard, N.; Daigneault, A.; Bourbonniere, L.; Anand, S.P.; Balthazard, R.; et al. Identification of SARS-CoV-2-specific immune alterations in acutely ill patients. *J Clin Invest* **2021**, *131*, doi:10.1172/JCI145853.
157. Brunet-Ratnasingham, E.; Anand, S.P.; Gantner, P.; Dyachenko, A.; Moquin-Beaudry, G.; Brassard, N.; Beaudoin-Bussieres, G.; Pagliuzza, A.; Gasser, R.; Benlarbi, M.; et al. Integrated immunovirological profiling validates plasma SARS-CoV-2 RNA as an early predictor of COVID-19 mortality. *Sci Adv* **2021**, *7*, eabj5629, doi:10.1126/sciadv.abj5629.
158. Syed, F.; Li, W.; Relich, R.F.; Russell, P.M.; Zhang, S.; Zimmerman, M.K.; Yu, Q. Excessive Matrix Metalloproteinase-1 and Hyperactivation of Endothelial Cells Occurred in COVID-19 Patients and Were Associated With the Severity of COVID-19. *J Infect Dis* **2021**, *224*, 60-69, doi:10.1093/infdis/jiab167.
159. Rovito, R.; Bono, V.; Augello, M.; Tincati, C.; Mainoldi, F.; Beaudoin-Bussieres, G.; Tauzin, A.; Bianchi, S.; Hadla, M.; Yellenki, V.; et al. Association between SARS-CoV-2 RNAemia and dysregulated immune response in acutely ill hospitalized COVID-19 patients. *Sci Rep* **2022**, *12*, 19658, doi:10.1038/s41598-022-23923-1.
160. WHO. COVID-19 vaccine tracker and landscape. **2022**.
161. Barouch, D.H. Covid-19 Vaccines - Immunity, Variants, Boosters. *N Engl J Med* **2022**, *387*, 1011-1020, doi:10.1056/NEJMra2206573.
162. WHO. 11 Vaccines Granted Emergency Use Listing (EUL) by WHO. **2022**.
163. Hsieh, C.L.; Goldsmith, J.A.; Schaub, J.M.; DiVenere, A.M.; Kuo, H.C.; Javanmardi, K.; Le, K.C.; Wrapp, D.; Lee, A.G.; Liu, Y.; et al. Structure-based design of prefusion-stabilized SARS-CoV-2 spikes. *Science* **2020**, *369*, 1501-1505, doi:10.1126/science.abd0826.
164. Polack, F.P.; Thomas, S.J.; Kitchin, N.; Absalon, J.; Gurtman, A.; Lockhart, S.; Perez, J.L.; Perez Marc, G.; Moreira, E.D.; Zerbini, C.; et al. Safety and Efficacy of the BNT162b2 mRNA Covid-19 Vaccine. *N Engl J Med* **2020**, *383*, 2603-2615, doi:10.1056/NEJMoa2034577.

165. Baden, L.R.; El Sahly, H.M.; Essink, B.; Kotloff, K.; Frey, S.; Novak, R.; Diemert, D.; Spector, S.A.; Rouphael, N.; Creech, C.B.; et al. Efficacy and Safety of the mRNA-1273 SARS-CoV-2 Vaccine. *N Engl J Med* **2021**, *384*, 403-416, doi:10.1056/NEJMoa2035389.
166. Tauzin, A.; Nayrac, M.; Benlarbi, M.; Gong, S.Y.; Gasser, R.; Beaudoin-Bussieres, G.; Brassard, N.; Laumaea, A.; Vezina, D.; Prevost, J.; et al. A single dose of the SARS-CoV-2 vaccine BNT162b2 elicits Fc-mediated antibody effector functions and T cell responses. *Cell Host Microbe* **2021**, *29*, 1137-1150 e1136, doi:10.1016/j.chom.2021.06.001.
167. Turner, J.S.; O'Halloran, J.A.; Kalaidina, E.; Kim, W.; Schmitz, A.J.; Zhou, J.Q.; Lei, T.; Thapa, M.; Chen, R.E.; Case, J.B.; et al. SARS-CoV-2 mRNA vaccines induce persistent human germinal centre responses. *Nature* **2021**, *596*, 109-113, doi:10.1038/s41586-021-03738-2.
168. Carreno, J.M.; Alshammary, H.; Tcheou, J.; Singh, G.; Raskin, A.J.; Kawabata, H.; Sominsky, L.A.; Clark, J.J.; Adelsberg, D.C.; Bielak, D.A.; et al. Activity of convalescent and vaccine serum against SARS-CoV-2 Omicron. *Nature* **2022**, *602*, 682-688, doi:10.1038/s41586-022-04399-5.
169. Neidleman, J.; Luo, X.; McGregor, M.; Xie, G.; Murray, V.; Greene, W.C.; Lee, S.A.; Roan, N.R. mRNA vaccine-induced T cells respond identically to SARS-CoV-2 variants of concern but differ in longevity and homing properties depending on prior infection status. *Elife* **2021**, *10*, doi:10.7554/eLife.72619.
170. Liu, J.; Chandrashekar, A.; Sellers, D.; Barrett, J.; Jacob-Dolan, C.; Lifton, M.; McMahan, K.; Sciacca, M.; VanWyk, H.; Wu, C.; et al. Vaccines elicit highly conserved cellular immunity to SARS-CoV-2 Omicron. *Nature* **2022**, *603*, 493-496, doi:10.1038/s41586-022-04465-y.
171. Collier, A.Y.; Yu, J.; McMahan, K.; Liu, J.; Chandrashekar, A.; Maron, J.S.; Atyeo, C.; Martinez, D.R.; Ansel, J.L.; Aguayo, R.; et al. Differential Kinetics of Immune Responses Elicited by Covid-19 Vaccines. *N Engl J Med* **2021**, *385*, 2010-2012, doi:10.1056/NEJMc2115596.
172. Keehner, J.; Horton, L.E.; Binkin, N.J.; Laurent, L.C.; Alliance, S.; Pride, D.; Longhurst, C.A.; Abeles, S.R.; Torriani, F.J. Resurgence of SARS-CoV-2 Infection in a Highly Vaccinated Health System Workforce. *N Engl J Med* **2021**, *385*, 1330-1332, doi:10.1056/NEJMc2112981.
173. Yoon, S.K.; Hegmann, K.T.; Thiese, M.S.; Burgess, J.L.; Ellingson, K.; Lutrick, K.; Olsho, L.E.W.; Edwards, L.J.; Sokol, B.; Caban-Martinez, A.J.; et al. Protection with a Third Dose of mRNA Vaccine against SARS-CoV-2 Variants in Frontline Workers. *N Engl J Med* **2022**, *386*, 1855-1857, doi:10.1056/NEJMc2201821.
174. Qu, P.; Faraone, J.; Evans, J.P.; Zou, X.; Zheng, Y.M.; Carlin, C.; Bednash, J.S.; Lozanski, G.; Mallampalli, R.K.; Saif, L.J.; et al. Neutralization of the SARS-CoV-2 Omicron BA.4/5 and BA.2.12.1 Subvariants. *N Engl J Med* **2022**, *386*, 2526-2528, doi:10.1056/NEJMc2206725.
175. Tuekprakhon, A.; Nutalai, R.; Dijokaite-Guraliuc, A.; Zhou, D.; Ginn, H.M.; Selvaraj, M.; Liu, C.; Mentzer, A.J.; Supasa, P.; Duyvesteyn, H.M.E.; et al. Antibody escape of SARS-CoV-2 Omicron BA.4 and BA.5 from vaccine and BA.1 serum. *Cell* **2022**, *185*, 2422-2433 e2413, doi:10.1016/j.cell.2022.06.005.
176. Wang, Q.; Guo, Y.; Iketani, S.; Nair, M.S.; Li, Z.; Mohri, H.; Wang, M.; Yu, J.; Bowen, A.D.; Chang, J.Y.; et al. Antibody evasion by SARS-CoV-2 Omicron subvariants

BA.2.12.1, BA.4 and BA.5. *Nature* **2022**, *608*, 603-608, doi:10.1038/s41586-022-05053-w.
177. Stephanie, R.L.-G.A.A.C.K.E.F.-D.Z.R.S.A.B.R.E.W.J.D.M.E.K.A. *Effectiveness of Bivalent mRNA Vaccines in Preventing Symptomatic SARS-CoV-2 Infection — Increasing Community Access to Testing Program, United States, September–November 2022*; CDC: 22 November 2022 2022.
178. Regev-Yochay, G.; Gonen, T.; Gilboa, M.; Mandelboim, M.; Indenbaum, V.; Amit, S.; Meltzer, L.; Asraf, K.; Cohen, C.; Fluss, R.; et al. Efficacy of a Fourth Dose of Covid-19 mRNA Vaccine against Omicron. *N Engl J Med* **2022**, *386*, 1377-1380, doi:10.1056/NEJMc2202542.
179. Chalkias, S.; Harper, C.; Vrbicky, K.; Walsh, S.R.; Essink, B.; Brosz, A.; McGhee, N.; Tomassini, J.E.; Chen, X.; Chang, Y.; et al. A Bivalent Omicron-Containing Booster Vaccine against Covid-19. *N Engl J Med* **2022**, *387*, 1279-1291, doi:10.1056/NEJMoa2208343.
180. Vicenti, I.; Gatti, F.; Scaggiante, R.; Boccuto, A.; Zago, D.; Basso, M.; Dragoni, F.; Zazzi, M.; Parisi, S.G. Single-dose BNT162b2 mRNA COVID-19 vaccine significantly boosts neutralizing antibody response in health care workers recovering from asymptomatic or mild natural SARS-CoV-2 infection. *Int J Infect Dis* **2021**, *108*, 176-178, doi:10.1016/j.ijid.2021.05.033.
181. Reynolds, C.J.; Pade, C.; Gibbons, J.M.; Butler, D.K.; Otter, A.D.; Menacho, K.; Fontana, M.; Smit, A.; Sackville-West, J.E.; Cutino-Moguel, T.; et al. Prior SARS-CoV-2 infection rescues B and T cell responses to variants after first vaccine dose. *Science* **2021**, *372*, 1418-1423, doi:10.1126/science.abh1282.
182. Collier, A.Y.; Yu, J.; McMahan, K.; Liu, J.; Atyeo, C.; Ansel, J.L.; Fricker, Z.P.; Pavlakis, M.; Curry, M.P.; Jacob-Dolan, C.; et al. Coronavirus Disease 2019 Messenger RNA Vaccine Immunogenicity in Immunosuppressed Individuals. *J Infect Dis* **2022**, *225*, 1124-1128, doi:10.1093/infdis/jiab569.
183. Boyarsky, B.J.; Werbel, W.A.; Avery, R.K.; Tobian, A.A.R.; Massie, A.B.; Segev, D.L.; Garonzik-Wang, J.M. Antibody Response to 2-Dose SARS-CoV-2 mRNA Vaccine Series in Solid Organ Transplant Recipients. *JAMA* **2021**, *325*, 2204-2206, doi:10.1001/jama.2021.7489.
184. Tauzin, A.; Beaudoin-Bussieres, G.; Gong, S.Y.; Chatterjee, D.; Gendron-Lepage, G.; Bourassa, C.; Goyette, G.; Racine, N.; Khrifi, Z.; Turgeon, J.; et al. Humoral immune responses against SARS-CoV-2 Spike variants after mRNA vaccination in solid organ transplant recipients. *iScience* **2022**, *25*, 104990, doi:10.1016/j.isci.2022.104990.
185. Tauzin, A.; Gong, S.Y.; Beaudoin-Bussieres, G.; Vezina, D.; Gasser, R.; Nault, L.; Marchitto, L.; Benlarbi, M.; Chatterjee, D.; Nayrac, M.; et al. Strong humoral immune responses against SARS-CoV-2 Spike after BNT162b2 mRNA vaccination with a 16-week interval between doses. *Cell Host Microbe* **2022**, *30*, 97-109 e105, doi:10.1016/j.chom.2021.12.004.
186. Tauzin, A.; Gong, S.Y.; Chatterjee, D.; Ding, S.; Painter, M.M.; Goel, R.R.; Beaudoin-Bussieres, G.; Marchitto, L.; Boutin, M.; Laumaea, A.; et al. A boost with SARS-CoV-2 BNT162b2 mRNA vaccine elicits strong humoral responses independently of the interval between the first two doses. *Cell Rep* **2022**, *41*, 111554, doi:10.1016/j.celrep.2022.111554.
187. Nayrac, M.; Dube, M.; Sannier, G.; Nicolas, A.; Marchitto, L.; Tastet, O.; Tauzin, A.; Brassard, N.; Lima-Barbosa, R.; Beaudoin-Bussieres, G.; et al. Temporal associations of B

and T cell immunity with robust vaccine responsiveness in a 16-week interval BNT162b2 regimen. *Cell Rep* **2022**, *39*, 111013, doi:10.1016/j.celrep.2022.111013.
188. Elsner, R.A.; Shlomchik, M.J. Germinal Center and Extrafollicular B Cell Responses in Vaccination, Immunity, and Autoimmunity. *Immunity* **2020**, *53*, 1136-1150, doi:10.1016/j.immuni.2020.11.006.
189. Lam, J.H.; Smith, F.L.; Baumgarth, N. B Cell Activation and Response Regulation During Viral Infections. *Viral Immunol* **2020**, *33*, 294-306, doi:10.1089/vim.2019.0207.
190. Qi, H.; Liu, B.; Wang, X.; Zhang, L. The humoral response and antibodies against SARS-CoV-2 infection. *Nat Immunol* **2022**, *23*, 1008-1020, doi:10.1038/s41590-022-01248-5.
191. Turner, J.S.; Kim, W.; Kalaidina, E.; Goss, C.W.; Rauseo, A.M.; Schmitz, A.J.; Hansen, L.; Haile, A.; Klebert, M.K.; Pusic, I.; et al. SARS-CoV-2 infection induces long-lived bone marrow plasma cells in humans. *Nature* **2021**, *595*, 421-425, doi:10.1038/s41586-021-03647-4.
192. Palm, A.E.; Henry, C. Remembrance of Things Past: Long-Term B Cell Memory After Infection and Vaccination. *Front Immunol* **2019**, *10*, 1787, doi:10.3389/fimmu.2019.01787.
193. Prevost, J.; Gasser, R.; Beaudoin-Bussieres, G.; Richard, J.; Duerr, R.; Laumaea, A.; Anand, S.P.; Goyette, G.; Benlarbi, M.; Ding, S.; et al. Cross-Sectional Evaluation of Humoral Responses against SARS-CoV-2 Spike. *Cell Rep Med* **2020**, *1*, 100126, doi:10.1016/j.xcrm.2020.100126.
194. Chen, Y.; Zuiani, A.; Fischinger, S.; Mullur, J.; Atyeo, C.; Travers, M.; Lelis, F.J.N.; Pullen, K.M.; Martin, H.; Tong, P.; et al. Quick COVID-19 Healers Sustain Anti-SARS-CoV-2 Antibody Production. *Cell* **2020**, *183*, 1496-1507 e1416, doi:10.1016/j.cell.2020.10.051.
195. Kuri-Cervantes, L.; Pampena, M.B.; Meng, W.; Rosenfeld, A.M.; Ittner, C.A.G.; Weisman, A.R.; Agyekum, R.S.; Mathew, D.; Baxter, A.E.; Vella, L.A.; et al. Comprehensive mapping of immune perturbations associated with severe COVID-19. *Sci Immunol* **2020**, *5*, doi:10.1126/sciimmunol.abd7114.
196. Long, Q.X.; Tang, X.J.; Shi, Q.L.; Li, Q.; Deng, H.J.; Yuan, J.; Hu, J.L.; Xu, W.; Zhang, Y.; Lv, F.J.; et al. Clinical and immunological assessment of asymptomatic SARS-CoV-2 infections. *Nat Med* **2020**, *26*, 1200-1204, doi:10.1038/s41591-020-0965-6.
197. Wajnberg, A.; Amanat, F.; Firpo, A.; Altman, D.R.; Bailey, M.J.; Mansour, M.; McMahon, M.; Meade, P.; Mendu, D.R.; Muellers, K.; et al. Robust neutralizing antibodies to SARS-CoV-2 infection persist for months. *Science* **2020**, *370*, 1227-1230, doi:10.1126/science.abd7728.
198. Isho, B.; Abe, K.T.; Zuo, M.; Jamal, A.J.; Rathod, B.; Wang, J.H.; Li, Z.; Chao, G.; Rojas, O.L.; Bang, Y.M.; et al. Persistence of serum and saliva antibody responses to SARS-CoV-2 spike antigens in COVID-19 patients. *Sci Immunol* **2020**, *5*, doi:10.1126/sciimmunol.abe5511.
199. Perreault, J.; Tremblay, T.; Fournier, M.J.; Drouin, M.; Beaudoin-Bussieres, G.; Prevost, J.; Lewin, A.; Begin, P.; Finzi, A.; Bazin, R. Waning of SARS-CoV-2 RBD antibodies in longitudinal convalescent plasma samples within 4 months after symptom onset. *Blood* **2020**, *136*, 2588-2591, doi:10.1182/blood.2020008367.
200. Beaudoin-Bussieres, G.; Laumaea, A.; Anand, S.P.; Prevost, J.; Gasser, R.; Goyette, G.; Medjahed, H.; Perreault, J.; Tremblay, T.; Lewin, A.; et al. Decline of Humoral Responses

against SARS-CoV-2 Spike in Convalescent Individuals. *mBio* **2020**, *11*, doi:10.1128/mBio.02590-20.
201. Anand, S.P.; Prevost, J.; Nayrac, M.; Beaudoin-Bussieres, G.; Benlarbi, M.; Gasser, R.; Brassard, N.; Laumaea, A.; Gong, S.Y.; Bourassa, C.; et al. Longitudinal analysis of humoral immunity against SARS-CoV-2 Spike in convalescent individuals up to 8 months post-symptom onset. *Cell Rep Med* **2021**, *2*, 100290, doi:10.1016/j.xcrm.2021.100290.
202. Gasser, R.; Cloutier, M.; Prevost, J.; Fink, C.; Ducas, E.; Ding, S.; Dussault, N.; Landry, P.; Tremblay, T.; Laforce-Lavoie, A.; et al. Major role of IgM in the neutralizing activity of convalescent plasma against SARS-CoV-2. *Cell Rep* **2021**, *34*, 108790, doi:10.1016/j.celrep.2021.108790.
203. Klingler, J.; Weiss, S.; Itri, V.; Liu, X.; Oguntuyo, K.Y.; Stevens, C.; Ikegame, S.; Hung, C.T.; Enyindah-Asonye, G.; Amanat, F.; et al. Role of Immunoglobulin M and A Antibodies in the Neutralization of Severe Acute Respiratory Syndrome Coronavirus 2. *J Infect Dis* **2021**, *223*, 957-970, doi:10.1093/infdis/jiaa784.
204. Chandrashekar, A.; Liu, J.; Martinot, A.J.; McMahan, K.; Mercado, N.B.; Peter, L.; Tostanoski, L.H.; Yu, J.; Maliga, Z.; Nekorchuk, M.; et al. SARS-CoV-2 infection protects against rechallenge in rhesus macaques. *Science* **2020**, *369*, 812-817, doi:10.1126/science.abc4776.
205. Dufloo, J.; Grzelak, L.; Staropoli, I.; Madec, Y.; Tondeur, L.; Anna, F.; Pelleau, S.; Wiedemann, A.; Planchais, C.; Buchrieser, J.; et al. Asymptomatic and symptomatic SARS-CoV-2 infections elicit polyfunctional antibodies. *Cell Rep Med* **2021**, *2*, 100275, doi:10.1016/j.xcrm.2021.100275.
206. Chen, X.; Rostad, C.A.; Anderson, L.J.; Sun, H.Y.; Lapp, S.A.; Stephens, K.; Hussaini, L.; Gibson, T.; Rouphael, N.; Anderson, E.J. The development and kinetics of functional antibody-dependent cell-mediated cytotoxicity (ADCC) to SARS-CoV-2 spike protein. *Virology* **2021**, *559*, 1-9, doi:10.1016/j.virol.2021.03.009.
207. Yu, Y.; Wang, M.; Zhang, X.; Li, S.; Lu, Q.; Zeng, H.; Hou, H.; Li, H.; Zhang, M.; Jiang, F.; et al. Antibody-dependent cellular cytotoxicity response to SARS-CoV-2 in COVID-19 patients. *Signal Transduct Target Ther* **2021**, *6*, 346, doi:10.1038/s41392-021-00759-1.
208. Hastie, K.M.; Li, H.; Bedinger, D.; Schendel, S.L.; Dennison, S.M.; Li, K.; Rayaprolu, V.; Yu, X.; Mann, C.; Zandonatti, M.; et al. Defining variant-resistant epitopes targeted by SARS-CoV-2 antibodies: A global consortium study. *Science* **2021**, *374*, 472-478, doi:10.1126/science.abh2315.
209. Barnes, C.O.; Jette, C.A.; Abernathy, M.E.; Dam, K.A.; Esswein, S.R.; Gristick, H.B.; Malyutin, A.G.; Sharaf, N.G.; Huey-Tubman, K.E.; Lee, Y.E.; et al. SARS-CoV-2 neutralizing antibody structures inform therapeutic strategies. *Nature* **2020**, *588*, 682-687, doi:10.1038/s41586-020-2852-1.
210. Yuan, M.; Wu, N.C.; Zhu, X.; Lee, C.D.; So, R.T.Y.; Lv, H.; Mok, C.K.P.; Wilson, I.A. A highly conserved cryptic epitope in the receptor binding domains of SARS-CoV-2 and SARS-CoV. *Science* **2020**, *368*, 630-633, doi:10.1126/science.abb7269.
211. Panel, C.-T.G. *Coronavirus Disease 2019 (COVID-19) Treatment Guidelines*; National Institutes of Health: 2022.
212. Takashita, E.; Kinoshita, N.; Yamayoshi, S.; Sakai-Tagawa, Y.; Fujisaki, S.; Ito, M.; Iwatsuki-Horimoto, K.; Chiba, S.; Halfmann, P.; Nagai, H.; et al. Efficacy of Antibodies and Antiviral Drugs against Covid-19 Omicron Variant. *N Engl J Med* **2022**, *386*, 995-998, doi:10.1056/NEJMc2119407.

213. FDA. *FDA releases important information about risk of COVID-19 due to certain variants not neutralized by Evusheld*; 2022.
214. Mornese Pinna, S.; Lupia, T.; Scabini, S.; Vita, D.; De Benedetto, I.; Gaviraghi, A.; Colasanto, I.; Varese, A.; Cattel, F.; De Rosa, F.G.; et al. Monoclonal antibodies for the treatment of COVID-19 patients: An umbrella to overcome the storm? *Int Immunopharmacol* **2021**, *101*, 108200, doi:10.1016/j.intimp.2021.108200.
215. Dong, J.; Zost, S.J.; Greaney, A.J.; Starr, T.N.; Dingens, A.S.; Chen, E.C.; Chen, R.E.; Case, J.B.; Sutton, R.E.; Gilchuk, P.; et al. Genetic and structural basis for SARS-CoV-2 variant neutralization by a two-antibody cocktail. *Nat Microbiol* **2021**, *6*, 1233-1244, doi:10.1038/s41564-021-00972-2.
216. FDA. Decisio - Summary of Product Characteristics for Evusheld. **2022**.
217. Loo, Y.M.; McTamney, P.M.; Arends, R.H.; Abram, M.E.; Aksyuk, A.A.; Diallo, S.; Flores, D.J.; Kelly, E.J.; Ren, K.; Roque, R.; et al. The SARS-CoV-2 monoclonal antibody combination, AZD7442, is protective in nonhuman primates and has an extended half-life in humans. *Sci Transl Med* **2022**, *14*, eabl8124, doi:10.1126/scitranslmed.abl8124.
218. Iketani, S.; Liu, L.; Guo, Y.; Liu, L.; Chan, J.F.; Huang, Y.; Wang, M.; Luo, Y.; Yu, J.; Chu, H.; et al. Antibody evasion properties of SARS-CoV-2 Omicron sublineages. *Nature* **2022**, *604*, 553-556, doi:10.1038/s41586-022-04594-4.
219. Westendorf, K.; Zentelis, S.; Wang, L.; Foster, D.; Vaillancourt, P.; Wiggin, M.; Lovett, E.; van der Lee, R.; Hendle, J.; Pustilnik, A.; et al. LY-CoV1404 (bebtelovimab) potently neutralizes SARS-CoV-2 variants. *Cell Rep* **2022**, *39*, 110812, doi:10.1016/j.celrep.2022.110812.
220. FDA. FDA Announces Bebtelovimab is Not Currently Authorized in Any US Region. **2022**.
221. Kao, R.Y.; Tsui, W.H.; Lee, T.S.; Tanner, J.A.; Watt, R.M.; Huang, J.D.; Hu, L.; Chen, G.; Chen, Z.; Zhang, L.; et al. Identification of novel small-molecule inhibitors of severe acute respiratory syndrome-associated coronavirus by chemical genetics. *Chem Biol* **2004**, *11*, 1293-1299, doi:10.1016/j.chembiol.2004.07.013.
222. Ding, S.; Ullah, I.; Gong, S.Y.; Grover, J.R.; Mohammadi, M.; Chen, Y.; Vézina, D.; Beaudoin-Bussières, G.; Verma, V.T.; Goyette, G.; et al. VE607 stabilizes SARS-CoV-2 Spike in the "RBD-up" conformation and inhibits viral entry. *iScience* **2022**, *25*, 104528, doi:10.1016/j.isci.2022.104528.
223. Rubin, D.; Chan-Tack, K.; Farley, J.; Sherwat, A. FDA Approval of Remdesivir - A Step in the Right Direction. *N Engl J Med* **2020**, *383*, 2598-2600, doi:10.1056/NEJMp2032369.
224. Lo, M.K.; Albarino, C.G.; Perry, J.K.; Chang, S.; Tchesnokov, E.P.; Guerrero, L.; Chakrabarti, A.; Shrivastava-Ranjan, P.; Chatterjee, P.; McMullan, L.K.; et al. Remdesivir targets a structurally analogous region of the Ebola virus and SARS-CoV-2 polymerases. *Proc Natl Acad Sci U S A* **2020**, *117*, 26946-26954, doi:10.1073/pnas.2012294117.
225. FDA. FDA's approval of Veklury (remdesivir) for the treatment of COVID-19—the science of safety and effectiveness. **2020**.
226. Kabinger, F.; Stiller, C.; Schmitzova, J.; Dienemann, C.; Kokic, G.; Hillen, H.S.; Hobartner, C.; Cramer, P. Mechanism of molnupiravir-induced SARS-CoV-2 mutagenesis. *Nat Struct Mol Biol* **2021**, *28*, 740-746, doi:10.1038/s41594-021-00651-0.
227. Owen, D.R.; Allerton, C.M.N.; Anderson, A.S.; Aschenbrenner, L.; Avery, M.; Berritt, S.; Boras, B.; Cardin, R.D.; Carlo, A.; Coffman, K.J.; et al. An oral SARS-CoV-2 M(pro)

inhibitor clinical candidate for the treatment of COVID-19. *Science* **2021**, *374*, 1586-1593, doi:10.1126/science.abl4784.
228. McKinnon, K.M. Flow Cytometry: An Overview. *Curr Protoc Immunol* **2018**, *120*, 5 1 1-5 1 11, doi:10.1002/cpim.40.
229. Cossarizza, A.; Chang, H.D.; Radbruch, A.; Acs, A.; Adam, D.; Adam-Klages, S.; Agace, W.W.; Aghaeepour, N.; Akdis, M.; Allez, M.; et al. Guidelines for the use of flow cytometry and cell sorting in immunological studies (second edition). *Eur J Immunol* **2019**, *49*, 1457-1973, doi:10.1002/eji.201970107.
230. Ding, S.; Laumaea, A.; Benlarbi, M.; Beaudoin-Bussières, G.; Gasser, R.; Medjahed, H.; Pancera, M.; Stamatatos, L.; McGuire, A.T.; Bazin, R.; et al. Antibody Binding to SARS-CoV-2 S Glycoprotein Correlates with but Does Not Predict Neutralization. *Viruses* **2020**, *12*, doi:10.3390/v12111214.
231. Petersen, R.L. Strategies Using Bio-Layer Interferometry Biosensor Technology for Vaccine Research and Development. *Biosensors (Basel)* **2017**, *7*, doi:10.3390/bios7040049.
232. Prévost, J.; Finzi, A. The great escape? SARS-CoV-2 variants evading neutralizing responses. *Cell Host Microbe* **2021**, *29*, 322-324, doi:10.1016/j.chom.2021.02.010.
233. Haynes, B.F.; Gilbert, P.B.; McElrath, M.J.; Zolla-Pazner, S.; Tomaras, G.D.; Alam, S.M.; Evans, D.T.; Montefiori, D.C.; Karnasuta, C.; Sutthent, R.; et al. Immune-correlates analysis of an HIV-1 vaccine efficacy trial. *N Engl J Med* **2012**, *366*, 1275-1286, doi:10.1056/NEJMoa1113425.
234. Alsahafi, N.; Debbeche, O.; Sodroski, J.; Finzi, A. Effects of the I559P gp41 change on the conformation and function of the human immunodeficiency virus (HIV-1) membrane envelope glycoprotein trimer. *PLoS One* **2015**, *10*, e0122111, doi:10.1371/journal.pone.0122111.
235. Alsahafi, N.; Anand, S.P.; Castillo-Menendez, L.; Verly, M.M.; Medjahed, H.; Prevost, J.; Herschhorn, A.; Richard, J.; Schon, A.; Melillo, B.; et al. SOSIP Changes Affect Human Immunodeficiency Virus Type 1 Envelope Glycoprotein Conformation and CD4 Engagement. *J Virol* **2018**, *92*, doi:10.1128/JVI.01080-18.
236. Castillo-Menendez, L.R.; Nguyen, H.T.; Sodroski, J. Conformational Differences between Functional Human Immunodeficiency Virus Envelope Glycoprotein Trimers and Stabilized Soluble Trimers. *J Virol* **2019**, *93*, doi:10.1128/JVI.01709-18.
237. Lu, M.; Ma, X.; Castillo-Menendez, L.R.; Gorman, J.; Alsahafi, N.; Ermel, U.; Terry, D.S.; Chambers, M.; Peng, D.; Zhang, B.; et al. Associating HIV-1 envelope glycoprotein structures with states on the virus observed by smFRET. *Nature* **2019**, *568*, 415-419, doi:10.1038/s41586-019-1101-y.
238. Callaway, E. Fast-spreading COVID variant can elude immune responses. *Nature* **2021**, *589*, 500-501, doi:10.1038/d41586-021-00121-z.
239. Asplund Hogelin, K.; Ruffin, N.; Pin, E.; Manberg, A.; Hober, S.; Gafvelin, G.; Gronlund, H.; Nilsson, P.; Khademi, M.; Olsson, T.; et al. Development of humoral and cellular immunological memory against SARS-CoV-2 despite B cell depleting treatment in multiple sclerosis. *iScience* **2021**, *24*, 103078, doi:10.1016/j.isci.2021.103078.
240. Wu, M.; Wall, E.C.; Carr, E.J.; Harvey, R.; Townsley, H.; Mears, H.V.; Adams, L.; Kjaer, S.; Kelly, G.; Warchal, S.; et al. Three-dose vaccination elicits neutralising antibodies against omicron. *Lancet* **2022**, *399*, 715-717, doi:10.1016/S0140-6736(22)00092-7.

241. Wall, E.C.; Wu, M.; Harvey, R.; Kelly, G.; Warchal, S.; Sawyer, C.; Daniels, R.; Hobson, P.; Hatipoglu, E.; Ngai, Y.; et al. Neutralising antibody activity against SARS-CoV-2 VOCs B.1.617.2 and B.1.351 by BNT162b2 vaccination. *Lancet* **2021**, *397*, 2331-2333, doi:10.1016/S0140-6736(21)01290-3.
242. Wang, Z.; Schmidt, F.; Weisblum, Y.; Muecksch, F.; Barnes, C.O.; Finkin, S.; Schaefer-Babajew, D.; Cipolla, M.; Gaebler, C.; Lieberman, J.A.; et al. mRNA vaccine-elicited antibodies to SARS-CoV-2 and circulating variants. *Nature* **2021**, *592*, 616-622, doi:10.1038/s41586-021-03324-6.
243. Gangavarapu, K.; Latif, A.A.; Mullen, J.L.; Alkuzweny, M.; Hufbauer, E.; Tsueng, G.; Haag, E.; Zeller, M.; Aceves, C.M.; Zaiets, K.; et al. Outbreak.info genomic reports: scalable and dynamic surveillance of SARS-CoV-2 variants and mutations. *medRxiv* **2022**, 2022.2001.2027.22269965, doi:10.1101/2022.01.27.22269965.
244. Moulana, A.; Dupic, T.; Phillips, A.M.; Chang, J.; Nieves, S.; Roffler, A.A.; Greaney, A.J.; Starr, T.N.; Bloom, J.D.; Desai, M.M. Compensatory epistasis maintains ACE2 affinity in SARS-CoV-2 Omicron BA.1. *Nat Commun* **2022**, *13*, 7011, doi:10.1038/s41467-022-34506-z.
245. Sanjuan, R.; Cuevas, J.M.; Moya, A.; Elena, S.F. Epistasis and the adaptability of an RNA virus. *Genetics* **2005**, *170*, 1001-1008, doi:10.1534/genetics.105.040741.
246. Gobeil, S.M.; Henderson, R.; Stalls, V.; Janowska, K.; Huang, X.; May, A.; Speakman, M.; Beaudoin, E.; Manne, K.; Li, D.; et al. Structural diversity of the SARS-CoV-2 Omicron spike. *Mol Cell* **2022**, *82*, 2050-2068.e2056, doi:10.1016/j.molcel.2022.03.028.
247. Zeng, C.; Evans, J.P.; Qu, P.; Faraone, J.; Zheng, Y.M.; Carlin, C.; Bednash, J.S.; Zhou, T.; Lozanski, G.; Mallampalli, R.; et al. Neutralization and Stability of SARS-CoV-2 Omicron Variant. *bioRxiv* **2021**, doi:10.1101/2021.12.16.472934.
248. Stalls, V.; Lindenberger, J.; Gobeil, S.M.; Henderson, R.; Parks, R.; Barr, M.; Deyton, M.; Martin, M.; Janowska, K.; Huang, X.; et al. Cryo-EM structures of SARS-CoV-2 Omicron BA.2 spike. *Cell Rep* **2022**, *39*, 111009, doi:10.1016/j.celrep.2022.111009.
249. Sajadi, M.M.; Habibzadeh, P.; Vintzileos, A.; Shokouhi, S.; Miralles-Wilhelm, F.; Amoroso, A. Temperature, Humidity, and Latitude Analysis to Estimate Potential Spread and Seasonality of Coronavirus Disease 2019 (COVID-19). *JAMA Netw Open* **2020**, *3*, e2011834, doi:10.1001/jamanetworkopen.2020.11834.
250. McFadden, E.R., Jr.; Pichurko, B.M.; Bowman, H.F.; Ingenito, E.; Burns, S.; Dowling, N.; Solway, J. Thermal mapping of the airways in humans. *J Appl Physiol (1985)* **1985**, *58*, 564-570, doi:10.1152/jappl.1985.58.2.564.
251. Lindemann, J.; Leiacker, R.; Rettinger, G.; Keck, T. Nasal mucosal temperature during respiration. *Clin Otolaryngol Allied Sci* **2002**, *27*, 135-139, doi:10.1046/j.1365-2273.2002.00544.x.
252. V'Kovski, P.; Gultom, M.; Kelly, J.N.; Steiner, S.; Russeil, J.; Mangeat, B.; Cora, E.; Pezoldt, J.; Holwerda, M.; Kratzel, A.; et al. Disparate temperature-dependent virus-host dynamics for SARS-CoV-2 and SARS-CoV in the human respiratory epithelium. *PLoS Biol* **2021**, *19*, e3001158, doi:10.1371/journal.pbio.3001158.
253. Planas, D.; Saunders, N.; Maes, P.; Guivel-Benhassine, F.; Planchais, C.; Buchrieser, J.; Bolland, W.H.; Porrot, F.; Staropoli, I.; Lemoine, F.; et al. Considerable escape of SARS-CoV-2 Omicron to antibody neutralization. *Nature* **2022**, *602*, 671-675, doi:10.1038/s41586-021-04389-z.

254. Lubinski, B.; Fernandes, M.H.V.; Frazier, L.; Tang, T.; Daniel, S.; Diel, D.G.; Jaimes, J.A.; Whittaker, G.R. Functional evaluation of the P681H mutation on the proteolytic activation of the SARS-CoV-2 variant B.1.1.7 (Alpha) spike. *iScience* **2022**, *25*, 103589, doi:10.1016/j.isci.2021.103589.
255. Uraki, R.; Ito, M.; Furusawa, Y.; Yamayoshi, S.; Iwatsuki-Horimoto, K.; Adachi, E.; Saito, M.; Koga, M.; Tsutsumi, T.; Yamamoto, S.; et al. Humoral immune evasion of the omicron subvariants BQ.1.1 and XBB. *Lancet Infect Dis* **2023**, *23*, 30-32, doi:10.1016/S1473-3099(22)00816-7.
256. Hoffmann, M.; Arora, P.; Nehlmeier, I.; Kempf, A.; Cossmann, A.; Schulz, S.R.; Morillas Ramos, G.; Manthey, L.A.; Jäck, H.-M.; Behrens, G.M.N.; et al. Profound neutralization evasion and augmented host cell entry are hallmarks of the fast-spreading SARS-CoV-2 lineage XBB.1.5. *Cellular & Molecular Immunology* **2023**, doi:10.1038/s41423-023-00988-0.
257. Yue, C.; Song, W.; Wang, L.; Jian, F.; Chen, X.; Gao, F.; Shen, Z.; Wang, Y.; Wang, X.; Cao, Y. ACE2 binding and antibody evasion in enhanced transmissibility of XBB.1.5. *Lancet Infect Dis* **2023**, *23*, 278-280, doi:10.1016/S1473-3099(23)00010-5.
258. Starr, T.N.; Greaney, A.J.; Hannon, W.W.; Loes, A.N.; Hauser, K.; Dillen, J.R.; Ferri, E.; Farrell, A.G.; Dadonaite, B.; McCallum, M.; et al. Shifting mutational constraints in the SARS-CoV-2 receptor-binding domain during viral evolution. *Science* **2022**, *377*, 420-424, doi:10.1126/science.abo7896.
259. Shang, J.; Wan, Y.; Luo, C.; Ye, G.; Geng, Q.; Auerbach, A.; Li, F. Cell entry mechanisms of SARS-CoV-2. *Proc Natl Acad Sci U S A* **2020**, *117*, 11727-11734, doi:10.1073/pnas.2003138117.
260. Fowler, D.M.; Araya, C.L.; Fleishman, S.J.; Kellogg, E.H.; Stephany, J.J.; Baker, D.; Fields, S. High-resolution mapping of protein sequence-function relationships. *Nat Methods* **2010**, *7*, 741-746, doi:10.1038/nmeth.1492.
261. Vergara, N.G.; Gatchel, M.; Abrams, C.F. Entropic overcompensation of the N501Y mutation on SARS-CoV-2 S binding to ACE2. *bioRxiv* **2022**, doi:10.1101/2022.08.30.505841.
262. Roy, R.; Hohng, S.; Ha, T. A practical guide to single-molecule FRET. *Nat Methods* **2008**, *5*, 507-516, doi:10.1038/nmeth.1208.
263. Asif, Z.; Chen, Z.; Stranges, S.; Zhao, X.; Sadiq, R.; Olea-Popelka, F.; Peng, C.; Haghighat, F.; Yu, T. Dynamics of SARS-CoV-2 spreading under the influence of environmental factors and strategies to tackle the pandemic: A systematic review. *Sustainable Cities and Society* **2022**, *81*, 103840, doi:https://doi.org/10.1016/j.scs.2022.103840.
264. Cai, J.; Deng, X.; Yang, J.; Sun, K.; Liu, H.; Chen, Z.; Peng, C.; Chen, X.; Wu, Q.; Zou, J.; et al. Modeling transmission of SARS-CoV-2 Omicron in China. *Nat Med* **2022**, *28*, 1468-1475, doi:10.1038/s41591-022-01855-7.
265. Munoz-Fontela, C.; Dowling, W.E.; Funnell, S.G.P.; Gsell, P.S.; Riveros-Balta, A.X.; Albrecht, R.A.; Andersen, H.; Baric, R.S.; Carroll, M.W.; Cavaleri, M.; et al. Animal models for COVID-19. *Nature* **2020**, *586*, 509-515, doi:10.1038/s41586-020-2787-6.
266. Shou, S.; Liu, M.; Yang, Y.; Kang, N.; Song, Y.; Tan, D.; Liu, N.; Wang, F.; Liu, J.; Xie, Y. Animal Models for COVID-19: Hamsters, Mouse, Ferret, Mink, Tree Shrew, and Non-human Primates. *Front Microbiol* **2021**, *12*, 626553, doi:10.3389/fmicb.2021.626553.

267. Kim, Y.I.; Kim, S.G.; Kim, S.M.; Kim, E.H.; Park, S.J.; Yu, K.M.; Chang, J.H.; Kim, E.J.; Lee, S.; Casel, M.A.B.; et al. Infection and Rapid Transmission of SARS-CoV-2 in Ferrets. *Cell Host Microbe* **2020**, *27*, 704-709 e702, doi:10.1016/j.chom.2020.03.023.
268. Lavine, J.S.; Bjornstad, O.N.; Antia, R. Immunological characteristics govern the transition of COVID-19 to endemicity. *Science* **2021**, *371*, 741-745, doi:10.1126/science.abe6522.
269. Lagace-Wiens, P.; Bullard, J.; Cole, R.; Van Caeseele, P. Seasonality of coronaviruses and other respiratory viruses in Canada: Implications for COVID-19. *Can Commun Dis Rep* **2021**, *47*, 132-138, doi:10.14745/ccdr.v47i03a02.

APPENDIX

Permissions to use copyright material

Chapter II: Gong, S. Y.; Chatterjee, D.; Richard, J.; Prévost, J.; Tauzin, A.; Gasser, R.; Bo, Y.; Vézina, D.; Goyette, G.; Gendron-Lepage, G.; Medjahed, H.; Roger, M.; Côté, M.; Finzi, A., Contribution of single mutations to selected SARS-CoV-2 emerging variants spike antigenicity. *Virology* **2021,** 563, 134-145.

Chapter III: Gong, S. Y.; Ding, S.; Benlarbi, M.; Chen, Y.; Vezina, D.; Marchitto, L.; Beaudoin-Bussieres, G.; Goyette, G.; Bourassa, C.; Bo, Y.; Medjahed, H.; Levade, I.; Pazgier, M.; Cote, M.; Richard, J.; Prevost, J.; Finzi, A., Temperature Influences the Interaction between SARS-CoV-2 Spike from Omicron Subvariants and Human ACE2. *Viruses* **2022**, 14, (10).